Functional characterization of the TTF complex and its role in neurodevelopmental disorders

Doctoral Dissertation (Thesis)

to obtain the degree of

"Doktor der Naturwissenschaften"

(Dr. rer. nat.)

awarded by the Julius-Maximilians-Universität Würzburg

submitted by

Cornelia Brosi

from Würzburg, Germany

Würzburg 2017

Submitted to the Faculty of Chemistry and Pharmacy on

December 21, 2017

Evaluators of the written Dissertation (Thesis)

Supervisor – 1. Evaluator: Prof. Dr. Utz Fischer

2. Evaluator: Prof. Dr. Alexander Buchberger

Examiners of the Public Defense

1. Examiner: Prof. Dr. Utz Fischer

2. Examiner: Prof. Dr. Alexander Buchberger

3. Examiner: PD Dr. Sibylle Jablonka

Date of the Public Defense

Doctoral Certificate awarded on

Table of contents

1. Summary

The eukaryotic gene expression requires extensive regulations to enable the homeostasis of the cell and to allow dynamic responses due to external stimuli. Although many regulatory mechanisms involve the transcription as the first step of the gene expression, intensive regulation occurs also in the post-transcriptional mRNA metabolism. Thereby, the particular composition of the mRNPs plays a central role as the components associated with the mRNA form a specific "mRNP code" which determines the fate of the mRNA. Many proteins which are involved in this regulation and the mRNA metabolism are affected in diseases and especially neurological disorders often result from an aberrant mRNP code which leads to changes in the regulation and expression of mRNPs.

The focus of this work was on a trimeric protein complex which is termed TTF complex based on its subunits TDRD3, TOP3β and FMRP. Biochemical investigations revealed that the three components of the TTF complex are nucleo-cytosolic shuttle proteins which localize in the cytoplasm at the steady-state, associate with mRNPs and are presumably connected to the translation. Upon cellular stress conditions, the TTF components concentrate in stress granules. Thus, the TTF complex is part of the mRNP code, however its target RNAs and function are still completely unknown. Since the loss of functional FMRP results in the fragile X syndrome and TOP3β is associated with schizophrenia and intellectual disability, the TTF complex connects these phenotypically related neuro-psychiatric disorders with each other on a molecular level.

Therefore, the aim of this work was to biochemically characterize the TTF complex and to define its function in the mRNA metabolism. In this work, evidence was provided that TDRD3 acts as the central unit of the TTF complex and directly binds to FMRP as well as to TOP3β. Thereby, the interaction of TDRD3 and TOP3β is very stable, whereas FMRP is a dynamic component. Interestingly, the TTF complex is not bound directly to mRNA, but is recruited via the exon junction complex (EJC) to mRNPs. This interaction is mediated by a specific binding motif of TDRD3, the EBM. Upon biochemical and biological investigations, it was possible to identify the interactome of the TTF complex and to define the role in the mRNA metabolism. The data revealed that the TTF complex is mainly associated with "early" mRNPs and is probably involved in the pioneer round of translation. Furthermore, TOP3β was found to bind directly to the ribosome and thus, establishes a connection between the EJC and the translation machinery. A reduction of the TTF components resulted in selective changes in the proteome in cultured cells, whereby individual protein subsets seem to be regulated rather than the global protein expression.

Moreover, the enzymatic analysis of TOP3β indicated that TOP3β is a type IA topoisomerase which can catalytically attack not only DNA but also RNA. This aspect is particularly interesting with regard to the connection between early mRNPs and the translation which has been revealed in this work.

The data obtained in this work suggest that the TTF complex plays a role in regulating the metabolism of an early mRNP subset possibly in the course of the pioneer round of translation. Until now, the link between an RNA topoisomerase and the mRNA metabolism is thereby unique and thus provides a completely new perspective on the steps in the post-transcriptional gene expression and its regulation.

2. Zusammenfassung

Die eukaryotische Genexpression bedarf einer umfassenden Regulation um die Homöostase der Zelle zu gewährleisten und um dynamische Reaktionen auf externe Einflüsse zu ermöglichen. Obwohl viele der regulatorischen Mechanismen die Transkription als ersten Schritt der Genexpression betreffen, findet auch eine intensive Regulierung auf der Ebene des post-transkriptionellen mRNA-Metabolismus statt. Dabei spielt die jeweilige Zusammensetzung der mRNPs eine zentrale Rolle, da je nachdem, mit welchen Faktoren eine mRNA assoziiert ist, ein sog. „mRNP-Code“ entsteht, der das Schicksal der mRNA bestimmt. Viele der an der Regulierung und dem mRNA-Metabolismus beteiligten Proteine sind in Krankheiten betroffen und gerade neurologische Erkrankungen resultieren häufig von einem fehlerhaften mRNP-Code, der zu Veränderungen in der Regulation und Expression von mRNPs führt.

Im Zentrum dieser Arbeit stand ein trimerer Proteinkomplex, der aufgrund seiner Untereinheiten TDRD3, TOP3β und FMRP als TTF-Komplex bezeichnet wird. Biochemische Daten haben gezeigt, dass die drei Komponenten des TTF-Komplexes nucleo-cytoplasmatische „Shuttle“-Proteine sind, die sich im „steady-state“ hauptsächlich im Cytoplasma befinden, mit mRNPs assoziieren und vermutlich mit der Translation in Verbindung stehen. Unter zellulären Stressbedingungen konzentrieren sich die TTF-Komponenten in Stress Granula. Der TTF-Komplex ist damit Teil des mRNP-Codes, dessen zelluläre Ziel-RNAs und Funktion bislang aber völlig unbekannt sind. Da der Verlust von funktionellem FMRP zu der Ausprägung des fragilen X Syndroms (FXS) führt und TOP3β mit Schizophrenie und geistiger Retardation in Verbindung steht, verbindet der TTF-Komplex phänotypisch verwandte neuro-psychiatrische Krankheiten auf molekularer Ebene miteinander.

Das Ziel dieser Arbeit war es daher, den TTF-Komplex biochemisch zu charakterisieren und seine Funktion im mRNA-Metabolismus zu definieren. Im Zuge dieser Arbeit gelang der Nachweis, dass TDRD3 als zentrale Einheit des TTF-Komplexes agiert und sowohl FMRP als auch TOP3β direkt bindet. Die Interaktion von TDRD3 und TOP3β ist hierbei sehr stabil, FMRP ist hingegen eine dynamische Komponente. Interessanterweise wird der TTF-Komplex nicht direkt an mRNA gebunden, sondern über den Exon-Junction-Komplex (EJC) an mRNPs rekrutiert. Diese Interaktion wird durch ein spezifisches Bindungsmodul in TDRD3, dem sog. EBM vermittelt. In einer Reihe von biochemischen und systembiologischen Studien konnte das Interaktom des TTF-Komplexes bestimmt und seine Rolle im mRNA-Metabolismus definiert werden. Die Daten offenbarten, dass der TTF-Komplex primär mit „frühen“ mRNPs assoziiert ist und sehr wahrscheinlich an der „pioneer round of translation“ beteiligt ist. Weiterhin zeigte sich, dass TOP3β das Ribosom direkt bindet und somit eine Verbindung des EJC und der Translationsmaschinerie etabliert. Die Reduktion von Komponenten des TTF-Komplexes in

kultivierten Zellen führte zu selektiven Änderungen im Proteom, wobei einzelne Proteinteilgruppen, jedoch nicht die globale Expression durch den TTF-Komplex reguliert zu sein scheinen.

Die enzymatische Analyse von TOP3β hat darüber hinaus gezeigt, dass es sich um eine Topoisomerase vom Typ IA handelt, die nicht nur DNA sondern auch RNA angreifen kann. Dieser Aspekt ist besonders interessant im Zusammenhang der in dieser Arbeit aufgedeckten Verbindung von frühen mRNPs mit der Translation.

Die im Rahmen dieser Arbeit erhaltenen Daten legen nahe, dass der TTF-Komplex eine Rolle bei der Regulation des Metabolismus „früher“ mRNP-Teilgruppen möglicherweise im Zuge der „Pionierrunde“ der Translation spielt. Dabei ist die Verbindung einer RNA-Topoisomerase mit dem mRNA-Metabolismus bisher einzigartig und eröffnet so eine ganz neue Sichtweise auf die post-transkriptionellen Schritte der Genexpression und ihre Regulation.

3. Introduction

3.1. mRNA processing - an important step in the eukaryotic gene expression

The eukaryotic gene expression entails the translation of protein-coding genes into the corresponding proteins. The first step in this process is the transcription of the protein-encoding DNA sequence into a messenger RNA (mRNA) template. This entity then carries the genetic information into the cytoplasm where the translation into a protein occurs. As mRNA is transcribed by RNA polymerase II (RNAP II) into a non-translatable precursor mRNA (pre-mRNA), the transcript undergoes major processing steps before it reaches maturity and can serve as a coding template for translation (Figure 1). As soon as the 5' end of the pre-mRNA emerges from the RNAP II, the terminus receives a 7-methylguanosine (m7Gppp) cap. This modification is catalyzed by the capping enzyme machinery (Shatkin, 1976). Most eukaryotic protein-coding genes are segmented, so the nascent transcripts contain non-coding sequences (introns). These introns interrupt the open reading frame and need to be removed so that the coding segments (exons) can be ligated in frame. This process is referred to as pre-mRNA splicing and is catalyzed by the spliceosome, a macromolecular assembly of unprecedented complexity (Wahl et al., 2009). Finally, the 3' end of the nascent pre-mRNA is cleaved and a poly-adenosine (poly(A)) tail is added by the poly(A)-polymerase (PAP), whereupon the maturation of the mRNA will be completed (Proudfoot, 2011).

The nuclear mRNA maturation steps described above occur most likely co-transcriptional in an ordered fashion. This spatio-temporal regulation is orchestrated by post-translational modifications of the C-terminal domain (CTD) of the RNAP II. The CTD consists of numerous repeats of the heptameric sequence $Y_1S_2P_3T_4S_5P_6S_7$ in which the serine 2, 5 and 7 can be phosphorylated. The phosphorylation pattern of the serine residues changes along with the progressing RNAP II and thus allows recruitment of the different components of the processing machineries to the nascent pre-mRNA at different stages of transcription (Phatnani and Greenleaf, 2006). One processing event in turn can influence the other downstream processing events (Proudfoot et al., 2002).

mRNAs associate with a large variety of RNA-binding proteins (RBPs) at all stages of their lifecycle. As a consequence, mRNA maturation not only affects the mRNA sequences themselves but also determines the set of mRNA-associated proteins (Lee and Tarn, 2013). The resulting mRNA protein complexes (mRNPs) are the functional units that determine the fate of the corresponding mRNA (Gehring et al., 2017).

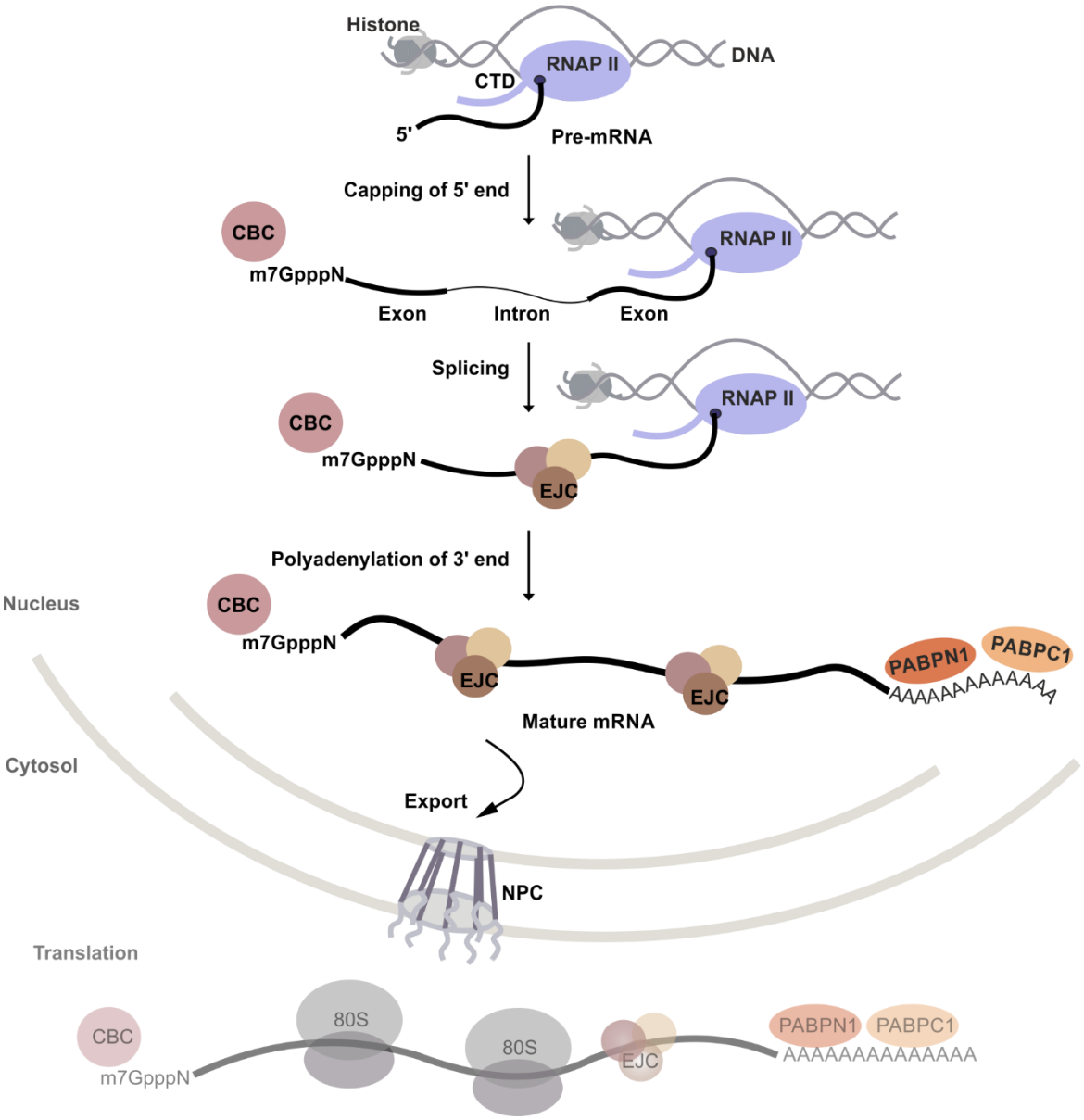

Figure 1: **The processing of pre-mRNA and generation of mature mRNPs as part of the eukaryotic gene expression.** The pre-mRNA is transcribed by the RNA polymerase II (RNAP II) and the nascent transcript is co-transcriptionally processed. Processing steps include the capping of the 5' end, removal of the introns by the spliceosome and cleavage and polyadenylation of the 3' end. The C-terminal domain (CTD) of the RNAP II recruits transcription and processing factors, and coordinates the progress of the transcription and processing. The mature mRNA is occupied with several proteins, such as the cap binding complex (CBC) at the m7Gppp-cap, the exon junction complex (EJC) upstream of exon-exon junctions and both the nuclear and the cytoplasmic version of the poly(A)-binding protein, PABPN1 and PABPC1, on the poly(A) tail. Such mature mRNPs can be exported into the cytoplasm and translated by the 80S ribosome into proteins.

3.2. The mRNP code regulates the post-transcriptional gene expression

Although the production of mRNA is in many cases regulated at the level of transcription in eukaryotes, it has become clear in the past years that regulation of gene expression does not stop at that point. As soon as the nascent transcript emerges from the RNAP II, mRNA-processing factors and mRNA-binding proteins as well as noncoding RNAs start to associate with the nascent transcript and form mRNPs. These mRNP components regulate and mediate the processing, monitor the correct maturation and determine the post-transcriptional fate of the corresponding mRNA. Depending on the composition of an mRNP different effectors "read" this mRNP code and initiate the respective downstream events in the determined lifecycle of the mRNP (Gehring et al., 2017).

The mRNP code consists of common and mRNP-specific factors

As described above, there are processing steps which every pre-mRNP must pass (Proudfoot et al., 2002) upon its maturation. As a consequence, common factors associate with every mRNP at a certain time point in the lifecycle of the mRNP. The 5' terminal cap of mRNAs associates with the cap-binding complex (CBC) consisting either of the nuclear cap binding proteins 1 (NCBP1, also CBP80) and 2 (NCBP2, also CBP20) or of the nuclear cap binding proteins 1 and 3 (NCBP3) in the nucleus (Gebhardt et al., 2015; Gonatopoulos-Pournatzis and Cowling, 2014; Izaurralde et al., 1994). In addition, every intron-containing mRNA associates with the spliceosome and undergoes the splicing reaction. The spliceosome leaves a mark 20-24 nt upstream of the newly emerged exon-exon junction (Le Hir et al., 2000). The core of this so called exon junction complex (EJC) consists of the four proteins eIF4AIII, MAGOH or MAGOHB, Y14 and BARENTZ (BTZ) (Ballut et al., 2005; Singh et al., 2013). The EJC core is assembled by the spliceosome around the DEAD-box helicase eIF4AIII which is bound in a sequence-unspecific manner to the RNA. In this position, eIF4AIII is fixed by a hetero-dimer consisting of Y14 and MAGOH. Eventually, the fourth protein BTZ binds both eIF4AIII and MAGOH as well as one nucleotide of the mRNA. Thus, BTZ stabilizes the complex and completes the core of the EJC (Ballut et al., 2005). This EJC core stays associated with the mRNA during export and the first round of translation, whereas various peripheral EJC proteins only associate with the common EJC core during certain steps of the early mRNA metabolism. For example, the variable integration of the peripheral proteins ACINUS or PININ into the complex is restricted to the nucleus, whereas NXF1 and NXT1 mediate the export of bulk mRNPs through the nuclear pore complex (NPC) and leave the EJC in the cytosol, while UPF2 joins the EJC at that point (Hir et al., 2016). Moreover, every poly(A)-tail which is added to the 3'end during the processing is bound by the poly(A)-binding proteins PABPN1 and PABPC1, respectively.

Apart from the common mRNP components, there are also factors that are only present in a specific subset of mRNPs. These include besides variable peripheral EJC proteins for example, regulators of

alternative splicing events such as SR proteins. SR proteins can bind in various combinations to exonic splicing enhancer (ESE) sites to determine the inclusion or exclusion of an exon upon splicing (Zhou and Fu, 2013). Another example of specific mRNP components are translation and turnover RBPs like the human antigen R (HuR). HuR binds to AU-rich elements in the 3' untranslated region (UTR) and thus regulates the translation efficiency and the stability of the corresponding mRNAs (Pullmann et al., 2007). Moreover, HuR can also recruit the export factor CRM1 to a subset of mRNPs to mediate their export apart from the common NFX1/NXT1 pathway (Delaleau and Borden, 2015).

Some of the described mRNP components bind directly to the mRNA. Their binding can depend on a specific sequence, for example, the binding of PABPC1 to the poly(A) stretch (Kühn and Wahle, 2004), or can occur independently of any sequence like the binding of the EJC core which is deposited 20-24 nt upstream of the exon-exon junction (Le Hir et al., 2000). Other components do not bind directly to RNA, but rather associate with the mRNP via binding to mRNA-associated proteins. The EJC core, for example, serves as a binding-platform for peripheral factors mediating the export, translation initiation or nonsense-mediated decay factors (Björk and Wieslander,2017).

Remodeling of the mRNP occurs during the first round of translation

Upon progression of an mRNP through its lifecycle, the composition of the mRNP changes and the mRNP is remodeled. This concerns not only the mRNA structure itself, which is changed upon pre-mRNA maturation, but also involves the complement of associated proteins and factors (Proudfoot et al., 2002). Upon co-transcriptional processing, certain proteins associate with emerging mRNP structures and therefore the mature mRNP exhibits a certain composition. This includes among other factors, the CBC at the 5' cap structure, the EJC complex deposited near the exon-exon-junctions and a mainly nuclear version of the PABP protein PABPN1 at the poly(A) tail, as mentioned above. The resulting mature mRNPs are called "early mRNPs" (Maquat et al., 2010) and are competent for export. The CBC, the transcription, splicing and 3' end processing together mediate the recruitment of the export complex (TREX complex) which then promotes the export of the early mRNP through the nuclear pore complex (NPC) via the NFX1/NXT1 export factor (Katahira, 2012; Lee and Tarn, 2013). This ensures that only mature mRNPs are exported. In the cytoplasm, early mRNPs usually engage a first round of translation, also referred to as the pioneer round of translation which remodels the mRNP once again (Figure 2) (Maquat et al., 2010b; Sato and Maquat, 2009). While the CBC, as part of the early mRNP, is required for the initiation of the pioneer round of translation, translation in the steady state mode requires the eukaryotic initiation factor 4E (eIF4E). The replacement of the CBC by eIF4E occurs in a translation-independent manner and is mediated by Importin-α, which associates with the cap-bound CBC. Subsequently, its binding to Importin-β induces the dissociation of the CBC from the 5' cap which is then occupied by eIF4E (Sato and Maquat, 2009). The first translating ribosome

displaces the EJC from the open reading frame (ORF) of the mRNP via interacting with the EJC removal factor PYM (Gehring et al., 2009). Furthermore, the mainly nuclear version of the poly(A)-binding protein PABPN1 is exchanged by the mainly cytosolic version PABPC1. This exchange also depends on the translation. Therefore, PABPN1, CBC EJC and possibly many more factors are only present in early mRNPs, whereas eIF4E is part of mRNPs that have already completed the pioneer round of translation (Hosoda et al., 2006; Sato and Maquat, 2009).

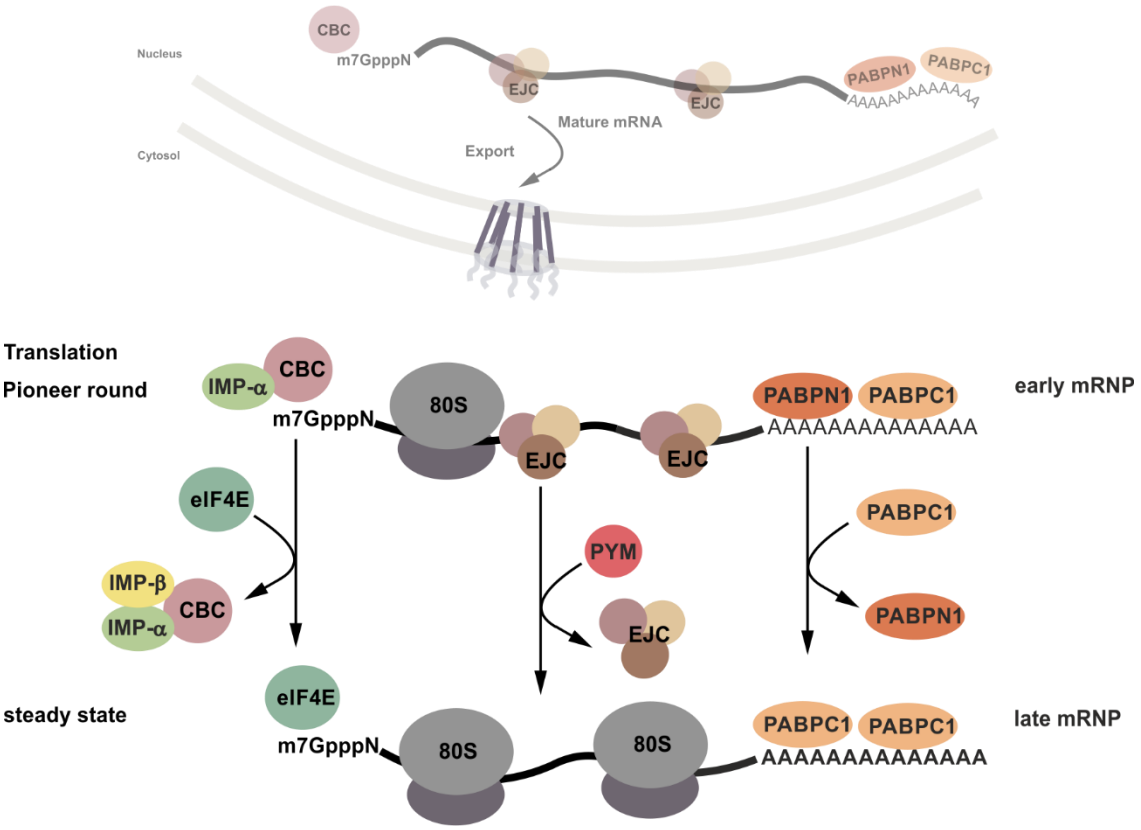

Figure 2: **Remodeling of the mRNP during the pioneer round of translation.** The cap binding complex (CBC) is replaced by the eukaryotic translation initiation factor 4E (eIF4E) via interaction with Importin-α (IMP-α) and Importin-β (IMP-β). The exon junction complex (EJC) is removed by the translating ribosome and the factor PYM. The nuclear version of the poly(A)-binding protein (PABPN1) is exchanged for the cytoplasmic version (PABPC1). After the pioneer round of translation, the steady state translation takes place, initiated by eIF4E. Adapted from (Maquat et al., 2010).

Remodeling enables specific functions related to the lifecycle of the mRNP

The mRNP composition determines the fate of the mRNP and the usual content of mature early mRNPs enables their export and mediates the first round of translation. Thereby, the exchange and removal of the factors specific for the early mRNPs that occur during this pioneer round of translation provide the opportunity for surveillance. Since the EJC is removed by the translating ribosome, a premature stop codon, which could e.g. result from an aberrant splicing event, provokes the release of the ribosome through translation termination before the ribosome could remove further downstream

EJCs. These left EJCs trigger the recruitment of the nonsense-mediated decay (NMD) machinery. The NMD presents a surveillance mechanism which ensures degradation of transcripts with a premature termination codon (PTC) and thereby prevents the synthesis of truncated translational products (Nicholson et al., 2010).

Many factors and mechanisms exist which regulate the metabolism of an mRNA and determine the fate of the mRNP. In the context of a cell or organism, the interplay of their regulations and the fine tuning of the proteomic output, especially in response to different stimuli, must be guaranteed to enable the correct function of the cell. With that, not only the general steps of the mRNA metabolism and their surveillance are important, but particularly selective mechanisms which involve only a subset of mRNAs play an important role.

3.3. mRNA-binding proteins

The mRNP code which executes and modulates the mRNA processing and determines the fate of the mRNP consists of small, non-coding RNAs, metabolites and a large number of proteins. Many of these proteins bind directly to the mRNA and therefore are referred to as mRNA-binding proteins (mRBPs).

The mRBPs contain one or several RNA-binding domains or motifs and often help to recruit further factors to the mRNP. Among the RNA-binding proteins there are proteins with canonical mRNA-binding domains, such as the RNA recognition motif (RRM), the heterogeneous nuclear RNP K-homology (KH) domain, the double-stranded RNA-binding domain (dsRBD), RNA-binding zinc-finger domains (ZnF), but also Arginine-Glycine-motifs (RGG/RG motifs), the oligonucleotide and oligosaccharide-binding fold (OB-fold) and numerous others (Castello et al., 2012; Douglas L. Theobald et al., 2003; Lunde et al., 2007; Thandapani et al., 2013). However, many RNA-binding motifs or domains can also account for other interactions than RNA-binding and there are several examples of annotated RNA-binding domains mediating protein-protein-interactions. For example, RGG/RG motifs bind not only to RNA, but also mediate protein-protein interactions upon methylation of the arginine residues. Typically these methylated arginines are recognized by Tudor domain containing proteins, as first shown for the interaction of the Tudor domain of the SMN protein with symmetrically dimethylated RG motifs found in some Sm-proteins (Brahms et al., 2001; Tripsianes et al., 2011). Remarkably, a rather large proportion of mRNP components which were recently identified as direct RNA binders lack any known RNA-binding motif (Beckmann et al., 2016). Therefore, it is challenging to identify RNA-binding proteins and even, if a protein contains an annotated RNA-binding domain, further validation will be necessary to confirm the RNA-binding of the domain in the cellular context of the protein.

3.4. The mRNA metabolism and neuropsychiatric diseases

Many diseases are caused by defects in the mRNA metabolism (Linder et al., 2015). These diseases can derive either from impaired processing, RNA modification or an incorrect mRNP code. Upon impairment of processing factors the maturation of the transcripts is affected in general at a certain processing step. In spinal muscular atrophy (SMA), for example, decreased levels of functional SMN protein (Lorson et al., 1998, 1999; Monani et al., 1999) affect the assembly of the spliceosome (Chari et al., 2008; Fischer et al., 1997; Meister et al., 2001). However, also the processing of single mRNAs can be affected, for example upon mutation of a processing consensus sequence in the mRNA such as the mutation of splice sites or poly(A) sites in the β-globin mRNA which causes β-thalassemia (Cao and Galanello, 2010).

RNA modifications of mRNAs can occur at specific sequences and are written, erased or read by specific enzymes and proteins. Therefore, single mRNAs or a subset of mRNAs can be affected at various steps of the mRNA metabolism, if the consensus sequence in an mRNA or the effector protein of this modification is impaired in a disease. For example, N6-methyladenosine (m^6A) modifications are frequently found with mRNAs. They can influence splicing, export, translation or stability of the mRNPs and the deletion or mutation of WTAP, a component of the m^6A methyltransferase complex, is linked to cancer (Maity and Das, 2016). Moreover, also mature ribosomal RNA (rRNA) and transfer RNAs (tRNAs) are modified. Therefore, the impairment of these modifications impacts either translation efficiency or accuracy in general or could affect only a subset of mRNPs with a specific codon frequency.

Recently, the mRNP code has gained importance as defects of components of the mRNP code cause a wide range of diseases and especially neurological manifestations are frequently linked to an aberrant mRNP code (Zhou et al., 2014).

Mutations in the *UPF3B* gene which encodes for an mRNP-associated protein involved in NMD lead to X-linked syndromic mental retardation (XLMR). Mutation-carriers often also exhibit, apart from intellectual disability, autistic phenotypes, childhood onset schizophrenia and attention deficit hyperactivity disorder (Addington et al., 2011; Laumonnier et al., 2010; Tarpey et al., 2007). In neuronal progenitor cells the absence of the UPF3B-associated NMD manifests as differentiation-deficits and affects neurite growth in hippocampal neurons (Jolly et al., 2013).

Fragile X mental retardation syndrome: mental retardation and mRNP code

The fragile X mental retardation syndrome (FXS) is another well studied neurodevelopmental disorder characterized by intellectual disability (ID). Notably, defects in only one gene which encodes for the fragile X mental retardation protein FMRP account for the FXS. In the most cases, the underlying impairment of the *FMR1* gene expression results from inherited CGG-repeat expansions adjacent to the promotor region. In the normal condition, about 30 repeats of the CGG-sequence are present at this region. In contrast, more than 200 CGG-repeat expansions are observed in FXS leading to epigenetic silencing of the *FMR1* gene during embryonic development (Oberle et al., 1991). 55-200 repeats are regarded as pre-mutation which usually expand to the FXS causing repeat level in the following generation when they are passed by a female pre-mutation carrier (Feng et al., 1995; Oberle et al., 1991). However, apart from the common CGG-repeat expansions, also missense mutations of the FMRP protein were identified which account for FXS in patients.

FMRP possesses two autosomal paralogues, the fragile-X related proteins 1 and 2 (FXR1 and FXR2). They share about 60% sequence identity to FMRP with high identity especially in the N-terminal part (Siomi et al., 1995; Zhang et al., 1995). In FXS patients, the expression level of these autosomal homologues is unaffected. However, they are unable to complement the loss of FMRP neurons (Coffee et al., 2010).

The phenotype of FXS patients often varies and can include, besides different ranges of intellectual and cognitive deficits, hyperactivity, socio-emotional disability and autism. Moreover, affected men typically present additional physical symptoms, like a long face with prominent chin and ears and macroorchidism (Chonchaiya et al., 2009). Analysis of FXS mouse models reveals alterations in the morphology of dendritic spines and indicates changes in the synapse development or function which may explain the neurological phenotype of FXS (Comery et al., 1997; Gatto and Broadie, 2009; Nimchinsky et al., 2001; van Spronsen and Hoogenraad, 2010).

The fragile X mental retardation protein FMRP – an mRNA-binding protein

The fragile X mental retardation protein is not only highly abundant in the brain and in neuronal cells, but is ubiquitously expressed in various tissues (Fagerberg et al., 2014). On the subcellular level, FMRP localizes mainly in the cytoplasm, but shuttles due to its nuclear localization signal (NLS) and a crm1-dependent nuclear export signal (NES) between nucleus and cytosol (Eberhart et al., 1996). Under stress conditions FMRP was found to concentrate in stress granules (SG). SG are cytoplasmic foci in which mRNAs are stalled together with initiation factors and several mRNA-associated proteins during the inhibition of translation initiation (Mazroui et al., 2002; Protter and Parker, 2016). FMRP harbors three canonical RNA-binding domains, two KH domains, named KH1 and KH2, as well as an RGG box, and binds to specific mRNAs (Ascano et al., 2012; Darnell et al., 2011; Siomi et al., 1993). Recently, a

third KH domain, named KH0, was discovered N-terminal of the other two KH domains. However, it is not clear whether it binds to RNA or DNA or if it is capable of both (Myrick et al., 2015a). In addition, the extreme N-terminus of FMRP contains two tandem agenet modules which form an aromatic cage in the fashion of a Tudor domain (Figure 3A). It has been proposed that these two modules bind to lysine methylations at the chromatin and function in the DNA damage response (Alpatov et al., 2014; Myrick et al., 2015a). However, other studies suggest that the N-terminal part of FMRP is rather responsible for other protein-protein interactions (Bardoni et al., 1999; He and Ge, 2017; Siomi et al., 1996).

In Addition, it has been shown that FMRP binds to its autosomal homologues FXR1 and FXR2 and FMRP was also found to homo-oligomerize (Ceman et al., 1999; Zhang et al., 1995).

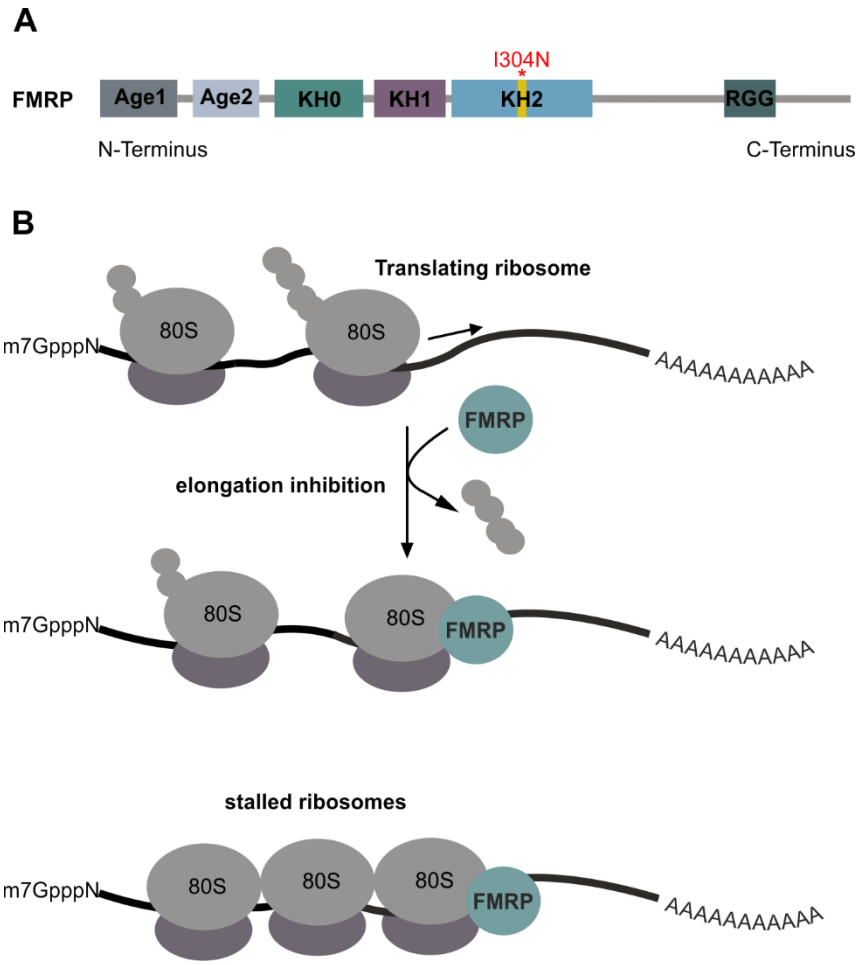

Figure 3: **The fragile X mental retardation protein FMRP. (A) The domain composition of FMRP**. The N-terminus of FMRP contains two tandem agenet domains (Age1 and 2) and a KH domain, termed KH0. The KH0 domain is followed by another two KH domains, the KH1 and KH2 domain. The KH2 domain contains the amino acid affected in the patient mutation I304N (marked in yellow). The RGG box resides in the C-terminal region of FMRP. Adapted from (Myrick et al., 2015a). **(B) FMRP as translational repressor.** FMRP plays a role as translational repressor in the mRNA metabolism by stalling elongating ribosomes. Adapted from (Harigaya and Parker, 2014).

In the past, many potential functions for FMRP as a component of specific mRNPs in the mRNA metabolism have been discussed, such as a role in the export, cytosolic localization, translation or stability of the corresponding mRNPs (Fridell et al., 1996; Ling et al., 2004; Zalfa et al., 2007). It was demonstrated that FMRP associates with polyribosomes (polysomes) and that it can repress the translation by stalling translating ribosomes (Darnell et al., 2011; Laggerbauer et al., 2001; Li et al., 2001; Stefani et al., 2004; Tamanini et al., 1996) (Figure 3B). Furthermore, FMRP was found to directly bind the 80S ribosome at the subunit interphase close to the central perturbance of the 60S subunit. Therefore, FMRP was proposed to interfere with the translation factor binding or to interact with the mRNA as potential mechanisms for its function as translational repressor (Chen et al., 2014).

As mentioned before, patients were described with FXS resulting from rare single point mutation (De Boulle et al., 1993; Myrick et al., 2014, 2015b). Of special interest for this work is a substitution of isoleucine 304 with asparagine (I304N) in the KH2 domain. The I304N mutant failed to form homo-oligomers *in vitro* and the ability to inhibit translation was shown to be affected in some cases (Laggerbauer et al., 2001). The I304N mutation was found to have only a slight influence on the RNA-binding ability of FMRP per se, even if the binding-selectivity varies for some sequences between the mutant and the wild type (wt) form (Ascano et al., 2012; Laggerbauer et al., 2001). However, the association with polysomes is disrupted by this mutation (Feng et al., 1997), whereas the direct binding to the 80S ribosome is not affected *in vitro* (Chen et al., 2014). Strikingly, the interaction with the Tudor domain containing protein 3 (TDRD3) which was identified as direct binding partner of FMRP (Linder et al., 2008) is completely abolished by the I304N mutation. This finding proposes an important contribution of this protein-protein interaction to the correct function of FMRP, especially in the context of FXS.

The TTF complex may provide a molecular link between FXS and schizophrenia

Investigation of the protein levels in the cerebella showed a reduction of FMRP also in some patients diagnosed with schizophrenia, bipolar disease or major depression in comparison to healthy controls (Fatemi et al., 2010). Moreover, recent functional investigations revealed that a subset of cellular FMRP forms a complex together with TDRD3 and the DNA topoisomerase III beta (TOP3β) at mRNPs (Goulet et al., 2008; Linder et al., 2008; Stoll et al., 2013; Xu et al., 2013). This complex, termed TTF (TDRD3, TOP3β, FMRP) complex, was not only detected in various human cells of non-neuronal tissues, but is also present in the mouse brain (Stoll et al., 2013). Finnish isolate studies revealed that the deletion or missense mutation of TOP3β is associated with the risk of schizophrenia and intellectual disability (Stoll et al., 2013) or autism (Iossifov et al., 2012; Xu et al., 2012). Therefore, the TTF complex

provides a potential molecular link between the fragile X syndrome and schizophrenia. However, at present the function of the TTF complex remains completely unknown.

The Tudor domain containing protein 3 (TDRD3) - a multidomain protein and component of the TTF complex

TDRD3 belongs to the family of Tudor domain containing proteins and members of this family are assigned to function in the mRNA metabolism (Ponting, 1997). The Tudor domain typically comprises about 60 amino acids and mediates usually protein-protein interactions via the recognition of arginine methylations (Côté and Richard, 2005). The Tudor domain of TDRD3 is located at the C-terminal part of the protein and adopts a 5-stranded β-barrel fold similar to the SMN Tudor domain structure. Nevertheless, it binds with higher affinity to asymmetrically dimethylated arginine residues (aDMA), unlike the SMN protein which prefers symmetrically dimethylated arginines (Liu et al., 2012; Sikorsky et al., 2012). It was shown that the TDRD3 Tudor domain can bind to aDMA marks on histone tails, more precisely the H3R17me2a and the H4R3me2a mark, and TDRD3 was proposed to acts as transcriptional coactivator (Yang et al., 2010). Moreover, there are reports that the Tudor domain of TDRD3 can specifically bind to an aDMA of the R1810 residue on the C-terminal domain of the transcribing RNA Polymerase II (Sikorsky et al., 2012; Sims et al., 2011).

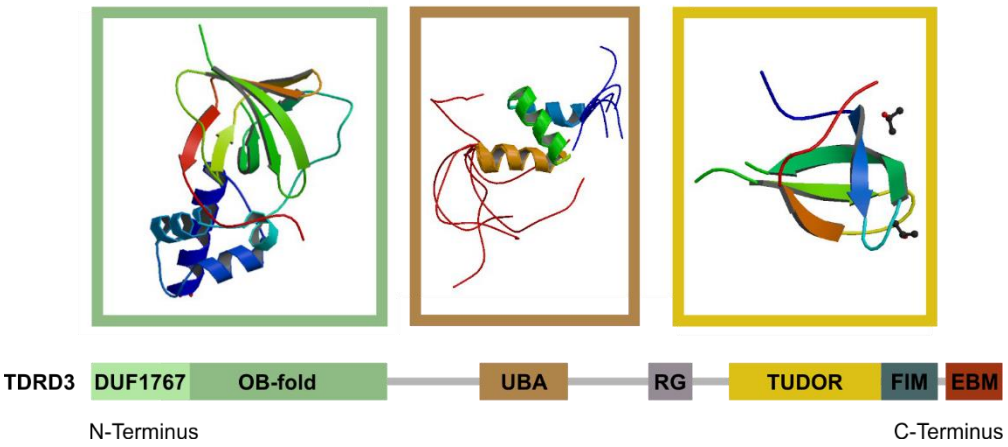

Figure 4: **The domain structure of TDRD3**. The N-terminal domain consists of an OB fold associated with a DUF1767 motif (light green frame, structure DOI: 10.2210/pdb5gvd/pdb), followed by an UBA domain (light brown frame, structure DOI: 10.2210/pdb1wji/pdb) and a predicted RG motif in the central part. In its C-terminus TDRD3 harbors a Tudor domain (yellow frame, structure DOI: 10.2210/pdb3s6w/pbd), the FMRP interaction motif (FIM) and an EBM.

Besides the Tudor domain, TDRD3 consists of multiple other domains and possesses a unique domain combination (Figure 4). The central part of the protein contains an ubiquitin binding associated (UBA) domain. It has been shown that the UBA domain of TDRD3 binds Lysine 48-linked tetraubiquitin *in vitro*, a modification which usually serves as a degradation signal (Linder et al., 2008). Moreover,

sequence analysis has identified a predicted RG motif in the central region of the protein (Thandapani et al., 2013). However, the function of these two motifs in the TDRD3 context remains unknown.

TDRD3 binds directly to FMRP and *in vitro* binding studies revealed that the binding occurs via a stretch of 20 amino acids adjacent to the Tudor domain in the C-terminal part (Linder et al., 2008) which was termed the FMRP interaction motif (FIM) (Stoll et al., 2013). In addition, a conserved EJC-binding motif (EBM) was identified in the extreme C-Terminus of TDRD3. It was shown that TDRD3 associates with the EJC proteins and strikingly also with mRNPs dependent on this motif *in vivo* (Kashima et al., 2010; Stoll et al., 2013).

In the N-terminus TDRD3 contains an OB fold domain combined with a DUF1767 motif which is homolog to the OB fold of the Topoisomerase III alpha (TOP3α)-interacting protein RMI1 (Goulet et al., 2008; Linder et al., 2008; Yin et al., 2005). TDRD3 was shown to co-immunoprecipitate with TOP3β in an RNase-insensitive manner and binding studies with *in vitro* translated TDRD3 truncations revealed that the binding to the topoisomerase occurs via the N-terminus of TDRD3 (Stoll et al., 2013).

TDRD3 is ubiquitously expressed and localizes mainly in the cytoplasm. Nevertheless, it shuttles between nucleus and cytosol in a CRM1 dependent manner due to its nuclear export signal (NES) (Goulet et al., 2008; Linder et al., 2008; Stoll et al., 2013). Also, it was found to co-localize with FMRP in SGs upon arsenic stress (Goulet et al., 2008; Linder et al., 2008) and associates with poly(A)-containing RNAs (Ahmad et al., 2017; Kashima et al., 2010; Stoll et al., 2013) and polysomes *in vivo* (Goulet et al., 2008; Linder et al., 2008). Interestingly, binding studies revealed that not only the EBM is important for the association of TDRD3 with mRNPs. *In vivo*, also the Tudor domain seems to play a role for the mRNP association of TDRD3 and its binding to FMRP although the binding ability per se to both mRNPs and FMRP is not influenced by the Tudor domain mutant, as shown by *in vitro* experiments (Stoll et al., 2013). These findings propose that TDRD3 is an mRNP-associated protein with a potential role in the mRNA metabolism like other Tudor domain containing proteins of this protein family. However, its multidomain composition which provides numerous interaction possibilities and the potential of their functional coordination within one single protein makes TDRD3 a unique member of this family. The function of TDRD3 remains elusive, though it is proposed to function as recruitment factor for the TTF complex which attaches the complex to selective mRNPs via interactions mediated by the Tudor domain and the EBM (Stoll et al., 2013).

The TTF component TOP3β – a curiosity among topoisomerases

Topoisomerases can help to maintain the genome stability by solving topological issues that typically occur on the DNA during transcription, replication, recombination and chromatin remodeling. The

catalytical mechanism of the topological conversion comprises a cycle of cleavage and re-ligation which allows the passage of another strand through the transient gap.

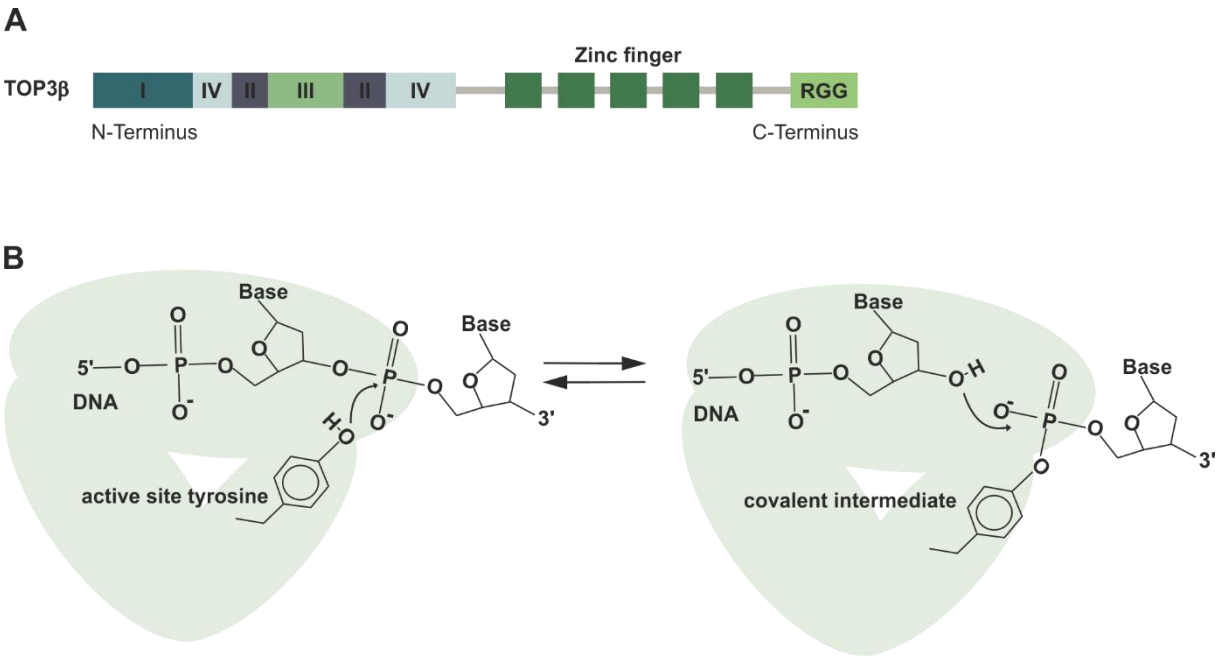

Figure 5: **The type IA topoisomerase TOP3β. (A) The domain structure of TOP3β**. The N-terminus contains the common catalytical core, the TOPO domain, divided into domain I-IV. The zinc finger motif and the RGG box reside in the C-terminus of TOP3β. Adapted from (Goto-Ito et al., 2017). **(B) The catalytical mechanism of type IA topoisomerases.** The active site tyrosine attacks the phosphate diesterbond of the nucleic acid (here depicted: DNA) and forms a covalent intermediate with the 5' end phosphate via a transesterification reaction, whereby the nucleic acid strand is cleaved. Upon attack of the 3' end hydroxyl group, the cleaved strand is re-ligated in a second transesterification. Adapted from (Viard and de la Tour, 2007).

The eukaryotic topoisomerase TOP3β is classified as type IA topoisomerase like its paralogue TOP3α (Bugreev and Nevinsky, 2009). Type IA topoisomerases are monomeric enzymes. The catalytical active core, the TOPO domain, is highly conserved among the representatives of this class, whereas the C-terminus highly varies both in size and sequence. In the case of TOP3β, the C-terminus contains besides a zinc finger motif also an RGG box (Figure 5 A) (Viard and de la Tour, 2007; Xu et al., 2013). Type IA topoisomerases cleave only one strand of the nucleic acid substrate to mediate the passage of the other strand. They can act both on single stranded (ss) or double stranded (ds) nucleic acids, but usually they require an exposed single stranded region in the substrate to exert their activity (Champoux, 2001; Wang, 1996). As the catalytical reaction consists of two transesterification reactions, no external energy in terms of ATP is necessary. In the first step, the hydroxyl group oxygen of the active site tyrosine attacks the phosphodiester in the nucleic acid back bone. Subsequently, a covalent ester bond between the 5' end of the phosphate group and the active site tyrosine is formed by the first transesterification reaction and a free hydroxyl group on the 3' end of the cleavage site is generated.

As a result, the 3' part of the nucleic acid is covalently bound to the enzyme in the intermediate state, whereas the 5' part is tightly but non-covalently attached. After strand passage, the gaped nucleic acid is re-ligated by the second transesterification reaction. At the re-ligation step, the oxygen of the free hydroxyl group of the 3' end on the 5' part of the gapped strand attacks the tyrosine-bound phosphate and resolves the covalent intermediate (Figure 5 B) (Viard and de la Tour, 2007; Wang, 2002).

TOP3β shares this catalytical mechanism with the other type IA enzymes and it has been shown that mouse and human TOP3β can relax hypernegatively supercoiled DNA (Seki et al., 1998; Yang et al., 2014). Additionally, the drosophila version was observed, apart from relaxing hypernegatively supercoiled DNA, to also cleave D-loops and R-loops *in vitro* (Wilson et al., 2000; Wilson-Sali and Hsieh, 2002). R-loops are hybrid structures in which one DNA strand of a dsDNA is replaced by a corresponding RNA strand, whereas in D-loops, the strand is replaced by another DNA strand, accordingly. D-loops can form during recombination and replication, while R-loops can arise during transcription due to negative supercoils behind the transcribing RNAP II which allow hybridization of a looping-back transcript (Wilson-Sali and Hsieh, 2002; Yang et al., 2014). Furthermore, it was shown that also human TOP3β can reduce the R-loop formation *in vitro*. TDRD3 helps to recruit TOP3β to the chromatin and as the R-loop formation was increased at TDRD3-target genes upon depletion of TDRD3, TOP3β is thought to prevent the formation of these R-loops by removing negative supercoils behind the transcribing RNAP II (Yang et al., 2014). However, if one takes a closer look at the cellular characteristics of the TOP3β topoisomerase several intriguing features attract the attention and especially distinguish this protein from other topoisomerases.

TOP3β shuttles due to its NES between nucleus, and cytoplasm and its main localization is in the cytosol. Moreover, TOP3β co-localizes with TDRD3 and FMRP in SGs upon arsenic stress. It has been shown that TOP3β is arranged together with FMRP and TDRD3 into the TTF complex and associates with mRNPs and polysomes. However, these associations depend on the presence of functional TDRD3 (Stoll et al., 2013; Xu et al., 2013). Based on these findings, doubts were raised whether TOP3β might not also play a role at different cellular processes, apart from relaxing hypernegatively supercoiled DNA during transcription (Yang et al., 2014). As briefly mentioned before, TOP3β can be also connected to neuronal disease: The deletion of the *TOP3β* gene as well as a single missense mutation causing an arginine 472 glycine (R472G) substitution in the protein were found to be connected with schizophrenia and intellectual disability, whereas other missense point-mutations of TOP3β were reported to be linked to autism (Iossifov et al., 2012; Stoll et al., 2013; Xu et al., 2012). Consistent with its relation to these neuronal disorders, aberrant neuromuscular junctions which have been described upon deletion of FMRP in *drosophila melanogaster* were also observed in a TOP3β null-mutant (Xu et al., 2013). Nevertheless, the potential cellular role of this mRNP-associated topoisomerase remains

completely elusive. Which functional importance results from the arrangement of this enzyme in a complex with TDRD3 and FMRP, which function has this complex and what function might each component adopt within the complex, how might the actions of the single TTF proteins be orchestrated and at which steps in the mRNA metabolism might the complex be involved are some striking questions that arise from these intriguing facts. It is therefore the aim of this work to biochemically characterize the TTF complex and to define its function in the mRNA metabolism. Moreover, to understand the role and the functioning of the TTF complex might also help to comprehend how the phenotypically related neuropsychiatric disorders schizophrenia and fragile X syndrome are linked on a molecular level.

4. Results

4.1. TDRD3 forms a complex with FMRP and TOP3β and binds directly to the EJC

The Tudor domain protein TDRD3 was identified as direct interactor of the FXS connected protein FMRP (Linder et al., 2008). Moreover, TDRD3 was found to associate with the topoisomerase TOP3β in an RNase insensitive manner and experiments with *in vitro* translated TDRD3 protein suggested that TDRD3 binds with its N-terminal DUF1767/OB fold domain to the topoisomerase (Stoll et al., 2013). Using an *in vitro* pull down assay with purified recombinant proteins I analyzed whether the interaction of TDRD3 with TOP3β is direct rather than mediated by other factors (Figure 6A). For this, both proteins were separately expressed and purified from *E. coli*. Both GST- and His-tagged TOP3β was immobilized on a glutathione Sepharose column (lane 3) and incubated with His-tagged TDRD3 (lane 1). The TDRD3-6xHis protein bound stoichiometrically to the immobilized GST-TOP3β-6xHis (lane 5) but not to immobilized GST-6xHis alone (lane 4). Thus, TDRD3 binds directly to TOP3ß.

TOP3β co-immunoprecipitates not only with TDRD3, but also with FMRP, and it was previously shown that their association is not mediated by RNA (Stoll et al., 2013; Xu et al., 2013). However, the interaction depends rather on the binding of TDRD3 to FMRP and TOP3β fails to associate with FMRP in the absence of TDRD3 (Stoll et al., 2013). These findings point strongly towards the formation of a complex of the proteins TDRD3, FMRP and TOP3β, whereat TDRD3 acts as an adaptor for the other two proteins. Indeed, this trimeric assembly, termed TTF complex, could be co-purified upon co-expression of the respective recombinant proteins in the baculovirus expression system (Figure 6B). For this experiment, Sf21 cells were co-transfected with a virus expressing GST-tagged TOP3β, a virus containing untagged TDRD3 and a virus with the FMRP-6xHis construct. To ensure that only the entire TTF complex rather than its individual subunits was isolated from the lysates of the expression culture, the proteins were purified first via the GST-tagged TOP3β using glutathione Sepharose followed by a second purification step via His-tagged FMRP using Ni-NTA (lane 1-12). With this strategy, all three proteins could be eluted stoichiometrically from the Ni-NTA column (lane 4-7) and the identity of each protein was verified via Western blot (Figure 6B, right panel, WB). This result confirms the formation of a stable hetero-trimeric TTF complex, whereat TDRD3 acts as bridging factor between FMRP and TOP3β. It further shows that no additional factor is required to mediate the observed interactions within the TTF complex.

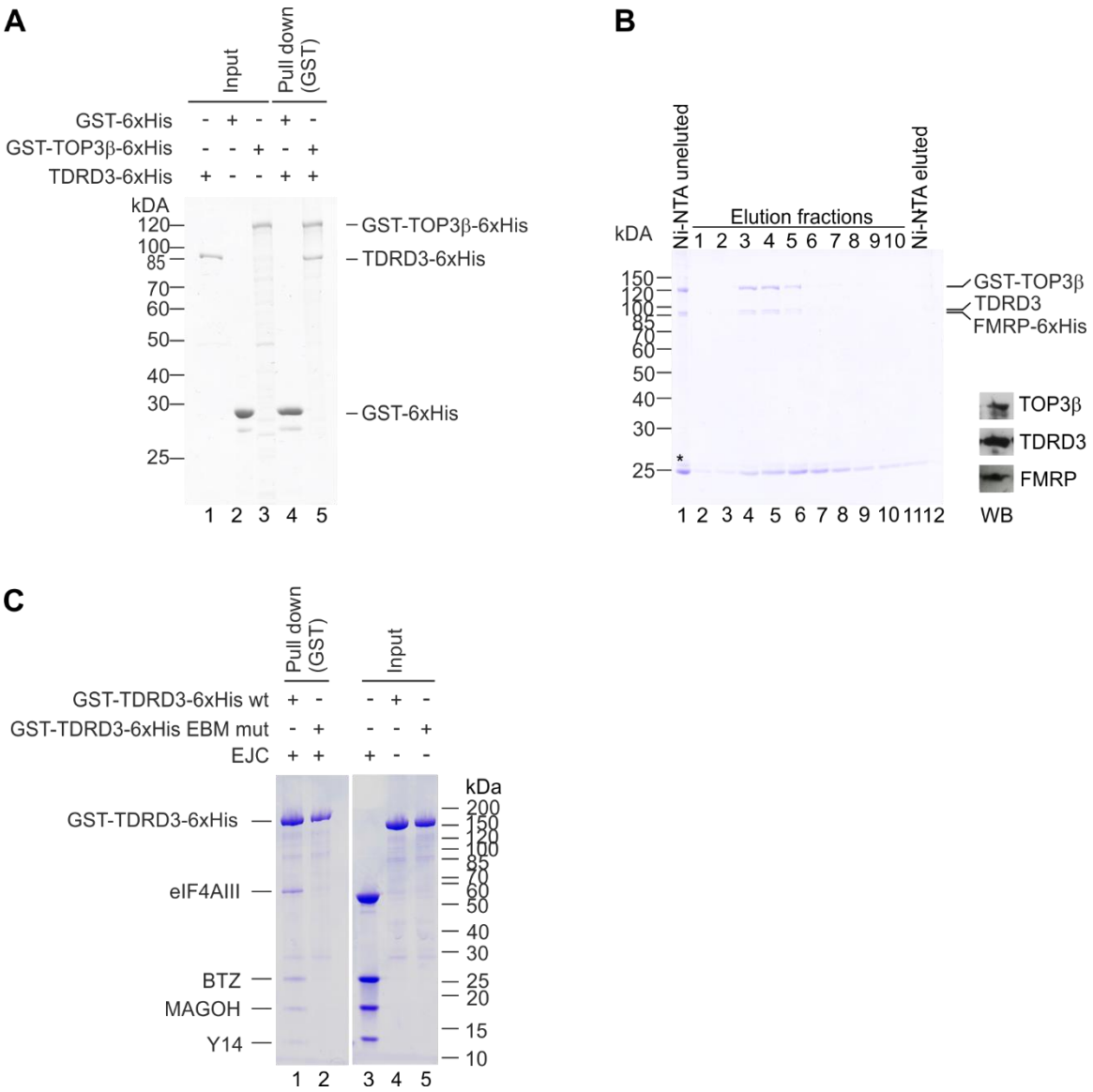

Figure 6: **Interaction network of the TTF complex. (A) TDRD3 and TOP3β are direct interactors.** Pull down assay with immobilized GST-TOP3β-6xHis. The input is shown in lane 1-3, respectively. Purified recombinant TDRD3 interacts stoichiometrically with immobilized GST-TOP3β-6xHis (lane 5) but fails to bind GST-6xHis alone (lane 4). **(B) Co-purification of TOP3β, TDRD3 and FMRP indicates the formation of the hetero-trimeric TTF complex.** GST-TOP3β, TDRD3 and FMRP-6xHis were co-expressed in Sf21 cells. The three proteins were co-purified first via glutathione Sepharose (not shown) followed by Ni-NTA (lane 1-12). The trimeric complex eluted stoichiometrically (lane 4-7) from the Ni-NTA column (column before elution in lane 1 and after elution in lane 12). The identity of each protein was confirmed via Western blot of the pooled peak-fractions (WB, right panel). The star marks unspecific protein-contaminations **(C) TDRD3 binds directly to the EJC.** Pull down assay with immobilized GST-TDRD3-6xHis wt or EBM mutant, respectively (lane 1 and 2). The input is shown in lane 3-5. Purified EJC consisting of eIF4AIII, BTZ, Y14 and MAGOH binds to the wt (lane 1), but not to the EBM mutant of GST-TDRD3-6xHis (lane 2).

Having established the mode of interactions that holds together the TTF complex, I next analyzed the association with mRNPs and the translation machinery. It was previously shown that a functional exon

junction binding motif (EBM) in TDRD3 was necessary not only for its own association but also for the association of TOP3β with mRNPs and polysomes (Stoll et al., 2013). Although TDRD3 associates with proteins of the EJC in co-immunoprecipitation experiments, this association is lost upon RNAse treatment (Kashima et al., 2010; Stoll et al., 2013). This might result from the disassembly of the EJC upon RNase digestion of the bound mRNA or it might occur because their interaction is only indirect and is bridged by the mRNA. To investigate, if TDRD3 binds directly to the EJC, a pull down assay with purified proteins was performed (Figure 6C). In this approach, recombinant wild type (wt) or EBM mutant GST-TDRD3-6xHis was immobilized on a glutathione Sepharose column (lane 4 and 5) and incubated with the purified EJC core complex assembled on a short RNA oligo (lane 3) which was a generous gift from Prof. Elena Conti (Max Planck institute for biochemistry, Martinsried). GST-TDRD3-6xHis wt bound the EJC core consisting of MAGOH, Y14, BTZ and eIF4AIII (lane 1), whereas the EBM mutant version failed to interact with the complex (lane2). These results provide evidence that the EJC directly binds to the TTF complex through the EBM present in TDRD3. The experiment revealed also that TDRD3 is capable of binding to the EJC core and that no additional peripheral EJC protein is required for this interaction.

4.2. Identifying the TTF complex interactome I: biochemical purifications

The experiments described in the preceding chapters illustrate the interaction network within the TTF complex and with the EJC. The TTF complex is believed to be recruited to mRNPs via TDRD3. Moreover, each TTF protein associates with polysomes (Stoll et al., 2013; Xu et al., 2013). In accordance with this finding, some common interactors were already identified for the three TTF components. Of note, most of them are mRNP-associated proteins or ribosomal components (Chen et al., 2014; Khandjian et al., 1996; Napoli et al., 2008; Singh et al., 2012; Stoll et al., 2013).

To obtain a first overview about the interactome of the TTF complex, anti-FLAG immunoprecipitation (IP) experiments of each TTF complex subunit were performed. For this purpose, stable cell lines were generated which express the N-terminal FLAG/HA-tagged protein of interest upon induction with tetracycline (Figure 7A). In brief, Flp-In T-REx 293 cells were co-transfected with a pFRT FLAG/HA vector containing the open reading frame (ORF) of the respective TTF protein adjacent to the N-terminal FLAG/HA-tag and the POG44 plasmid containing the FLP recombinase. Upon recombination, the protein of interest was integrated at the FRT (Flp recombination target) site with the promotor controlled by a tetracycline repressor element into the genome of the Flp-In T-REx 293 cells (see material and methods section for details). For IP experiments, the stable cell lines were grown to 50% confluency and the expression of the FLAG/HA-tagged TTF protein was induced with tetracycline. As a

control Flp-In T-REx 293 wt cells were grown and treated in an identical manner. Cells were lysed 14 hours after induction and IPs were performed using anti-FLAG antibody coupled agarose beads. The bound proteins were eluted with FLAG-peptide, and were separated by SDS-PAGE and visualized by silver-staining in the first approach (Figure 7B). The protein-bands of the immunoprecipitated FLAG/HA-tagged TTF proteins were clearly visible on the gel which confirms the efficient and specific IP procedure (marked by black arrows). Along with the FLAG/HA-tagged protein of interest, numerous additional factors were co-precipitated (lane 6-8) which were not visible in the control IP.

The comparison of the protein bands in the different IPs of FLAG/HA-TDRD3, -TOP3β and -FMRP displayed no major difference in the overall pattern of interactors. However, the intensity of the interactors in the FLAG/HA-TOP3β IP (lane 7) generally appears weaker compared to the the TDRD3 IP (lane 6) and to some extent also to the FMRP IP (lane 8). This observation suggests that interactors co-precipitate less efficiently with overexpressed FLAG/HA-TOP3β than with -TDRD3 and -FMRP.

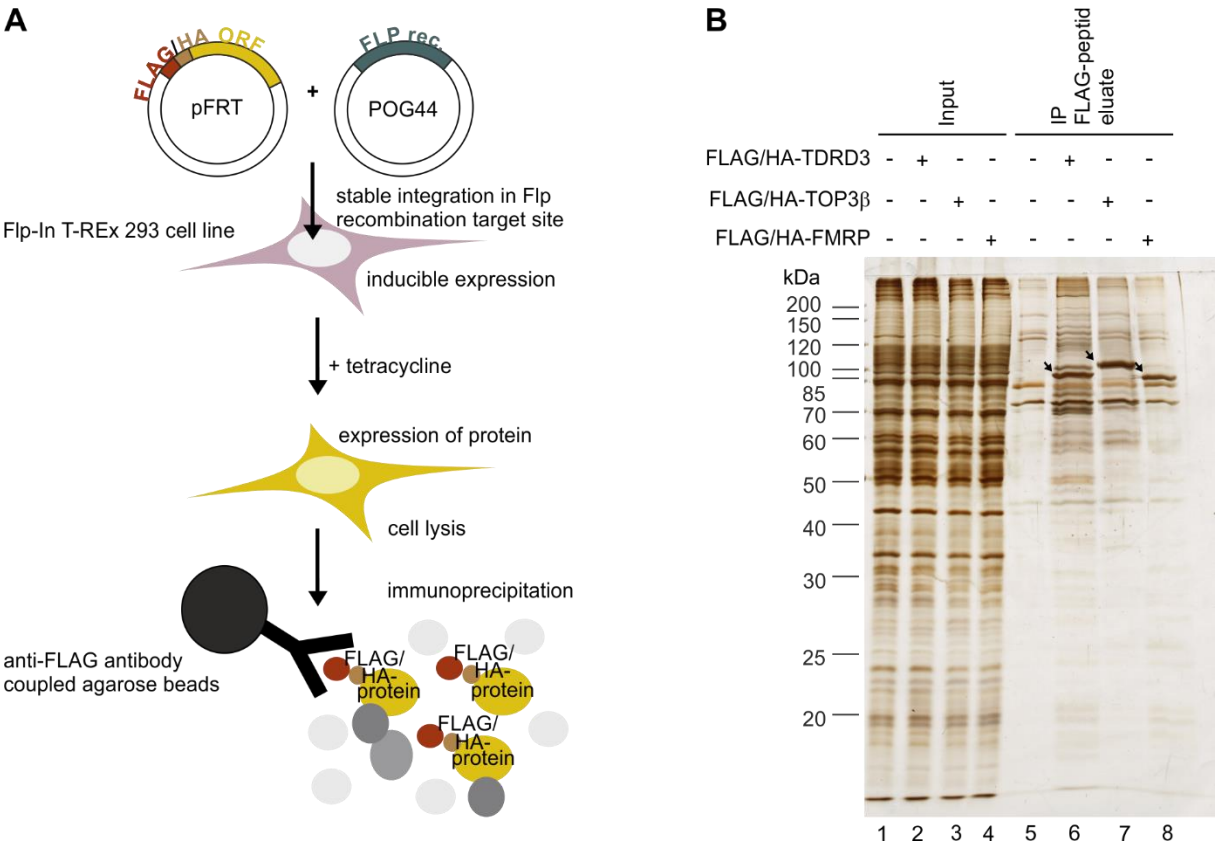

Figure 7: **Biochemical purifications of the TTF interactome. (A) Scheme of the generation of Flp-In T-REx 293 cell lines that stably express the FLAG/HA-tagged protein of interest upon induction and their use for anti-FLAG immunoprecipitations.** Flp-In T-REx 293 cells are co-transfected with a pFRT FLAG/HA vector containing the open reading frame (ORF) of the protein of interest and the POG44 plasmid containing the Flp recombinase gene. Upon recombination within the cells, the protein of interest

is integrated into the Flp recombination target site with the promotor controlled by the tetracycline repressor element in the host cell genome. Upon addition of tetracycline the expression of the FLAG/HA-tagged protein is induced. After the FLAG/HA-tagged protein was expressed for a certain period, cells are lysed and IP is performed using anti-FLAG agarose beads . **(B) Immunoprecipiations of the respective FLAG/HA-TTF proteins.** Silver-stained SDS-PAGE of the anti-FLAG IPs from stable Flp-In T-REx 293 cells expressing the respective FLAG/HA-tagged TTF protein or from Flp-In T-REx 293 wt cells for control, as indicated. The co-precipitated proteins were eluted via FLAG-peptide. The Input (0.5%) is shown in lane 1-4, respectively. The immunoprecipitated FLAG/HA-proteins are marked by arrows.

4.3. Identifying the TTF complex interactome II: mass spectrometric analysis

The identification of the proteins associated with the TTF complex and its corresponding mRNPs are expected to provide insight into the composition of the mRNPs and into its mode of action.

To obtain a full proteomic dataset of the proteins associated with the TTF complex, all proteins which co-immunoprecipitated with the FLAG/HA-tagged TTF proteins were identified by mass spectrometry. These studies were performed in triplicates to ensure the reproducibility of the obtained data set. The mass spectrometry analysis of the samples as well as the bioinformatic and statistical evaluation of the data were performed by Dr. Jens Vanselow (AG Schlosser, Rudolf-Virchow Center of Würzburg, Proteomics unit).

In Addition, for the anti-FLAG IP of FLAG/HA-TDRD3 a fourth approach in which the stable isotope labeling by amino acids in cell culture (SILAC) technique was used was included in the analysis to provide more sensitivity in the detection of the proteins enriched in the IP over the control. For this, the FLAG/HA-TDRD3 expressing cells were grown in media containing only stable heavy isotope-labeled lysine and arginine residues. These heavy amino acids then were integrated into the proteins produced in these cells over six passages. After performance of the IP, the eluate was equally mixed with the eluate of a control IP from Flp-In T-REx 293 wt cells which were grown in medium containing only light amino acids prior to the analysis. After performance of the mass spectrometry, the ratio between heavy and light peptides was calculated.

The median enrichment of proteins in the respective anti-FLAG IP experiments of FLAG/HA-TDRD3, -TOP3β and -FMRP was calculated in comparison to the control IP and depicted in a scatter plot diagram, respectively (Figure 8A-C).

The analysis revealed that 265 associated proteins were significantly enriched in the IP of overexpressed FLAG/HA-tagged TDRD3 (Figure 8A, colored dots). Especially the SILAC approach in

addition to the three normal IP experiments provided a very good sensitivity and contributed to the faithful detection of the proteins which co-immunoprecipitated with FLAG/HA-TDRD3. Among these interactors, TOP3β as well as FMRP are highly enriched which is in accordance with the formation of the TTF complex. A gene ontology (GO) term analysis revealed that mainly ribosomal proteins, mRNA-binding and mRNP-associated proteins, proteins localized in the cytoplasm as well as proteins involved in translation are associated with FLAG/HA-TDRD3 (see Figure 19 in the supplementary information). These findings are also consistent with our previous finding that TDRD3 associates with mRNPs and polysomes (Stoll et al., 2013).

The analysis of the proteome of FLAG/HA-tagged TOP3β showed a very similar set of co-precipitated factors (Figure 8B). As expected, TDRD3 and FMRP are among the most highly enriched interactors. However, their enrichment is generally lower than in FLAG/HA-TDRD3 IPs. Accordingly, only 121 high confidence interactors were found in the FLAG/HA-TOP3β IP. This result is also consistent with a less efficient co-IP of the interactors as became already evident in the silver-stained SDS-PAGE of the IP. Nevertheless, the GO term analysis of the enriched interactors along the same lines as described above gave a very similar result as in the case of TDRD3 (see Figure 19 in the supplementary information).

The analysis of the proteome of FLAG/HA-tagged FMRP likewise showed a very similar set of co-precipitating factors as compared to TDRD3 and TOP3ß. Although FMRP shares most of its identified 183 interactors with TDRD3 and TOP3β, the distribution of the enrichment shows a slightly different pattern regarding the two other TTF components (Figure 8C). Although TDRD3 and TOP3β are among the identified proteins, their enrichment is lower than the enrichment of many other interactors, and the enrichment of TDRD3 is not even statistically significant in this analysis. This observation is consistent with the finding that FMRP is the most abundant component of the TTF complex which associates also with non-TTF mRNPs and has also TTF-independent functions (Stoll et al., 2013). Nevertheless, the GO term analysis of the FMRP interactors reveals the enrichment of the same major terms as were enriched for the interactors of TDRD3 and TOP3β (see Figure 19 in the supplementary information).

All in all, among the interactors which have been identified in the IPs of the individual TTF components, there are 110 significant interactors that were common for all three TTF proteins. This strongly suggest that the TTF complex constitutes a functional unit acting in a specific cellular pathway.

Bioinformatic analysis of the TTF complex proteome

To identify (the) pathway(s) in which the TTF complex plays a role, we performed a detailed bioinformatics analysis of common and specific interactors of the TTF complex and its individual

components. These studies were performed together with Dr. Jens Vanselow (AG Schlosser, Rudolf-Virchow Center of Würzburg, Proteomics unit).

In the analysis, the significant interactors were grouped dependent on the IP experiments they were enriched in (Figure 8D). The proteins which were not significantly enriched in any of the IP experiments compared to the control were regarded as unspecific background proteins (423 proteins represented by the first column).

Common interactors of the TTF components

There are 110 interactors significantly enriched in the IPs of all three TTF proteins (Figure 8D, red column, Table 1). Among these, there are the autosomal homologs of FMRP, FXR1 and FXR2, which are already known to directly interact with FMRP and TDRD3 (Laggerbauer et al., 2001; Linder et al., 2008). Also, numerous ribosomal proteins, which account for almost half of the enriched interactors, and mRNA-binding proteins, like the already identified interactor PABPC1, but also PABPC4, LARP4 and LARP1, associated significantly with each TTF protein (see Table 1 in the supplementary information).

In addition, the EJC core protein MAGOHB as well as proteins of the peripheral EJC PININ (PNN) and ACINUS (ACIN1) which are restricted to the nucleus and involved in splicing (Hir et al., 2016; Rodor et al., 2016; Wang et al., 2002) were found in the IPs of the TTF proteins.

Interactors of one or two individual TTF components

Amazingly only a few factors turned up in the proteomics study that were specific for only one or two TTF components (see Table 1 in the supplementary information).

There are 11 interactors which were significantly enriched with the IP of FLAG/HA-TDRD3 and -TOP3β, but were not significantly associated with FLAG/HA-FMRP in the experiments (Figure 8D, fourth column). Among these proteins, there are the other proteins of the EJC core, eIF4AIII, Y14 and BTZ. However, it was shown in the past that FMRP associates with the EJC (Singh et al., 2012) and the statistical cut-off likely underestimates the associated factors. The recently identified cap-binding complex protein NCBP3 was also among the 11 proteins which are significantly enriched only in the IPs of FLAG/HA-TDRD3 and -TOP3β. On a side note, CBP80 (NCBP1) and CBP20 (NCBP2) which were already identified as interactors of TDRD3 and TOP3β (Stoll et al., 2013) were among the proteins that associated with all TTF proteins, however they are not ranged as significantly enriched in the samples and were therefore grouped as unspecific background proteins in the classification (Figure 8D, first column).

Only 14 proteins were found to associate with FMRP but not with TDRD3 or TOP3β. These include the ubiquitin-associated protein 2 like (UBAP2L) and Nucleophosmin (NPM1). Only one protein, the serine-threonine kinase RIOK1, was found to be enriched with FMRP and TOP3β, but not with TDRD3 and it

is likely that this protein appeared non-specifically in the IP experiment. This is consistent with the fact that TDRD3 is the bridging factor between FMRP and TOP3β and mediates their association (Stoll et al., 2013).

Nine proteins are only associated with TOP3β and among them are, for example MMS19 and CIAO1, components of the cytosolic iron-sulfur protein assembly complex, and the tyrosine phosphatase PTPN13. However, the potential role of their association with TOP3β is not clear.

Interestingly, TDRD3 and FMRP show a slightly higher number of common interactors (i.e. 58) which were not found to be associated with TOP3β. These include the RNA helicase DDX5 and Argonaut-2 (AGO2) that have already been shown to associate with FMRP previously (Ishizuka et al., 2002) as well as the stress granule assembly factor G3BP1. Of note, these factors all play a role in the mRNA metabolism which fits well with the proposed function of these proteins.

Surprisingly, the initiation factor of the cap-dependent steady state translation eIF4E was not found in any IP of the TTF proteins and was not even detected at rather low levels, like some proteins ranged as unspecific background in the IPs, although there were reports that FMRP co-immunoprecipitates with eIF4E in the mouse brain (Napoli et al., 2008).

Functional analysis of the TTF interactome

Next, a bioinformatic GO term analysis was used to gain insight into potential cellular pathways involving the TTF complex. For this purpose, the proteins are generally classified according to their biological function and pathways and receive the respective gene ontology (GO) terms. In the analysis, the enrichment of Go terms among the group of significant interactors was determined, though redundant terms were manually excluded.

The GO term analysis of the common TTF-associated proteins (Figure 8E) clearly identifies the translation machinery as the cellular pathway of TTF action. GO terms that score high are the cytosolic ribosome, cytosolic part, poly(A) RNA-binding and translation. The enrichment of these terms among the common TTF interactors illustrates also the described association of the TTF proteins with mRNPs and polysomes (Khandjian et al., 1996; Linder et al., 2008; Stoll et al., 2013; Tamanini et al., 1996; Xu et al., 2013) and reflects also the same major terms as found in the analysis of interactors for each individual TTF protein (Figure 19).

The overall analysis of the interactome of the TTF components revealed that TDRD3, TOP3β and FMRP share most of their interactors and it is likely that they act as one complex at the translational machinery in the mRNA metabolism. Nevertheless, FMRP is also part of other mRNP complexes independently of TDRD3, but was found in this analysis to interact with only surprisingly a few factors, which were not also found to interact with TDRD3 and TOP3β.

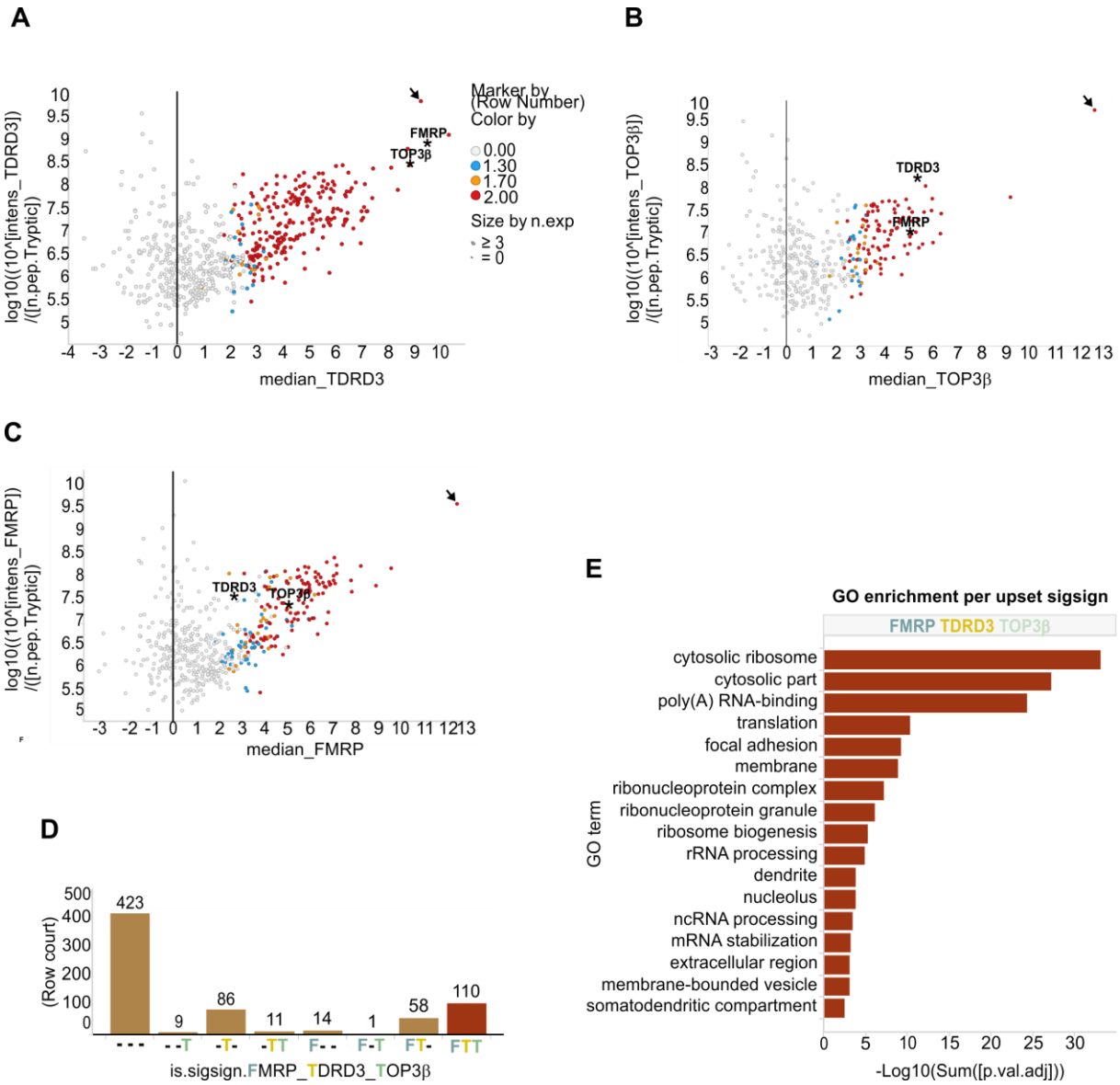

Figure 8: **Analysis of the mass spectrometry data of the anti-FLAG immunoprecipitation (IP) experiments from Flp-In T-REx 293 FLAG/HA-TDRD3, -TOP3β and -FMRP cells.** The co-immunoprecipitated proteins were eluted with FLAG-petide and analyzed via mass spectrometry. **(A) Proteins identified in the FLAG/HA-TDRD3 IP in four independent experiments are plotted against the proteins in the respective Flp-In T-REx 293 control IPs.** In one IP approach, proteins were labeled with SILAC. Cells expressing FLAG/HA-TDRD3 were labeled with heavy isotope-containing amino acids, Flp-In T-REx 293 control cells with light amino acids. **(B) Proteins identified with FLAG/HA-TOP3β in three independent IP experiments are plotted against the proteins in the Flp-In T-REx 293 control IP. (C) Proteins identified in the FLAG/HA-FMRP IP in three experiments are plotted against the proteins in the Flp-In T-REx 293 control IP.** (A-C) The statistical classification of interactors is indicated by color. Grey dots (0.00): no significant enrichment (p-value >0.05); blue (1.30): slightly enriched (p-value <0.05 and >0.02); orange (1.70): enriched (p-value <0.02 and >0.01); red (2): strongly enriched (p-value <0.01). The size of the dots indicates the number of experiments in which the protein was detected. The arrows mark the immunoprecipitated protein in the respective experiments, stars mark the other two associated TTF components, accordingly. **(D)**

Classification of the TTF interactors based on their significant enrichment in the respective IP experiments. The columns represent the proteins which were significantly enriched in the respective IPs: yellow T: FLAG/HA-TDRD3; light green T: FLAG/HA-TOP3β; blue F: FLAG/HA-FMRP; and the combination thereof accordingly. The first column marked with three dashes contains unspecific background proteins and interactors which were not significant in the TTF IPs. The red column represents the proteins which were significantly associated with each of the TTF proteins and are further analyzed in (E). **(E) GO term enrichment analysis of the common TTF interactome.** Redundant GO terms like mRNA-binding and poly(A)-binding were manually excluded from the analysis.

Validation of the TTF proteomics analysis

The proteomic dataset obtained via mass spectrometry analysis provided a good insight in the full interactome of the TTF complex proteins. However, the measurements might have not always been completely accurate and the range of significance of the interactors was set via statistical methods. This enables in principle an under- or overestimation of the identified interactome or individual interactors. Therefore, the obtained dataset needs to be validated for single interactors using an independent method. For this, the anti-FLAG IP experiments were repeated, and selected candidates were analyzed via WB (Figure 9C).

PABPC1 is already known to associate with the TTF proteins via the mRNA (Napoli et al., 2008; Stoll et al., 2013). As PABPC1 could be detected in each IP via WB (Figure 9C), it was proven that intact mRNPs with their corresponding protein-content could be precipitated in this experiment along with the TTF proteins. In the proteomic analysis of the interactome, MAGOHB but not its homologue MAGOH has been identified. However, both proteins share 87% identical amino acids and the monoclonal anti-MAGOH antibody which was used in the past to detect MAGOH in TDRD3 IPs (Stoll et al., 2013) likely recognizes both MAGOH and MAGOHB, as it was raised against the full length protein. Therefore, it was also used in this experiment to confirm the interaction with MAGOHB and indeed MAGOH/MAGOHB could be detected with each TTF protein in the WB. Furthermore, CBP20, which is known to associate with TDRD3 (Stoll et al., 2013), could also be identified as interactor of TOP3β and FMRP, even though their association with this protein was not ranged as significant in the mass spectrometry analysis.

Among the newly identified significantly enriched proteins in the IP experiments, the interaction with LARP1, LARP4 and the ribosomal proteins rpS6 which is part of the small subunit of the ribosome and rpL7 which is part of the large subunit was tested via WB. Their association could be confirmed for each FLAG/HA-tagged TTF protein, respectively. However, the association with the mRNA-binding proteins and also with ribosomal proteins, even though to a lesser extent, was generally much stronger for FLAG/HA-TDRD3 than for FLAG/HA-TOP3β. This is consistent with the reduced intensity of the interactors in the FLAG/HA-TOP3β IP that was already observed in the mass spectrometry analysis and

in the silver-stained SDS-PAGE (Figure 7B compare lane 6 and 8, Figure 8B, Figure 9B) of the co-precipitated interactome.

Notably, the association of FMRP with PABPC1 and LARP4 was relatively prominent, whereas its association with CBP20, LARP1 and MAGOH was rather weak. This finding could reflect the association of FMRP with different mRNP subsets or at different stages in the mRNA metabolism, independently of TDRD3.

Since eIF4E unexpectedly was not detected at all in the mass spectrometry, its association was also tested via WB. Although the eukaryotic translation initiation factor was clearly detectable in the input of the IP, eIF4E could also not be detected in any of the IPs via WB.

4.4. TDRD3 associates with mRNPs and polysomes independently of its interaction with TOP3β and FMRP

TDRD3 was shown to mediate the association of TOP3β with mRNPs and polysomes and is also likely to recruit FMRP to the TTF-containing mRNPs (Stoll et al., 2013). The next question that I addressed was whether the assembly of the TTF complex is important for the association of TDRD3 itself with the mRNPs and might impact the mRNP composition. This was tested using stable cell lines expressing FLAG/HA-tagged wild-type and deletion mutants of TDRD3.

A cell line expressing FLAG/HA-TDRD3 lacking the NTD, the interaction motif for TOP3β, was used to test the impact of TOP3β on the binding pattern of TDRD3. To abolish its interaction with FMRP, the FMRP interaction motif (FIM) of TDRD3 was deleted. Lastly, a cell line expressing a double deletion mutant lacking both the NTD and the FIM was examined. The respective cell lines were used for anti-FLAG co-IP experiments to investigate the respective domains for their influence on the TDRD3-interactome.

The anti-FLAG IP eluates from the different cell lines were separated by SDS-PAGE and visualized via silver-staining. The respective bands of the overexpressed and precipitated FLAG/HA-TDRD3 wt, ΔNTD, ΔFIM or ΔNTD ΔFIM proteins were clearly visible in the silver-stained gel (Figure 9B, lane 9-12, marked by arrow). This shows, that the FLAG/HA-TDRD3 deletion mutants were precipitated efficiently and in equal amounts as compared to the full length TDRD3 protein (wt). Surprisingly, the overall protein patterns were very similar among the different IPs. This suggests, that the association of TDRD3 with mRNPs and the translation machinery is not or only marginally dependent on its interaction with TOP3β or FMRP.

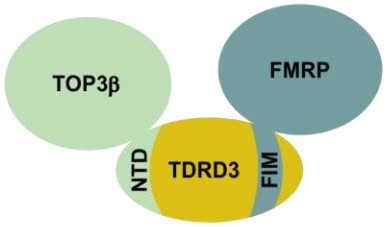
A
TOP3β
FMRP
NTD
TDRD3
FIM

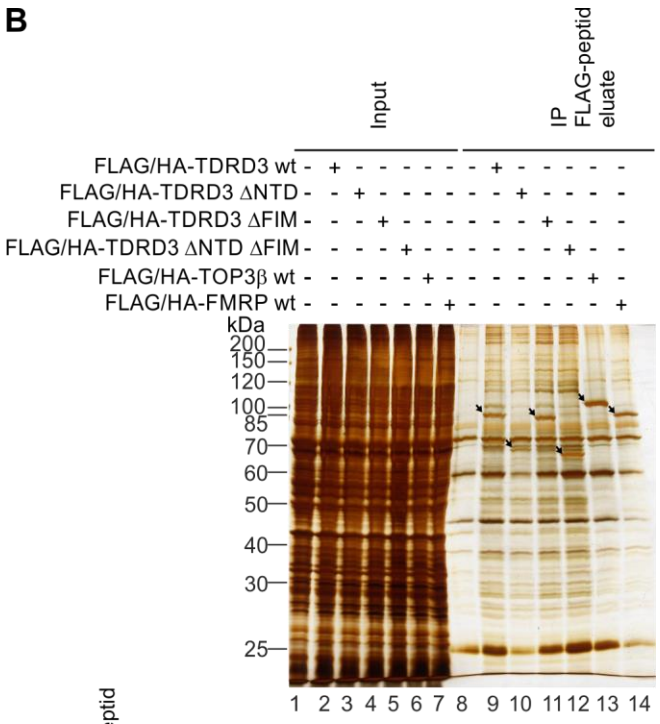
B
Input
IP FLAG-peptid eluate
FLAG/HA-TDRD3 wt
FLAG/HA-TDRD3 ΔNTD
FLAG/HA-TDRD3 ΔFIM
FLAG/HA-TDRD3 ΔNTD ΔFIM
FLAG/HA-TOP3β wt
FLAG/HA-FMRP wt
kDa
200
150
120
100
85
70
60
50
40
30
25
1 2 3 4 5 6 7 8 9 10 11 12 13 14

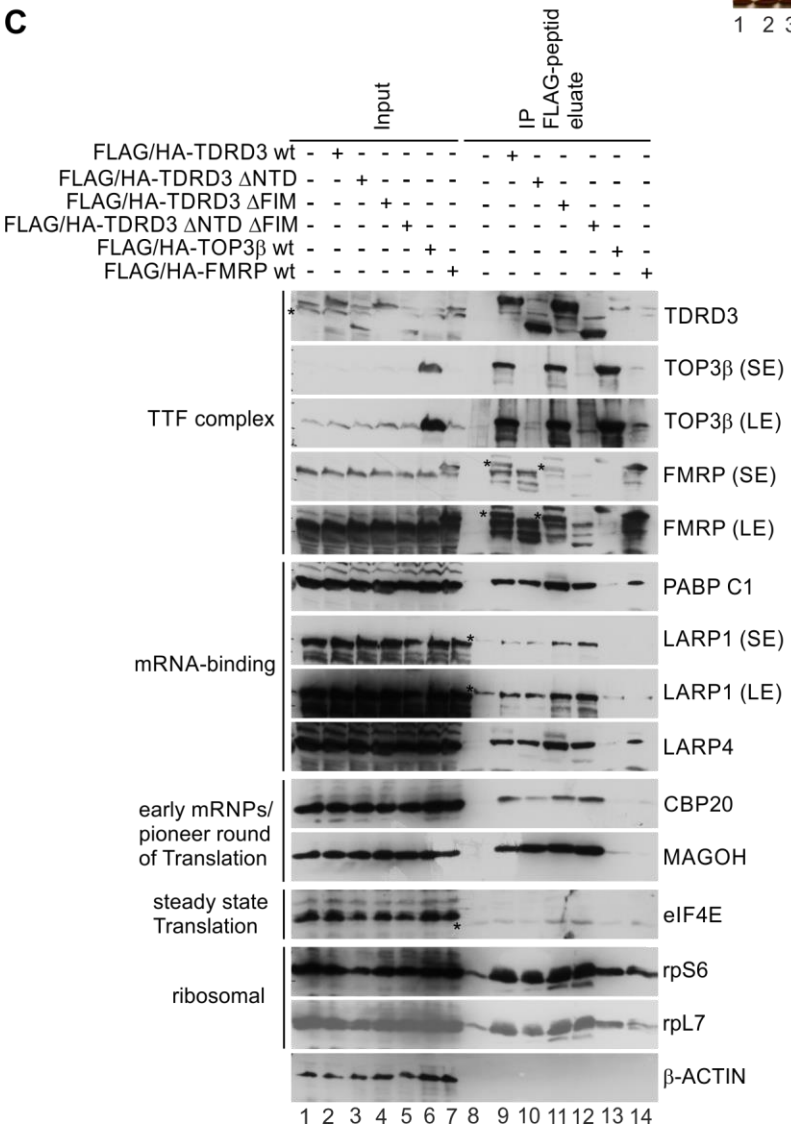
C
Input
IP FLAG-peptid eluate
FLAG/HA-TDRD3 wt
FLAG/HA-TDRD3 ΔNTD
FLAG/HA-TDRD3 ΔFIM
FLAG/HA-TDRD3 ΔNTD ΔFIM
FLAG/HA-TOP3β wt
FLAG/HA-FMRP wt
TTF complex
mRNA-binding
early mRNPs/ pioneer round of Translation
steady state Translation
ribosomal
TDRD3
TOP3β (SE)
TOP3β (LE)
FMRP (SE)
FMRP (LE)
PABP C1
LARP1 (SE)
LARP1 (LE)
LARP4
CBP20
MAGOH
eIF4E
rpS6
rpL7
β-ACTIN
1 2 3 4 5 6 7 8 9 10 11 12 13 14

Figure 9: **The interaction of TDRD3 with TOP3β and FMRP has no influence on its association with mRNPs. (A) Internal interaction map of the TTF complex.** TDRD3 interacts with TOP3β via its N-terminal domain (NTD) consisting of a DUF1767 domain associated with an OB fold domain. The interaction with FMRP occurs via the FMRP interaction motif (FIM) in the C-terminal part of TDRD3. **(B,C) The loss of the interaction with TOP3β and FMRP has no apparent influence on the overall association of FLAG/HA-TDRD3 with mRNPs (B) Silver-stained SDS-PAGE of FLAG-eluted TTF proteins or interaction mutants thereof after anti-FLAG IP.** The anti-FLAG IPs were performed using stable Flp-In T-REx 293 cell lines expressing FLAG/HA-tagged TDRD3 wt or with deletion of the NTD (ΔNTD), the FIM (ΔFIM) or both (ΔNTD ΔFIM) or cells expressing FLAG/HA-TOP3β wt or -FMRP wt or Flp-In T-REx 293 wt cells as control. The silver-stained SDS-PAGE shows the FLAG-peptide eluates after IP. The Input (0.5%) is shown in lane 1-7. The arrows mark the respective bands of the immunoprecipitated proteins. **(C) Immunoblotting of selected TTF interactors in the IP experiments of the FLAG/HA TTF proteins.** The association with selected common interactors of the TTF components was checked on WB (Lane 8,9,13 and 14) of the respective anti-FLAG IPs (same as in B). Stars mark cross-reactions of the antibodies and residual signals of proteins which have been detected on the membrane before. For some interactors, a shorter exposure (SE) and a longer exposure (LE) is depicted, respectively.

To verify the loss of the interaction with TOP3β or FMRP, the precipitated proteins were initially analyzed via immunoblotting. As expected, both mutants lacking the NTD (FLAG/HA-TDRD3 ΔNTD and ΔNTD ΔFIM) failed to interact with TOP3β (Figure 9C, lane 10 and 12), whereas TOP3β precipitates with FLAG/HA-TDRD3 wt and the FIM deletion mutant in equal amounts (lane 9 and 11). Likewise, the deletion of the FIM in the FLAG/HA-TDRD3 ΔFIM and ΔNTD ΔFIM impaired the interaction with FMRP (lane 11 and 12), but did not affect the interaction with TOP3β (lane 11).

Then, the association of individual mRNP-associated proteins was analyzed by immunoblotting. The mRNP components LARP1, LARP4 and PABPC1 were found to interact with FLAG/HA-TDRD3 and with the deletions-mutants in equal amounts (lane 9-12). The same was found for MAGOH and CBP20, marker-proteins for early mRNPs. The steady state translation initiation factor eIF4E was, however, absent from any of these IPs. These findings suggest that its interactions with TOP3β and FMRP are not required for TDRD3 to associate with early mRNPs.

Next, I tested the association of the different TDRD3 mutants with the translation machinery. As the interaction with the ribosomal proteins rpS6 and rpL7 was not affected at any of the deletion mutants of FLAG/HA-TDRD3 (shown in Figure 9C), the possibility was raised that also the association with polysomes remained intact. To test this assumption, the association of wt and mutant FLAG/HA-TDRD3 with polysomes was analyzed via density gradient centrifugation. For this, the stable cell lines expressing of the respective FLAG/HA-tagged TDRD3 versions were treated with cycloheximide shortly before lysis to stall the polysomes for the analysis. After density gradient centrifugation, the gradients were fractionated, and the RNA profile was monitored to verify the position of the polysomal fractions

within the gradient. The immunodetection of FLAG/HA-TDRD3 full length, ΔNTD, ΔFIM and ΔNTD ΔFIM in the gradient fractions revealed that all tested variants co-sedimented with the polysomal fractions to a very similar extent (Figure 10). In striking contrast however, a FLAG/HA-TDRD3 protein carrying a mutation in the Tudor domain showed a markedly reduced polysomal association, consistent with earlier reports (Stoll et al., 2013). The EBM mutant did not associate with the polysomal fractions, as was also shown in previous experiments (Stoll et al., 2013). These results confirm that apparently neither the interaction with TOP3β nor with FMRP nor both proteins are necessary for TDRD3 to associate with mRNPs and polysomes and no major changes in the mRNP composition could be observed.

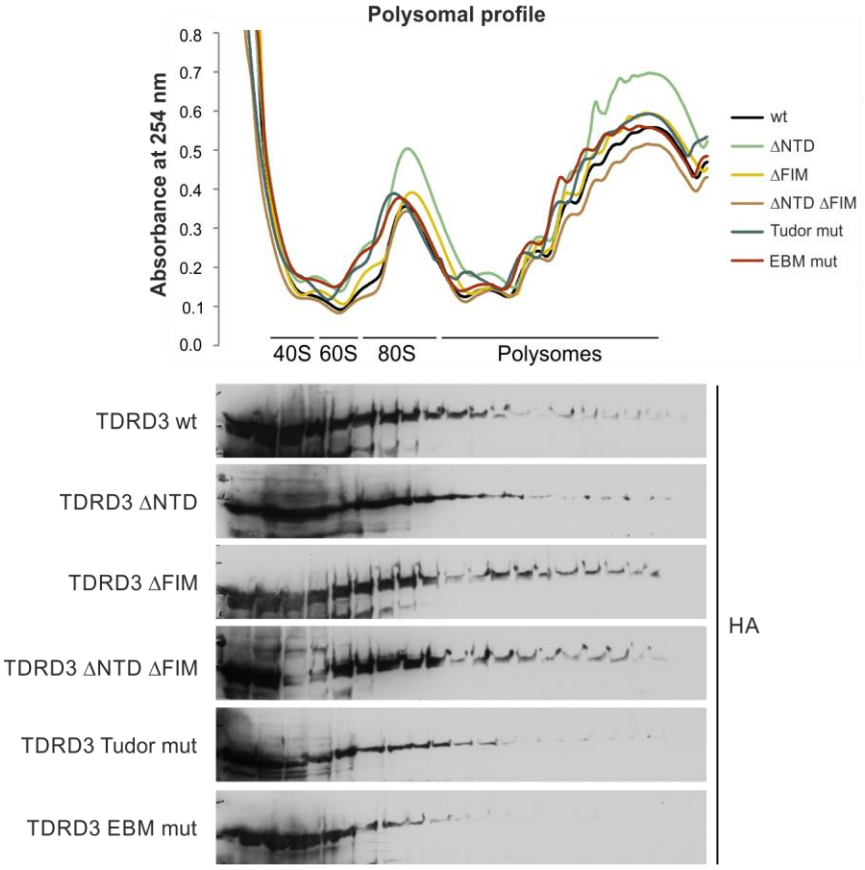

Figure 10: **FLAG/HA-TDRD3 associates with polysomes independently of its interaction with TOP3β and FMRP.** Flp-In T-REx 293 cell lines expressing either FLAG/HA-TDRD3 wt or the respective deletion mutants ΔNTD, ΔFIM, ΔNTD ΔFIM, the Tudor mutant or EBM mutant were used for polysomal gradient fractionation. After density gradient centrifugation, the co-sedimentation of the proteins was analyzed via WB. The respective FLAG/HA-TDRD3 versions were detected via immunoblotting against the HA-tag.

4.5. TDRD3 and TOP3β are tightly connected and associate with the pioneer round of translation

TDRD3 and TOP3β form a stable hetero-dimer which associates rather transiently with FMRP

Many common interactors of the three TTF proteins were identified and it is likely that these interactors form a unit that contains the ribosome and mRNPs. The question emerged, how permanently these interactions around or even within the TTF complex form in the cell and if there might be some interactors which connect stably to the TTF complex and might potentially even directly contribute to its function.

Therefore, the dissociation of the TDRD3 interactome was investigated by SILAC. Briefly, stable Flp-In T-REx 293 cell lines expressing FLAG/HA-TDRD3 upon induction with tetracycline were labeled over six passages with lysine and arginine containing heavy isotopes. As a negative control Flp-In T-REx 293 wt cells were grown in medium containing only light amino acids. The lysates of both cell lines were then divided into two parts, respectively. One part of each lysate was used to mix both lysates in a 1:1 ratio and thereafter an anti-FLAG IP was performed. After the IP, the FLAG-peptide eluate was analyzed via mass spectrometry and the ratio between heavy and light proteins was calculated (Figure 11A, lower panel). This enabled us to investigate which proteins stay associated with TDRD3 during the IP and which proteins dissociate during the incubation and thus exchange with proteins in the mixed lysate. Factors that completely have dissociated and re-bound in the frame of the experiment would be present in equal amounts, lightly and heavily labeled. Interactors which were present in the eluate with more than 50% heavy-labeled lysines and arginines have not completely been exchanged during the IP.

The second part of each lysate was used to perform the anti-FLAG IPs of FLAG/HA-TDRD3 and the control separately. The FLAG-peptide eluted proteins of both IPs were mixed afterwards and analyzed along the same lines as the first sample. However, the ratio between heavy and light proteins displays the co-precipitated interactors of FLAG/HA-TDRD3 in this second experimental set-up, regardless of whether they have dissociated and re-bound during the experiment. In this case, each interactor found in the FLAG/HA-TDRD3 IP contains heavy amino acids, whereas the unspecific proteins present in the control-IP contain light amino acids, respectively (Figure 11A, upper panel).

A large number of significantly enriched interactors of FLAG/HA-TDRD3 could be identified in the SILAC IP experiment and some of them already have been verified via WB in the previously described experiments (upper panel). Surprisingly, only TOP3β was found to be tightly connected with FLAG/HA-TDRD3 during the incubation time. Even the third TTF component FMRP was completely exchanged during the course of the IP (lower panel). This indicates that all three TTF proteins, TDRD3, TOP3β and

FMRP, seem to be rather transiently associated together as hetero-trimer. On the contrary, TDRD3 and TOP3β are apparently stably connected in the cell and thus form a separate, hetero-dimeric TT subunit. However, it is not clear in which processes the trimeric TTF complex might participate within the cell and at which steps only the TT dimer or FMRP alone might be present.

The TDRD3-TOP3β subunit of the TTF complex is restricted to the pioneer round of translation

It became clear that the TTF components are associated with early mRNPs and the translation machinery, as described in previous chapters. However, the question, if the TTF complex might be associated with the pioneer round of translation or if it also participates in the steady state translation, remained still unanswered until now.

To investigate whether the TTF complex is a specific component of early mRNPs, Flp-In T-REx 293 wt cells were treated with Actinomycin D (ActD) at a concentration which inhibits the global transcription of the cells for 2 h (Loreni et al., 2000). I assumed that the pool of newly transcribed early mRNPs which undergo their first round of translation is minimized due to this short transcription block and that the majority of translating mRNPs are translated via the eIF4E-initiated steady state translation. Cells were additionally treated with cycloheximide shortly before their lysis to enable the analysis of the polysomal association of the TTF proteins. The polysomes of the lysates were separated via density gradient centrifugation and their position in the gradient fractions was determined by monitoring the absorbance of the RNA during the fractionation. The co-sedimentation of the endogenous TTF proteins in the fractions of the gradient was analyzed via WB (Figure 11B).

The treatment with ActD resulted in a slight decrease in the overall translation level as compared to the control. However, the sedimentation of PABPC1 which takes part in, but is not restricted to the steady state translation of mRNPs in the polysomal fractions was not affected. In Contrast, the association of CBP20 which initiates the pioneer round of translation as part of the cap binding complex and of MAGOH/B, a core-component of the EJC, with the polysomal fractions was slightly decreased, although still not abolished completely. Both proteins are restricted to the pioneer round of translation as they are being removed during the mRNP remodeling upon transit to the steady state translation. Interestingly, the short transcription block had severe effects on the co-sedimentation of both TDRD3 and TOP3β with the polysomal fractions. Their association with polysomes was completely lost. However, there was no effect on the polysomal co-sedimentation of FMRP which shows like PABPC1 no response to the ActD treatment. To confirm that the sedimentation of the TTF proteins into the heavier fractions containing the polysomes resulted from their co-sedimentation with translating mRNPs, cell lysate was digested with RNase A prior to the gradient centrifugation. The RNA profile indicates that the RNase A treatment eliminated the polysomes in the lysate. Moreover, the sedimentation of each TTF protein as well as of PABPC1, CBP20 and MAGOH into the heavier fractions

of the gradient was abolished. This confirms, that their sedimentation in the heavier gradient-fractions resulted indeed from their association with polysomes in the experiment. These results strongly suggest that TDRD3 and TOP3β are associated with the pioneer round of translation and leave the mRNPs and the translation machinery at some point during the transit to the steady state translation. On the contrary, FMRP seems to remain associated with the mRNPs after the pioneer round of translation.

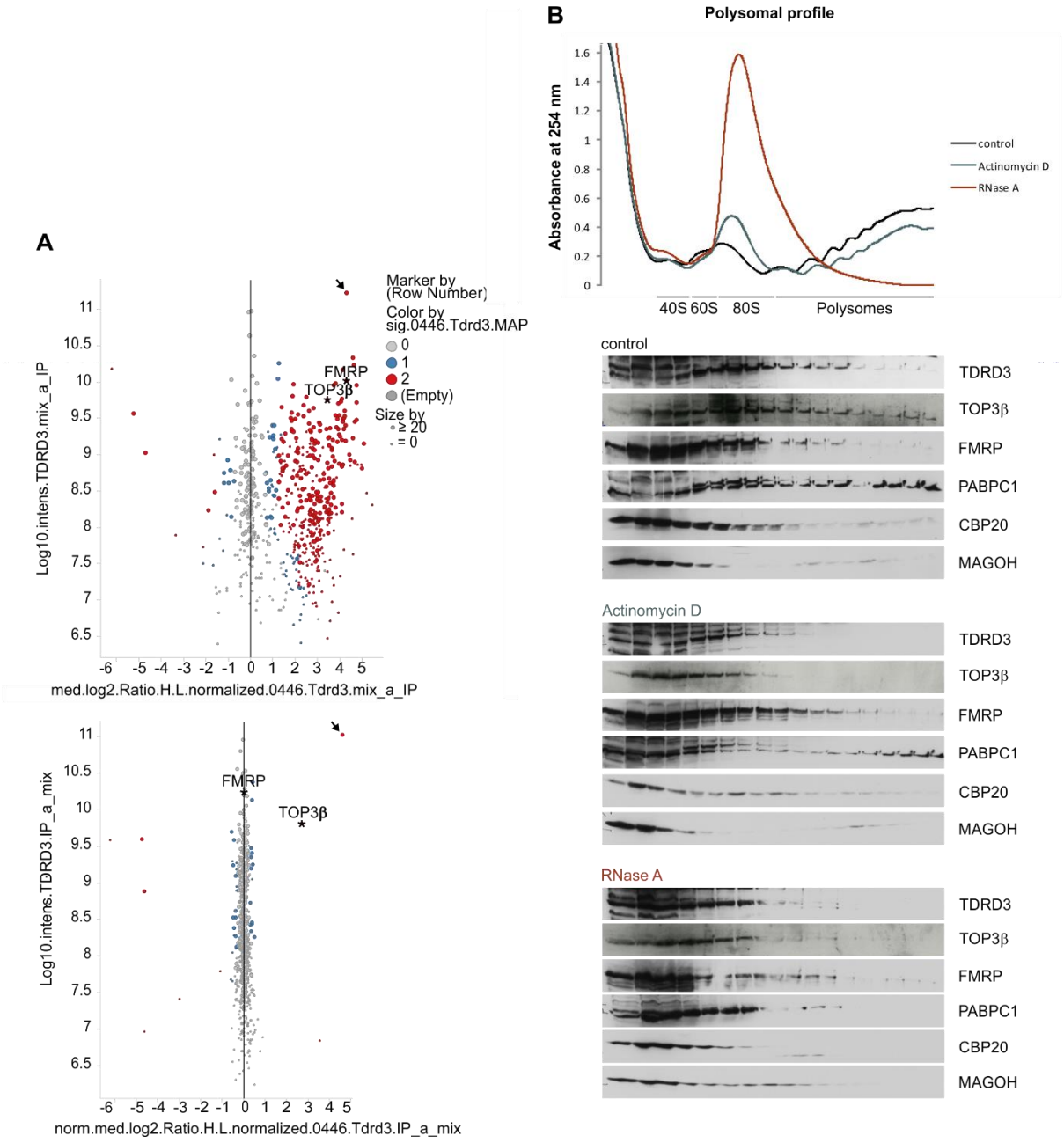

Figure 11: **TDRD3 and TOP3β form a stable hetero-dimeric sub-complex and are associated with the pioneer round of translation. (A) The "TT unit" of the TTF complex: SILAC-labeling and anti-FLAG IP experiments of FLAG/HA-TDRD3.** Flp-In T-REx 293 FLAG/HA-TDRD3 cell lines were labeled with heavy amino acids and Flp-In T-REx 293 wt control cells were labeled with light amino acids, respectively. Upper panel: Lysates

were kept separately during the anti-FLAG IP and FLAG-peptide eluates were mixed afterwards (mix_a_IP). Proteins which precipitated with FLAG/HA-TDRD3 were therefore labeled with heavy amino acids, unspecific proteins which precipitated with the control contain light amino acids. Lower panel: Lysates of both cell lines were mixed before the anti-FLAG IP was performed (IP_a_mix) to monitor the exchange of the heavy labeled proteins with proteins containing light amino acids during the IP experiment. Interactors of FLAG/HA-TDRD3 which remained associated with TDRD3 during the course of the IP contain heavy isotope-labeled amino acids, complete dissociation and re-binding resulted in a 1:1 ratio of proteins with heavy and light amino acids. Stars mark TOP3β and FMRP; arrow marks FLAG/HA-TDRD3. Grey dots (0): non-significant; blue (1): slightly significant; red (2): highly significant enrichment of the heavily over the lightly labeled protein. The size of the dots correlates with the number of unique peptides which were measured. **(B) Analysis of the TTF proteins in polysomal gradient fractions upon transcription inhibition.** Polysomal gradient fractionation of Flp-In T-REx 293 wt cells which have been either pre-treated with Actinomycin D or untreated control cells was performed. For the RNase control sample, untreated cell lysate was digested with RNase A prior to centrifugation. The sedimentation of the endogenous proteins was analyzed via immunoblotting.

4.6. TOP3β binds directly to the 80S ribosome via its RGG box

FMRP acts as translational repressor and stalls translating ribosomes (Darnell et al., 2011; Laggerbauer et al., 2001). It was shown, that FMRP binds directly to the 80S ribosome at the inter-phase of both subunits near the central protuberance. Therefore, it was proposed, that FMRP might inhibit the translation by interfering with the binding of translation factors or via interacting with the mRNA (Chen et al., 2014). As it was shown in Stoll et al., 2013 and in this work (see chapter 4.6. and 4.5.), also TDRD3 and TOP3β are associated with mRNPs during their first round of translation. It is likely, that the entire TTF complex situated at these mRNPs interacts with ribosomes during the pioneer round of translation. As FMRP and TOP3β both contact directly the mRNA and FMRP binds directly to the 80S ribosome, it is tempting to speculate that also TOP3β might directly interact with the ribosome. To investigate this, I tested whether purified 80S ribosomes directly bind to purified recombinant GST-TOP3β. 80S ribosomes were obtained from HeLa cells via hypotonic lysis and a two-step purification protocol as described in material and methods and the in the figure legend (Figure 12A). The obtained crude 80S pellet was resuspended and further purified via a sucrose gradient. The peak fractions which contained the 80S particles were pooled, pelleted and finally resuspended in low salt buffer. GST-TOP3β was recombinantly expressed in Sf21 insect cells via baculovirus. The recombinant protein was purified using glutathione Sepharose and was mixed with the purified 80S ribosome in a ratio of 1:1. The samples were separated by density gradient centrifugation and the sedimentation of 80S and GST-TOP3β was analyzed via SDS-PAGE of the gradient fractions followed by Coomassie-staining.

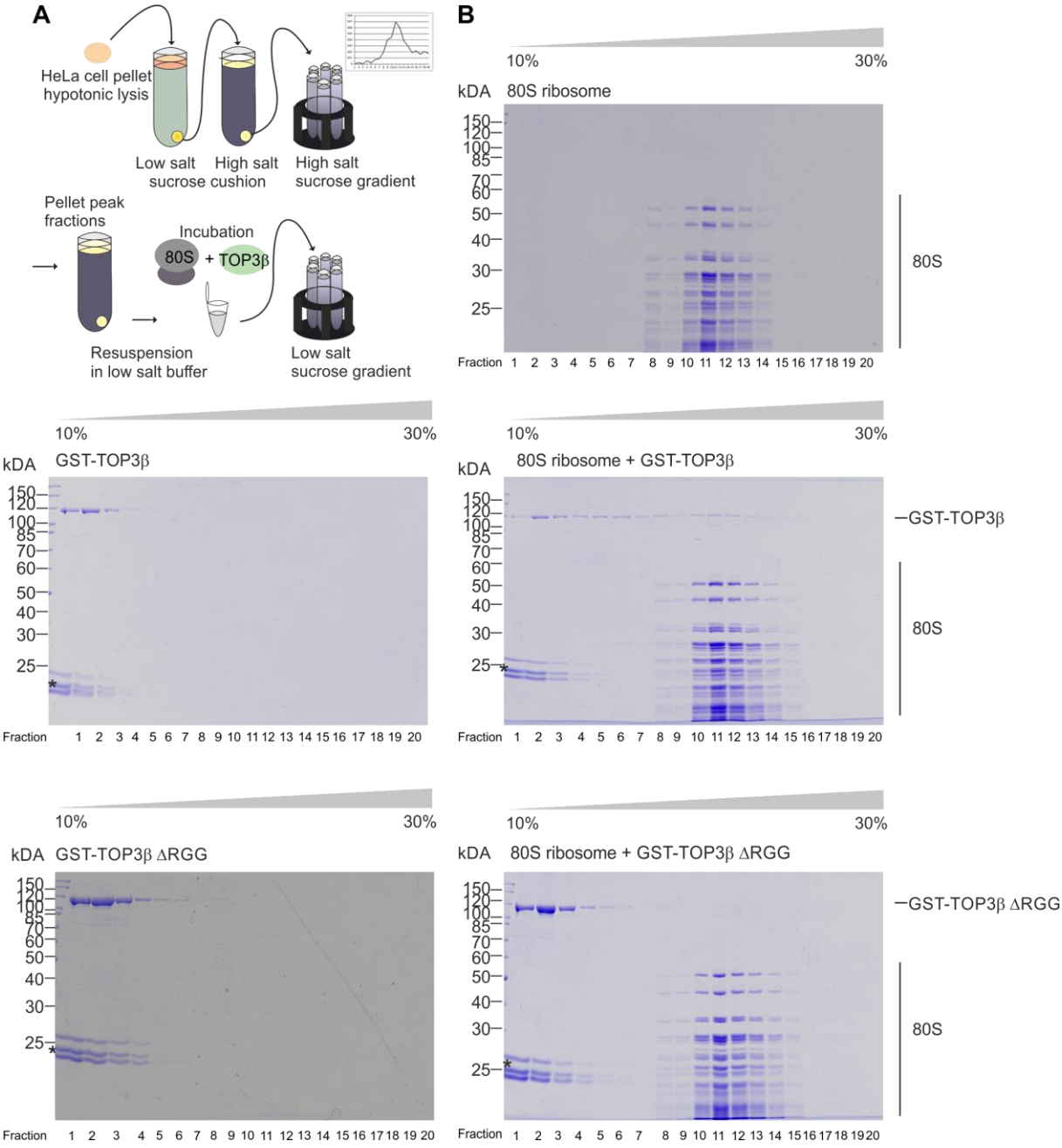

Figure 12: **TOP3β interacts directly with the 80S ribosome. (A) Purification of 80S ribosomes from HeLa cells and incubation with GST-TOP3β to investigate their interaction.** Scheme representing the purification strategy of 80S ribosomes. HeLa cells were pelleted and lysed via hypotonic lysis. The 80S ribosomes were then purified from the lysate first via a low salt sucrose cushion, followed by a high salt sucrose cushion and further purification via density gradient centrifugation. The fractions of the gradient which contained the ribosomes were pooled and pelleted. After resuspension in low salt buffer, the 80S particles were incubated with recombinant GST-TOP3β and their sedimentation was analyzed via density gradient centrifugation. **(B) GST-TOP3β binds directly to the 80S ribosome via its RGG box.** Density gradient centrifugation of purified 80S ribosomes alone, 80S ribosomes incubated either with GST-TOP3β wt or ΔRGG and of GST-TOP3β wt or ΔRGG alone. The fractions were analyzed via SDS-PAGE followed by Coomassie-staining. Stars marks unspecific protein-contaminations in the samples.

The purified 80S ribosome sedimented in fractions 8-15 of the gradient (Figure 12B, upper panel). GST-TOP3β alone did not enter into this part of the gradient under the same conditions but rather remained in the top fractions of the gradient (middle panel, left, fraction 1-4). This is in accordance with its lower molecular weight and S-value, and it further shows that the recombinant protein does not form aggregates. However, upon incubation with the 80S ribosome a significant fraction of GST-TOP3β shifts into the 80S containing fractions and co-sediments with the ribosome (B: middle panel, right fractions 10-14). These results show that GST-TOP3β directly binds to the 80S ribosome *in vitro* as it was previously also observed for FMRP. In the case of FMRP, the RGG box motif seems to be involved in the binding to the 80S ribosome (Chen et al., 2014). TOP3β has a highly conserved N-terminal TOPO domain like the other Type IA topoisomerases, whereas the C-terminal domains of these topoisomerases highly vary. The C-terminus of TOP3β contains zinc finger motifs and an RGG box motif which has been reported to mediate its RNA-binding (Ahmad et al., 2017; Xu et al., 2013). To examine, if the binding of TOP3β to the 80S ribosome is mediated via this motif, a GST-TOP3β ΔRGG mutant was expressed and purified. Interestingly, in contrast to the wt protein, GST-TOP3β ΔRGG remained in the light fractions of the gradient irrespective of whether it was loaded on the gradient alone or along with the 80S ribosome (lower panel). This shows that the RGG box of TOP3β is necessary for its binding to the 80S ribosome as the deletion of this motif abolished the binding completely.

4.7. TOP3β can recruit TDRD3 to the 80S ribosome

Since both FMRP and TOP3β were found to directly bind to the 80S ribosome, also the binding ability of the third TTF component TDRD3 was examined. For this GST-TDRD3-6xHis was recombinantly expressed and purified from *E. coli.* In brief, the recombinant protein was first purified via the GST-tag using glutathione Sepharose. The protein was eluted via removal of the GST-tag by PreScision protease digestion and purified in a second step via Ni-NTA. After elution with imidazole, TDRD3-6xHis was incubated with the 80S ribosome and the binding was analysed via density gradient centrifugation, as described above for TOP3ß. However, TDRD3-6xHis remained in the light fractions of the gradient and no interaction with the 80S particle could be observed (Figure 13A, lower panel). Nevertheless, consistent with the results shown in figure 12, GST-TOP3β bound efficiently to 80S ribosomes (Figure 13A) in the control experiment which was performed in parallel.

TDRD3 was shown to stably associate with TOP3β in the cell and it was a possibility that both were also in tight contact when they face the ribosome during the pioneer round of translation. Therefore, I investigated whether the binding of TOP3β to TDRD3 and 80S ribosomes is mutually exclusive or if TOP3β can mediate the indirect association of TDRD3 with the 80S ribosome *in vitro*. For this approach,

TDRD3 was co-expressed with GST-TOP3β in Sf21 cells via co-transfection of two baculovirus strains, each containing one of these proteins. Both recombinant proteins were co-purified together via GST-TOP3β using glutathione Sepharose. As shown in figure 13, the proteins formed a stoichiometric complex (termed TT complex, Figure 13B). The sedimentation of TDRD3, either as part of the TT complex with GST-TOP3β alone or as part of the TT complex incubated with 80S, was examined via density gradient centrifugation and immunoblotting after the fractionation (Figure 13C). Whereas TDRD3 with GST-TOP3β alone remained in the light fractions of the gradient, it co-sedimented in presence of GST-TOP3β with the 80S ribosome. These results show that although TDRD3 alone does not interact with the ribosome, the association of TDRD3 with the ribosome can be mediated by the TTF subunit TOP3β.

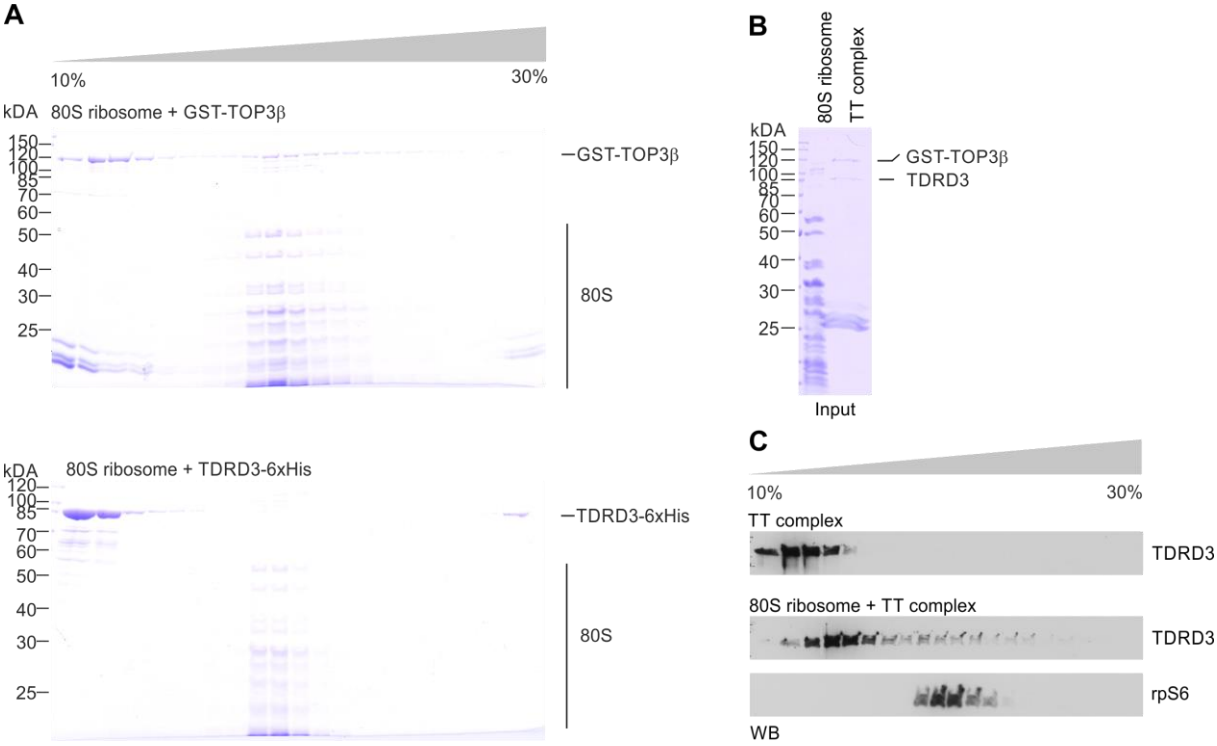

Figure 13: **TOP3β can recruit TDRD3 to the 80S ribosome. (A) TDRD3 alone does not bind to the 80S ribosome.** Either GST-TOP3β or TDRD3-6xHis were incubated with the 80S ribosome. After density gradient centrifugation, the sedimentation is analyzed via SDS-PAGE followed by Coomassie-staining. **(B) Co-purification of TDRD3 with GST-TOP3β: Formation of a stoichiometric TT complex.** GST-TOP3β and TDRD3 were co-expressed in Sf21 cells and co-purified via glutathione Sepharose. Upon elution a stoichiometric complex of GST-TOP3β and TDRD3, the TT complex, was obtained. This complex was further analyzed via density gradient centrifugation in (C): The respective input (10%) of 80S and the TT complex is shown in this Coomassie-stained SDS-PAGE. **(C) TOP3 can mediate the interaction of TDRD3 with the 80S ribosome.** The sedimentation of TDRD3 as part of the TT complex alone or upon incubation of the TT complex with the 80S ribosome was analyzed via density gradient centrifugation. Immunoblotting of TDRD3 and the ribosomal protein rpS6 revealed that TDRD3 partially co-sedimented with

80S in the heavier gradient fractions when it was in a complex with GST-TOP3β. The TT complex alone remained in the light fractions on top of the gradient.

4.8. TOP3β binds to rRNA of the 40S and the 60S ribosomal subunits

The previous experiments have shown that TOP3β is able to recruit TDRD3 to the 80S ribosome *in vitro*. Since TDRD3 and TOP3β are tightly associated *in vivo,* it is likely that both proteins bind as a complex to the ribosome in the cell. However, the potential functions of this complex at the 80S ribosome remain obscure. Insight into its function may come from information about its precise binding site at the ribosome. Therefore, I initially investigated to which ribosomal subunit TOP3β might bind. For this, the 40S and 60S ribosomal subunits were separately purified from HeLa cells. To analyze the binding, density gradient centrifugation of either GST-TOP3β alone or of 40S or 60S alone or of GST-TOP3β incubated with 40S or 60S was performed, respectively (Figure 14A). The sedimentation of the ribosomal subunits and GST-TOP3β was monitored via Western blot. GST-TOP3β alone remained at each of the conditions used for the gradient centrifugation of 40S and 60S in the light fractions on top of the gradient. Upon incubation with either the 40S subunit (left panel) or the 60S subunit (right panel) GST-TOP3β partly shifted to heavier fractions and was found to co-sediment with the 40S and 60S subunits, respectively. This indicates that GST-TOP3β binds directly to the small as well as to the large subunit of the ribosome.

The RGG box mediates the binding of TOP3β to the ribosome. Since this motif seems to be responsible for the RNA-binding of TOP3β (Ahmad et al., 2017; Xu et al., 2013), it was investigated if TOP3β binds to ribosomal RNA (rRNA). Therefore, either 80S, 40S or 60S were incubated with GST-TOP3β wt or the ΔRGG mutant, respectively (Figure 14B). After incubation, density gradient centrifugation was performed and the fractions which contained the respective ribosomal components were pooled and UV-crosslinked at 254 nm. Then, a GST pull down was carried out to obtain the respective ribosomal particles that were bound to GST-TOP3β. After intensive washing, an RNase digest was performed and the 5’ ends of the rRNA fragments were radioactively labeled. For elution, the glutathione Sepharose beads were boiled in sample buffer. The eluates were separated via SDS-PAGE and transferred to a blotting membrane. The signal of the labeled RNA on the corresponding autoradiograph revealed that GST-TOP3β wt was crosslinked to rRNA upon incubation with the 80S ribosome and the 40S subunit and also to the rRNA of the 60S subunit, however to a lesser extent (Figure 14C). The specificity of this signal was assured as the incubation of GST-TOP3β ΔRGG with the respective ribosomal particles produced no signal in this experiment. These results illustrate that GST-TOP3β interacts with the

ribosome and this interaction involves the contact to rRNA. It is, however, possible if not likely that also protein-protein-contribute to its binding.

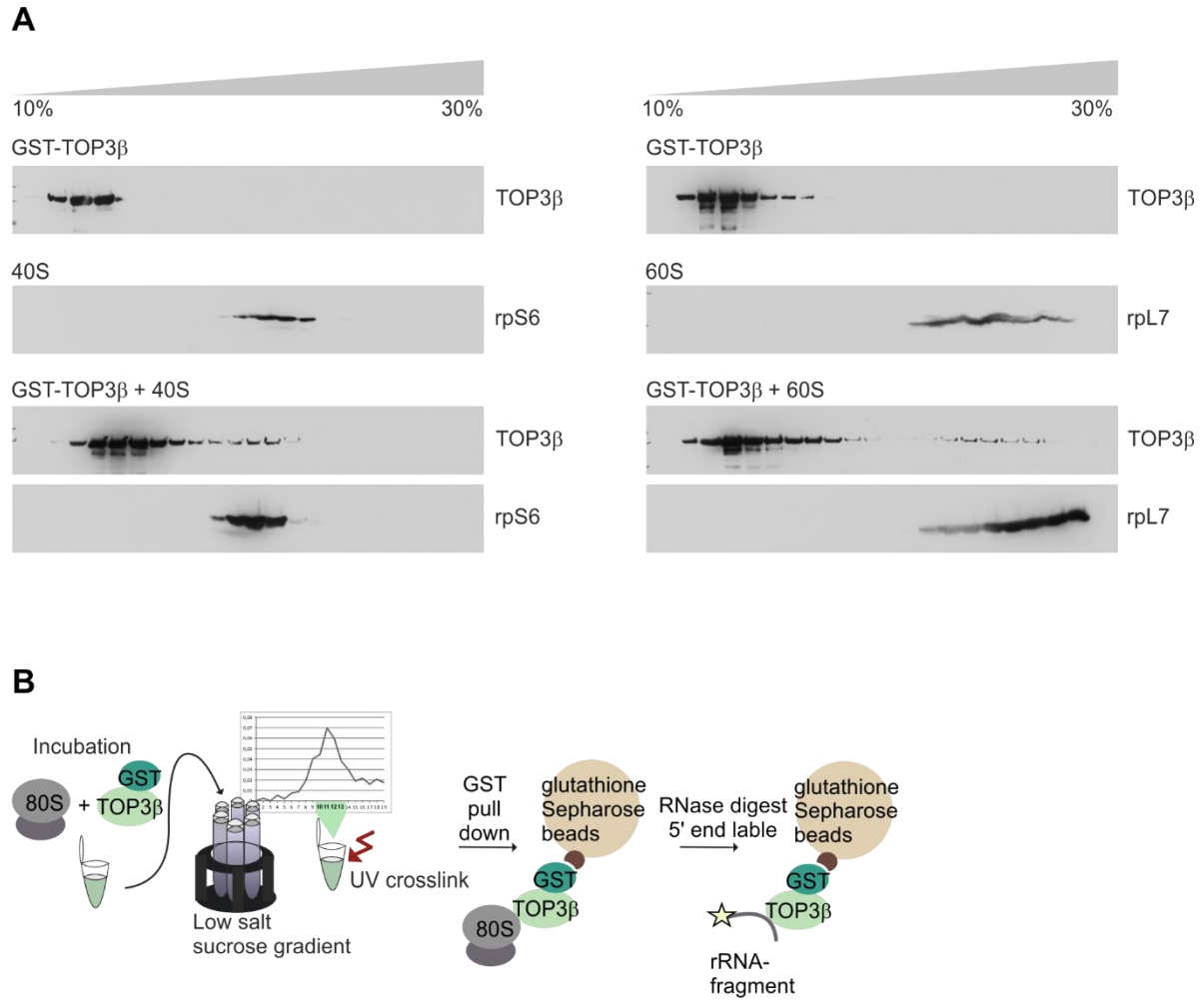

Figure 14: **TOP3β interacts with the 40S and the 60S ribosomal subunits and binds to the rRNA. (A) GST-TOP3β binds directly to 40S and 60S.** Density gradient centrifugation of GST-TOP3β alone, incubated with 40S (left panel) or 60S (right panel) or 40S and 60S alone. The gradient fractions were analyzed via WB. GST-TOP3β partially co-sediments with 40S and with 60S, showing that it interacts directly with the small and the large ribosomal subunit. **(B) Crosslinking and pull down strategy to monitor the direct binding to rRNA *in vitro*.** Ribosomal particles are incubated with GST-TOP3β and density

gradient centrifugation is performed. The pooled ribosomal peak fractions are UV-crosslinked, and a GST pull down is carried out thereof. After RNase digestion, the rRNA fragments are radioactively labeled at their 5' end. The samples are eluted, separated via SDS-PAGE and transferred to a membrane. The detection of the radiolabeled rRNA fragments occurs via autoradiography. **(C) TOP3β binds directly to rRNA of the 80S ribosome as well as of the 40S and 60s subunits.** Either GST-TOP3β wt or ΔRGG were incubated with 80S, 40S or 60S as described in (B), respectively. The autoradiograph reveals, that GST-TOP3β wt bound directly to the rRNA of 80S as well as of 40S and 60S. The deletion of the RGG box abolished this interaction.

4.9. TOP3β is a potential RNA topoisomerase but associates with polysomes independently of its catalytical activity and ribosome binding

The polysomal association of TOP3β

TOP3β binds directly to the ribosome *in vitro* via its RGG motif, as was shown in this work. Moreover, TOP3β mediates the interaction of TDRD3 with the 80S ribosome in *in vitro* experiments. However, it was shown that the association of TOP3β with polysomes *in vivo* depends on the EBM motif of TDRD3 and is thought to be, at least initially, mediated via the association with the mRNPs. To investigate this hypothesis and to test whether the direct contact of TOP3β with the 80S ribosome or with the ribosomal subunits might be necessary for its association with polysomes *in vivo*, I performed polysomal gradient fractionation with the TOP3β RGG deletion mutant. Furthermore, I included a catalytically inactive point mutation of TOP3β in the analysis to investigate whether the topoisomerase activity per se might be required for TOP3β to reach the translational machinery.

Therefore, stable cell lines were generated containing either the FLAG/HA-TOP3β ΔRGG deletion mutant which is defective in ribosome binding or catalytically inactive FLAG/HA-TOP3β with a mutation of the active site tyrosine into phenylalanine (Y336F). After lysis of the respective cells, polysomal gradient fractionation was performed. The fractions of the gradient were analyzed after centrifugation via immunoblotting. The comparison of FLAG/HA-TOP3β wt with the ΔRGG and the Y336F mutant revealed no difference in the sedimentation pattern: both mutants were found to associate with polysomes to the same extent as it was observed for the wt protein (Figure 15A). This shows, that the association of TOP3β with polysomes occurs independently of its ability to directly bind to the ribosome. This observation is consistent with the suggestion that TOP3β associates with polysomes via mRNPs. Also, the catalytical activity of the topoisomerase is not necessary for its association with polysomes.

TOP3β is a potential RNA topoisomerase

TOP3β is a shuttle protein which localizes mainly in the cytoplasm and is associated together with TDRD3 and FMRP at mRNPs (Stoll et al., 2013; Xu et al., 2013). Furthermore, TOP3β takes part in the first round of translation of these mRNPs, as was shown in this work, and possesses a putative RNA-binding motif which mediates its direct binding to the ribosome and to rRNA. Together, these findings suggest that TOP3β is a topoisomerase which exerts its catalytical activity on RNA rather than on DNA in the cell.

Type IA topoisomerases form an intermediate with the nucleic acid upon strand cleavage in which the 5' end of the phosphate group is covalently bound by the active site tyrosine. At the same time, the 5' end of the nucleic acid with the free 3' hydroxyl group is tightly, but non-covalently attached to the enzyme. After strand passage, the gap is usually re-ligated via nucleophilic attack by the free 3' hydroxyl group at the 5' part of the cleaved strand on the intermediate phosphate and the covalent intermediate is resolved. Upon denaturation of enzymes in the intermediate state, for example via the addition of SDS, the non-covalently bound 5' end of the cleaved nucleic acid is released, whereas the covalently bound 3' end is trapped on the denatured enzyme with no opportunity for re-ligation since the necessary free hydroxyl group is missing. This phenomenon was used to visualize the formation of a covalent intermediate with short DNA or RNA oligonucleotides *in vitro*. To provide evidence that these nucleic acids can potentially be used as a substrate by TOP3β, the respective oligonucleotides were radioactively labeled at the 5' end and incubated with recombinant GST-TOP3β. After the addition of SDS, the DNA or RNA oligonucleotides were separated on a denaturing polyacrylamide gel. Analysis of the autoradiograph corresponding to this gel revealed that the incubation with GST-TOP3β wt resulted in the formation of smaller bands representing the 5' end-fragments of the cleaved DNA (Figure 15C, lane 2) or RNA (lane 7) which were released from the intermediate upon denaturation. At the same time, both DNA and RNA full-length oligonucleotides which were only incubated with the reaction buffer remained intact, therefore a non-specific degradation can be excluded (lane 1 and 6). Also, the incubation with the active site mutant Y336F did not produce any cleaved fragments neither of the DNA nor of the RNA substrate. This shows that GST-TOP3β wt can cleave and form a covalent intermediate with both DNA and RNA substrates. However, the topoisomerase seems to vary in its specificity towards the DNA and the RNA, since incubation with the DNA substrate released mainly a larger fragment and only small amounts of a smaller fragment, whereas incubation of the enzyme with the RNA oligonucleotide produced mainly the smaller fragment and only small amounts of the larger fragment.

In addition, also the point mutation R472Q which was found to cause schizophrenia in a patient and the ΔRGG mutant of TOP3β were analyzed for potential topoisomerase activity on both substrates.

Surprisingly, incubation with the patient mutant R472Q (lane 3 and 8) as well as with the RGG box deletion mutant (lane 5 and 10) resulted in the formation of covalent intermediates with both the DNA and the RNA substrates to the same extent as it was observed for GST-TOP3β wt. Also, the ratio between the larger and the smaller fragments was the same as with GST-TOP3β wt on both substrates. These findings strongly suggest that the formation of the covalent DNA and RNA intermediates per se is neither influenced by the R472Q point mutation nor by the deletion of the RGG box.

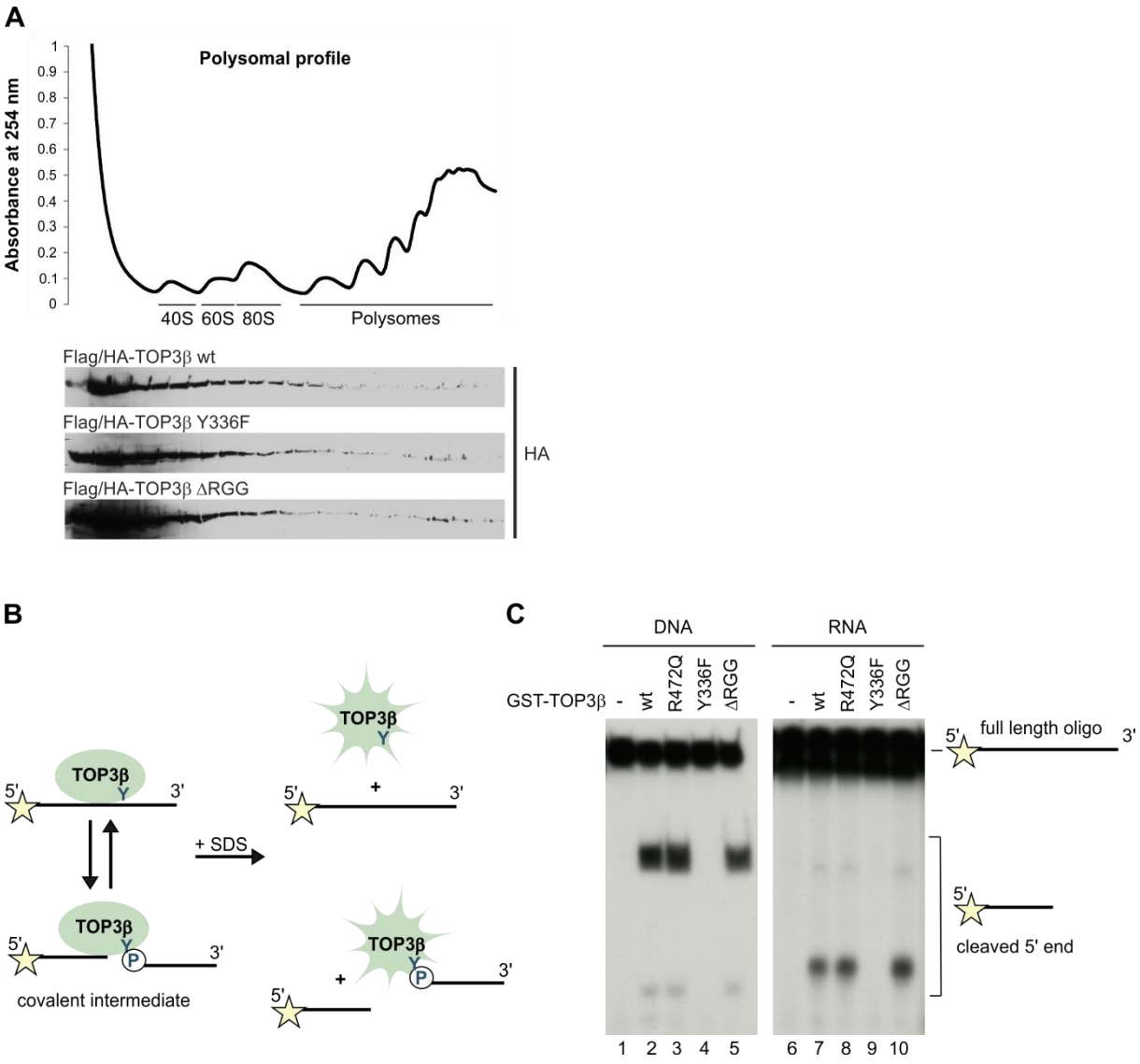

Figure 15: **TOP3β is a potential RNA topoisomerase that associates with polysomes independently of its catalytical activity and ribosome binding. (A) For its polysomal association, TOP3β requires neither its catalytical activity nor the ability to bind directly to the ribosome.** Polysomal fractionation of the respective stable Flp-In T-REx 293 cell lines shows that the active site mutant FLAG/HA-TOP3β Y336F and the deletion mutant FLAG/HA-TOP3β ΔRGG associate with polysomes to the same extent as the wt FLAG/HA-TOP3β. The overexpressed proteins were detected in the gradient fractions via immunoblotting of the HA-tag. **(B) Scheme of the visualization of the catalytical reaction of type IA topoisomerases on short linear oligonucleotides.** Denaturation of the intermediate with SDS results in the release of the cleaved 5' end of the nucleic

acid, while the 3' end is trapped on the denatured enzyme due to the covalent bound. Labeling of the 5' end enables the detection of the released 5' end fragment upon separation of the nucleic acids via gel electrophoresis. **(C) GST-TOP3β can form the covalent intermediate with DNA and RNA substrates.** The autoradiograph shows the 5' end labeled DNA or RNA substrates separated via gel electrophoresis. The incubation of a short DNA as well as of a short RNA oligonucleotide with purified GST-TOP3β wt or the R472Q or ΔRGG mutants resulted in cleaved 5' end fragments which were released upon denaturation of the enzymes at their intermediate state. The active tyrosine mutant GST-TOP3β Y336F fails to cleave the nucleic acids and forms no covalent intermediate.

4.10. TDRD3, TOP3β and FMRP regulate the expression of a subset of proteins

The data described so far are consistent with a potential role of the TTF complex in the regulation of the gene expression at the post-transcriptional level. This regulation may be at the global level or alternatively might be restricted to a specific subset of mRNPs to which the TTF complex is recruited at a yet undefined time point. If these assumptions are correct, one would expect that the ablation of TTF components has an impact on the protein expression profile of the affected cells. I analyzed such a scenario using a pulsed SILAC proteomics approach (described in materials and methods, according to Schwanhäusser et al., 2009).

For this, HEK 293 wt cells were transfected with a control siRNA or with siRNA either against TDRD3, TOP3β or FMRP. Thereafter, these knock down cells were incubated with medium containing medium-heavy amino acids, whereas control cells were incubated with heavy amino acids. Lysates of the knock down and the control cells were mixed in a ratio of 1:1 for analysis via mass spectrometry and the knock down efficiency was analyzed via immunoblotting. The experiments were performed in duplicates, respectively. Quantification and normalization of the immunoblot revealed that TOP3β was reduced by RNAi by 87% and 99% compared to control transfections. In equivalent experiments the level of TDRD3 was reduced by 80% and 84%, whereas FMRP was reduced by 55% and 82% in the experiments, respectively (Figure 16A).

The ratio of proteins with heavy amino acids (H) corresponding to the control cells and of proteins with medium-heavy amino acids (M) corresponding to the knock down of the respective TTF component was calculated after measuring the samples by mass spectrometry. This ratio displays the fold-change in the levels of newly synthesized proteins on a global level upon knock down of the respective TTF component. The protein ratios of both replicates were here depicted against each other in one plot (Figure 16B-D).

This analysis revealed that the knock down of TDRD3, TOP3β and FMRP reproducibly resulted in a significant change of a small subset of proteins each, but does not seem to impact the global protein

expression per se. Thereby, the reduction of TDRD3 seems to affect the expression of slightly less proteins than the reduction of TOP3β or FMRP. Notably, upon knock down of TOP3β, more proteins were found to be significantly down-regulated than up-regulated (Figure 16C), whereas the knock down of FMRP (Figure 16D) and TDRD3 (Figure 16B) produced a similar amount of up- and down-regulated proteins, respectively.

To confirm the changes in the proteome of these cell lines upon knock down, the expression of selected proteins was analyzed by an independent approach. After a knock down was performed along the same lines as described above, the level of selected proteins was monitored via WB (Figure 16E). The 6-phosphogluconate dehydrogenase (PGD) was found to be slightly significantly up-regulated upon depletion of TDRD3 and TOP3β in the pulsed SILAC approach. This could be confirmed via WB in this third siRNA mediated knock down experiment. Quantification of the WB revealed a 1.4- and a 2.5-fold up-regulation of PGD in the absence of TDRD3 and TOP3β, respectively (Figure 16F). The reduction of FMRP produced no significant change of PGD levels in the pulsed SILAC approach. However, the analysis of the WB corresponding to the third experiment showed a 0.11-fold reduction of PGD upon knock down of FMRP. This observation might be explained by the fact that the knock down of FMRP was more efficient in this third experiment (reduction by 86% in comparison to 55% and 82% in the pulsed SILAC experiments).

Next, also the protein-level of TOP2α was examined in the WB. The change in the expression of the topoisomerase TOP2α was highly significant in each pulsed SILAC experiment. The reduction of TDRD3 resulted in an up-regulation of this enzyme, whereas the absence of TOP3β or FMRP caused its down-regulation. The same regulation pattern could be also observed in the WB of this third knock down experiment and its quantification confirmed a 0.2- and 0.27-fold down-regulation upon knock down of TOP3β and FMRP and a 4-fold up-regulation upon reduction of TDRD3 levels.

All in all, the change of expression monitored via WB reflects the data obtained by mass spectrometry and the data of the three knock down experiments for the respective protein are in relatively good consistence with each other. The pulsed SILAC data revealed the proteome which is influenced by the TTF components on a global cellular level. However, as mentioned above, the TTF components seem not to influence the protein expression per se but rather affect the expression of only a small subset of proteins. Thereby, some proteins are regulated in the same manner by all three TTF components, whereas others are up regulated upon the reduction of one or two and down regulated or not regulated in the absence of the other TTF component(s) and vice versa. Therefore, it seems that each TTF component differs at least in parts in their influence on the expression of proteins.

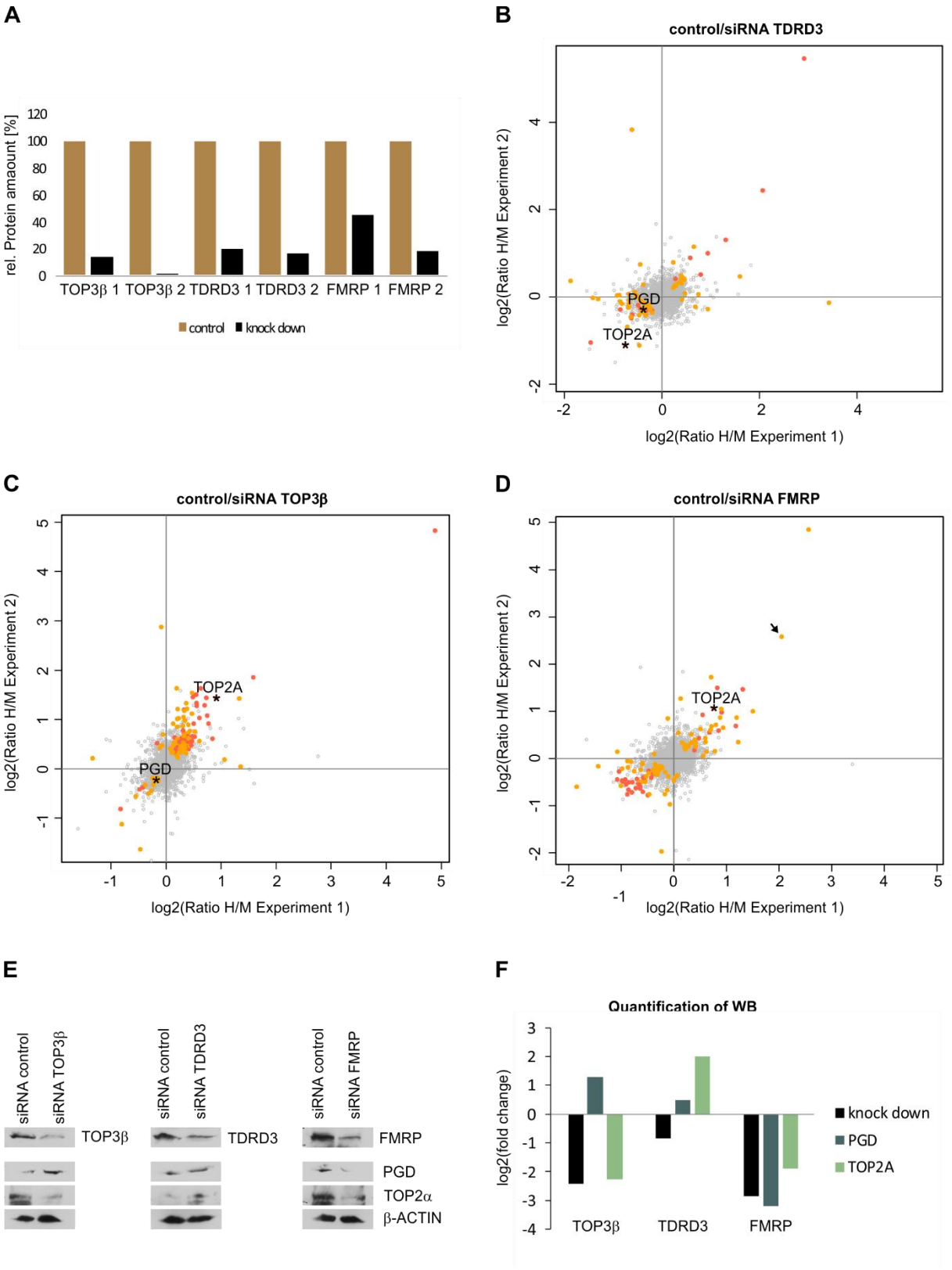

Figure 16: **TDRD3, TOP3β and FMRP regulate a subset of proteins in HEK 293 cells.** The change of protein levels upon knock down of TDRD3, TOP3β or FMRP is monitored via mass spectrometry of a pulsed SILAC experiment in HEK 293 cells. **(A) Validation of the knock down efficiency of the TTF components.** The knock down efficiency of TDRD3, TOP3β and FMRP in both replicates of the experiment is determined via normalized quantification of the immunoblot signal of the endogenous proteins in the

corresponding Western blot (WB). The relative protein amount in comparison to the control is depicted in the chart. **(B) Change of protein levels upon knock down of TDRD3.** The normalized ratios of proteins containing heavily labeled (H) amino acids representing the proteins of HEK 293 cells transfected with control siRNA and of proteins containing medium-heavily labeled (M) amino acids corresponding to the knock down of TDRD3 in HEK 293 cells from two independent experiments are plotted against each other in the scatter plot. Proteins which are significantly changed in their expression level upon the knock down of TDRD3 are marked in color, proteins which show no, or only minor changes are depicted in grey. Orange dots represent proteins which were calculated as slightly significantly changed in both experiments or strongly significant only in one experiment and not significant in the other. Red dots represent proteins which were strongly significantly regulated in either both experiments or strongly significant in one experiment and slightly significant in the other experiment. **(C) Change of protein levels upon knock down of TOP3β.** Same as in (B), but upon the knock down of TOP3β. **(D) Change of protein levels upon knock down of FMRP.** Same as in (B) and (C), but upon the knock down of FMRP. (B-D) The arrow marks the protein which was targeted by the siRNA for knock down. PGD and TOP2α which are selected for validation of the experiment (E and F) are marked by stars in the graph. **(E) Validation of the regulated proteins upon knock down of TDRD3, TOP3β.** The regulation of PGD and TOP2α upon knock down of TDRD3, TOP3β and FMRP is monitored via WB of a third independent experiment. **(F) The Quantification of the WB reflects the change of protein level for the selected proteins.** The fold change of the selected proteins upon knock down of TDRD3, TOP3β or FMRP in the third independent experiment based on the normalized quantification of the WB (E) is depicted in the scheme. Note: Calculation of fold change in (F): protein-ratio of siRNA TTF/siRNA control. Calculation in (B-D): protein-ratio of siRNA control (H)/siRNA TTF (M).

5. Discussion

The high diversity of different mRNP particles displays the complexity of the regulatory networks underlying the post-transcriptional regulation. In the recent years many proteins which have not been connected to the mRNP metabolism and its regulation so far were identified as mRNA-binding proteins (Castello et al., 2012). The recognition of these proteins as mRNP components emphasizes that we are only just beginning to understand the diversity of regulatory mechanisms and their potential. One intriguing example is the identification of TOP3β, which has been so far described as DNA topoisomerase, as an mRNA-binding protein (Castello et al., 2012; Stoll et al., 2013; Xu et al., 2013). However, the neither function of this mRNA-associated topoisomerase nor of the TTF complex in which TOP3β is integrated together with TDRD3 and FMRP is known. Therefore, the aim of this thesis was to biochemically characterize the TTF complex and to define its function in the mRNA metabolism.

In this work, I could show that TDRD3 is the central unit of the TTF complex that connect the two other proteins with each other and connects the complex with the EJC. I could identify the interacting proteome of the TTF mRNPs and link TDRD3 and TOP3β to the pioneer round of translation. Furthermore, I could show that TOP3β is capable of forming a covalent intermediate not only with DNA but also with RNA substrates. In addition, I found that TOP3β can directly bind to the 80S ribosome and to rRNA and could monitor the influence of each TTF component on the expression of the cellular proteome.

In the literature, FMRP was already shown to act as translational repressor (Darnell et al., 2011; Laggerbauer et al., 2001). As it was also found to directly bind to the 80S ribosome, it was proposed to repress the translation elongation due to this interaction. However, its function in the context of the TTF complex remains still speculative. TOP3β was shown to dissolve R-loops during the transcription by relaxing the DNA double-strand (Yang et al., 2014). However, the findings in this work and the facts discussed above make it very likely that TOP3β functions also in later steps of the mRNA metabolism where it could be required for the topological conversion of RNAs. In agreement with this, the Wang group reported that TOP3β can indeed topologically alter RNA substrates and thus act as an “RNA topoisomerase” (Xu et al., 2013). As recent studies have shown that RNA topoisomerase activity is also present in bacteria, archaea and in eukaryotes from yeast to humans (Ahmad et al., 2016; Siaw et al., 2016; Wang et al., 1996), the importance of this conserved catalytical activity for the cell seems to be emphasized. However, only TOP3β was found to associate with polysomes, whereas yeast and bacterial RNA topoisomerases fail to do so (Ahmad et al., 2016; Stoll et al., 2013; Xu et al., 2013). To our knowledge, TOP3β is the first topoisomerase which could be linked to the eukaryotic mRNA metabolism. Not only its association with mRNPs at polysomes, but also its integration into the TTF

complex with TDRD3 and FMRP characterize this topoisomerase and distinguish it from others. Although the function of the TTF complex remains still unclear, a role in the pioneer round of translation would be in good consistence with the obtained data.

5.1. TDRD3 is the central hub in the formation of the TTF complex and its binding to the EJC

Earlier studies by Stoll and coworkers had indicated that the interaction of TDRD3 with TOP3β and FMRP occurs in an RNase-insensitive manner. Therefore, TDRD3 was proposed to directly bind not only to FMRP (Linder et al., 2008) but also to TOP3β. Moreover, TDRD3 is thought to act as bridging factor between TOP3β and FMRP as these two proteins are not associated with each other in absence of TDRD3 (Stoll et al., 2013). In this thesis, I used a combination of biochemical and proteomics approaches to determine the mode of interactions within the TTF complex.

The biochemical reconstitution from recombinant sources and its biophysical characterization revealed that the TTF complex has a 1:1:1 stoichiometry and forms a hetero-trimeric unit (Figure 6B). This result confirms that TDRD3 indeed bridges FMRP and TOP3β in the complex and thus serves as adaptor within the complex, as it was proposed (Stoll et al., 2013). Furthermore, the co-purification of the three TTF components had demonstrated that no additional factor is required for the interactions within the complex or its stability. Nevertheless, it can`t be completely excluded that an additional factor, which is provided in the insect cell, might be transiently necessary for the initial formation of the complex.

Interaction of TDRD3 with TOP3β

In vitro binding experiments revealed a direct binding of TDRD3 to TOP3β which likely results in a stable hetero-dimer *in vitro* and *in vivo* (Figure 6A). The interaction between both proteins occurs via the N-terminal domain of TDRD3 (Stoll et al., 2013; Xu et al., 2013) which shares high similarity with the N-terminal domain of RMI1 (Yin et al., 2005). However, TDRD3 binds specifically to TOP3β, while RMI1 binds to TOP3α (Wu et al., 2006). TOP3α is the human paralog of TOP3β and they share homologous catalytical domains and differ mainly in their C-terminus. Whereas RMI1 associates with TOP3α and the RecQ helicase BLM to dissolve double Holliday junctions in mitotic cells (Raynard et al., 2006), TDRD3 associates with TOP3β and FMRP and recruits them to specific mRNPs (Stoll et al., 2013). The N-terminal domains of TDRD3 as well as of RMI1 consist of a DUF1767 domain and an OB-fold. The recently solved structure of the N-terminal Domain of TDRD3 bound to the catalytic domain of TOP3β revealed that the core-domain and an insertion-loop of the OB-fold of TDRD3 mediate the interaction

with the domain II in the catalytical TOPO domain of TOP3β. Moreover, TDRD3 seems to require both these interactions of the insertion loop and the core-domain for the discrimination between TOP3β and TOP3α (Goto-Ito et al., 2017). As the domain II in the TOPO domain of TOP3β appears to be rather flexible, an induced fit is proposed for the binding of TDRD3. Thereby, their interaction seems to be mainly hydrophobic and only a few single hydrogen bonds occur (Goto-Ito et al., 2017).

Interaction of TDRD3 with FMRP

Whereas TDRD3 binds via its N-terminal domain to TOP3β, the binding to FMRP occurs via the FIM in its C-terminal part. This interaction between TDRD3 and FMRP is abolished by a single missense-mutation in the KH2 domain of FMRP that leads to the isoleucine 304 asparagine (I304N) substitution (Linder et al., 2008). Interestingly, this mutation was found to cause the severe fragile X syndrome phenotype in a patient (De Boulle et al., 1993). However, TDRD3 seems to recruit FMRP only to the TTF-containing mRNPs. Consistent with this, FMRP is absent from the TOP3β-containing mRNPs in cells expressing exclusively a FIM deletion mutant of TDRD3, but it still associates with polysomes and other mRNPs (Stoll et al., 2013). Nevertheless, the I304N mutation impairs the association of FMRP with polysomes (Feng et al., 1997) although its ability to directly bind to the ribosome per se seems not to be affected (Chen et al., 2014). Therefore, the KH2-domain affected by the mutation might mediate the recruitment of FMRP to its target mRNPs in the cell. This recruitment might be mediated via the interaction of the KH2 domain with various recruitment-factors or else via its direct binding to mRNAs. However, the I304N mutation was shown to only slightly affect the ability of FMRP to bind to mRNPs per se (Feng et al., 1997; Laggerbauer et al., 2001) and seems rather to impact the sequence specificity to some extent (Ascano et al., 2012). Although the severe phenotype caused by the I304N mutation emphasizes the important role of the interactions mediated by the KH2 domain for the cellular function of FMRP, it is not yet known whether FMRP indeed might require additional factors for its overall association with mRNPs. Nevertheless, it has become quite clear that TDRD3 acts as such a recruitment-factor for FMRP within the context of the TTF complex, on which I focus in this work.

Association of the TTF complex with the EJC

TDRD3, was found to directly bind to the EJC core consisting of MAGOH/B eIF4AIII, BTZ and Y14 via its EBM (Figure 6C). Earlier reports have shown that the predicted EBM of TDRD3 is not only required for its own mRNP association but also for the recruitment of TOP3β to mRNPs and polysomes (Stoll et al., 2013). Therefore, the direct interaction of TDRD3 with the EJC provides the potential mechanism for the recruitment of the TTF complex to mRNPs: After the formation of the TTF complex via binding to TOP3β and FMRP, TDRD3 likely binds via its EBM to the EJC on mRNPs and thus loads TOP3β and FMRP with it onto the respective mRNP. However, it is still unknown to which EJCs the TTF complex is recruited and how the selection of the EJCs or the corresponding mRNAs occurs. There were reports

showing that TDRD3 associates with the chromatin via the binding of its Tudor domain to certain asymmetrically dimethylated arginines on histone-tails (Yang et al., 2010). As TDRD3 with a mutated Tudor domain was found to be diminished in its association with mRNPs and polysomes *in vivo* although these interactions were not affected *in vitro*, a hypothetical recruitment model (Figure 17) was established (Stoll et al., 2013). This model suggested that TDRD3 recruits TOP3β to transcription start sites (TSS) via interacting with the histone modifications (Yang et al., 2010, 2014) in the first step of the recruitment process (Figure 17A). From there, it is thought to be co-transcriptionally loaded together with TOP3β and FMRP as TTF complex onto the nascent mRNP via its binding to the EJC in the second recruitment-step (Figure 17B). Although TDRD3 was indeed found to be associated with the TSS of some genes and with the corresponding transcripts, TDRD3 was also associated with some mRNAs but not with the TSS of the corresponding gene and was found at the TSS of a gene but not at the respective mRNA (Morettin et al., 2017). These recent findings show that the recruitment model might not necessarily involve the chromatin association step (Figure 17B) and that there might be other mechanisms that direct the TTF complex to the EJCs of mRNPs or regulate its loading.

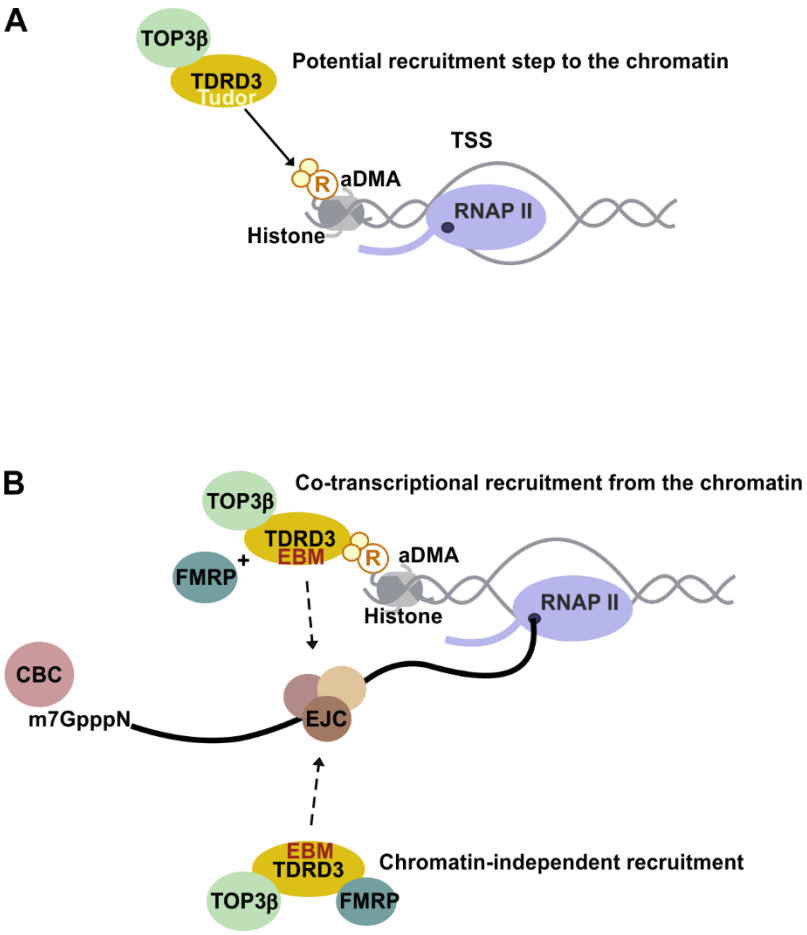

Figure 17: **Hypothetical model of the TTF recruitment to mRNPs via interaction of TDRD3 with the EJC. (A) TDRD3 interacts with asymmetrically dimethylated arginine-marks on histone-tails at promotor regions.** TDRD3 binds via its Tudor domain to certain asymmetrically dimethylated arginine residues of histone-tails at transcription start

sites (TSS) and thus recruits TOP3β with it to the chromatin (Yang et al., 2010, 2014). This association might possibly occur prior to a potential, co-transcriptional loading of the TTF complex to EJC of the nascent transcript. **(B) Recruitment of the TTF complex to mRNPs mediated by binding of TDRD3 to the EJC.** TDRD3 might be loaded together with TOP3β and FMRP from the TSS at the chromatin onto the EJC of the transcribed mRNPs. However, the chromatin association seems not to be necessarily involved in the recruitment to the mRNP and not each TSS association of TDRD3 seems to lead to the recruitment onto the respective transcript (Morettin et al., 2017). Alternative mechanisms or pathways are likely to exist which might mediate or regulate the attachment of the TTF complex to certain mRNPs via the interaction of TDRD3 with the EJC.

5.2. Contribution of TOP3β and FMRP to the cellular interactions of the TTF complex

As reported here and elsewhere, the role of TDRD3 as recruitment-factor and adaptor of the TTF complex has been established (Stoll et al., 2013). Nevertheless, it was not clear whether apart from TDRD3 also TOP3β or FMRP might play a functional role in the TTF assembly process or whether they might directly influence its mRNP association.

The contribution of TOP3β and FMRP to the TTF assembly on mRNPs

Via IP of TDRD3 deletion mutants which abolished the interaction with TOP3β, FMRP or both proteins, I could show that neither its interaction with TOP3β nor with FMRP were necessary for the association of TDRD3 with the other TTF component or with mRNPs (Figure 9). Early mRNP proteins like MAGOH and CBP20 as well as general mRNP proteins like PABPC1 were found to co-precipitate with the TDRD3 mutants to the same extent as with the wt protein. This suggests, that presumably neither TOP3β nor FMRP actively involved in the TTF complex assembly per se or in its association to early mRNPs.

Contribution of TOP3β and FMRP to the association with the translation machinery

The co-precipitation of TDRD3 with the translation machinery was not affected by the deletions in the IP (Figure 9). Consistent with this, also the co-sedimentation of the deletion mutants with polysomes was not altered compared to the full length protein (Figure 10). In contrast, the mutation of the Tudor domain and the mutation of the EBM decreased and abolished the polysomal association of TDRD3, as expected (Stoll et al., 2013). These findings indicate, that neither TOP3β nor FMRP are needed for

the polysomal association of TDRD3. Therefore, it is not likely that TOP3β and FMRP actively contribute to the initial steps that mediate the association of the TTF complex with translation.

Potential contribution of the TTF components to the fate of the mRNPs

Despite the findings described above, it is not clear whether TOP3β and FMRP might be necessary for the mRNPs to progress through the mRNA metabolism although they seem not to be actively required for the correct associations of the TTF complex itself. As there are no information available about the number of TTF complexes per mRNP at present, there could possibly be several TTF complexes present on each mRNA and not only one. In this case, the endogenous TDRD3 present in the cells could assemble the full TTF complex on an additional EJC of the same mRNA. Therefore, it can`t be excluded that an intact TTF complex would compensate on the transcript-level for the incomplete TTF complex which contains the mutated TDRD3. This intact TTF complex could then, for example, mediate the removal of R-loops to allow efficient transcription, mediate the export, the intracellular location or the translation of the mRNP, as will be discussed in detail in later sections.

5.3. The TTF interactome reflects early mRNPs and the translation machinery and links the TTF complex to the pioneer round of translation

The biochemical investigation of the TTF complex revealed important interactions to key factors of the translation machinery (Chen et al., 2014; Khandjian et al., 1996; Napoli et al., 2008; Singh et al., 2012; Stoll et al., 2013; Xu et al., 2013). These data, however, were insufficient to allow a detailed knowledge about the functional context in which the TTF complex acts. To close this gap, a comprehensive proteomics approach was chosen to determine the entire TTF complex interactome. To minimize the number of non-specific interactors, the respective experiments were performed in triplicates and selected interactors were validated in separate experiments. Already a visualization of the interactome on a silver-stained SDS-PAGE showed that the interactors of each TTF component are extremely numerous (Figure 7B). On a side note, interactors generally seem to rather sub-stoichiometrically co-precipitate with overexpressed FLAG/HA-TOP3β, unlike the interactors of TDRD3 and FMRP. As the overall association of TOP3β with mRNPs and polysomes depends strictly on its interaction with TDRD3 (Stoll et al., 2013), this observation might be explained by the assumption that increased levels of TOP3β would probably not be associated with mRNPs or reach polysomes due to limited availability of TDRD3 for recruitment. Despite this, the very similar band pattern observed in the IPs still suggested a good overlap of interactors between the TTF proteins. This was also confirmed by analysis of the interactors via mass spectrometry. Consistent with earlier findings by others and myself, TDRD3, TOP3β and FMRP were found to share a large number of common interactors. Hence, the TTF complex

is very likely to acts as a functional unit at the same pathways of the mRNA metabolism (Stoll et al., 2013).

The TTF interactome reveals the mRNP code of the TTF-associated mRNPs

The Functional analysis of the TTF interactome revealed that among the interactors of each individual TTF component proteins with the GO terms mRNA-binding proteins, cytoplasmic proteins and proteins of the translation machinery were enriched (Figure 19). Likewise, the same GO terms were also found to be enriched in the common TTF interactome (Figure 8E). Therefore, it has become quite clear that the TTF complex is associated with mRNPs and the translation machinery. Moreover, the identification of the interactors provided a good overview of the mRNP code of the TTF-containing mRNPs and could help to assign the complex to specific steps in the mRNA metabolism. Thus, the detection of the EJC core proteins and components of the CBC in the IPs of all three TTF proteins shows that TDRD3, TOP3β and FMRP associate with mRNPs already at their early stage in the mRNA metabolism, before or during the pioneer round of translation (Table 1). Moreover, the association with ACIN1 and PNN, peripheral EJC proteins which are restricted to the nucleus (Hir et al., 2016), suggests that the integration of the TTF complex into the mRNPs takes already place in the nucleus prior to the export to the cytosol. Therefore, this observation is consistent with the hypothesis that the TTF complex is probably loaded co-transcriptionally on the mRNPs.

The TTF complex is restricted to the pioneer round of translation

The interactome studies as well as biochemical studies of this thesis clearly link the TTF complex with the translation machinery and polysomes. It was therefore a surprise that eIF4E, a key factor in translation initiation could not be detected among the interactors in the proteomics study. Hence, it was tempting to speculate that the TTF complex is exclusively part of early mRNPs. This may indicate that the complex participates in the pioneer round of translation but does not take part in the steady state translation which involves eIF4E as part of eIF4F.

This assumption was supported by findings regarding the polysomal co-sedimentation pattern of the TTF proteins upon transcription inhibition. Here it was found that the co-sedimentation of TDRD3 and TOP3β with polysomes was completely abolished upon transcription inhibition. It is therefore likely that TDRD3 and TOP3β dissociate from the mRNPs and the translation machinery after the first round of translation as their polysomal association was found to be highly dependent on newly transcribed mRNAs (Figure 11B). Since TDRD3 and TOP3β are apparently restricted to the pioneer round of translation, the TTF complex as functional unit is only present at the mRNPs before and during the first round of translation. On the contrary, FMRP was still associated with polysomes upon transcription inhibition as it was also observed for PABPC1 (Figure 11B). This finding could suggest that FMRP remains associated with the mRNPs beyond the pioneer round of translation when TDRD3 and TOP3β

already have dissociated and participates in the steady state translation. However, the retained polysomal association of FMRP might be also explained by alternative scenarios. It is also possible that FMRP dissociates from some mRNPs, for example from the TTF-containing mRNP subset, already before or after the pioneer round of translation, but participates to a large extent in the steady state translation of other mRNPs. Since FMRP was shown to stall translating ribosomes on the mRNPs, it is also a possible that the retained polysomal co-sedimentation of FMRP upon transcription inhibition resulted at least in part from stalled ribosomes. In theory, these ribosomes could already be stalled during their first round of translation and have persisted in this state during the transcription inhibition. Hence, based on these results no definite conclusion can be drawn regarding the behaviour of FMRP upon translation.

Taken together, these findings suggest, that the trimeric TTF complex as a functional unit is present only at early mRNPs and that at least TDRD3 and TOP3β disassociate from the translation machinery after the pioneer round of translation. Therefore, it appears likely that the TTF complex plays a specific role prior or during the pioneer round of translation.

FMRP at distinct mRNP subsets and distinct steps in the mRNA metabolism

As FMRP is also associated with other mRNP subsets independently of the TTF complex (Stoll et al., 2013) and showed a different polysomal co-sedimentation behaviour as TDRD3 and TOP3β upon transcription inhibition, the following section particularly focuses on the FMRP interactome identified in this work.

Consistent with its TTF-independent mRNP association, TDRD3 and TOP3β were not among the most-enriched interactors in the FMRP IP (Figure 8C). However, in this experiment only a few factors were found to interact with FMRP, which were not also associated with TDRD3 (Figure 8D, Table 1). This leads to the impression, that although FMRP is part of distinct mRNP subsets, it still might take part to a certain extent in the same metabolic steps in the life of these mRNPs as it does as part of the TTF complex. However, the possibility can`t be excluded, that the interactome of FMRP identified in this experiment might be incomplete and some factors were simply not detected. This might also explain the fact that unexpectedly eIF4E was not present in the IP of FMRP although FMRP might also participate on the steady state translation. Nevertheless, some differences in the binding of individual interactors became still apparent in the WB (Figure 9C). FMRP was found to associate with the common mRNA-binding factors PABPC1 and LARP4 and the translation machinery represented by rpS6 and rpL7 approximately to the same extent as TDRD3. In contrast, the association with the early mRNP proteins MAGOH and CBP20 was rather weak when compared to their association with TDRD3 in the WB. Based on these differences it is tempting to speculate, that presumably rather a small part of FMRP is associated with early mRNPs in the cell. Moreover, also LARP1 was found to be decreased in its

association with FMRP when compared to the IP of TDRD3. This probably also reflects the association of FMRP with distinct mRNP subsets or processes that might involve a different mRNP code.

5.4. TDRD3 and TOP3β form a stable-subunit within the TTF complex

The TTF complex is assumed to function as one unit in the mRNA metabolism of early mRNPs, as was previously discussed. Since mRNPs are highly dynamic complexes and especially many factors are associated only transiently at early mRNPs, the dynamics of the TTF interactome were examined. For this, the interactions of TDRD3 as the adaptor and recruitment factor of the TTF complex were investigated regarding their stability. The analysis of IPs from cells labeled via SILAC, revealed that only the interaction between TOP3β and TDRD3 persisted through the course of the IP, whereas FMRP as well as every other interactor were found to interact rather transiently with TDRD3 and to disassociate and re-bind more dynamically (Figure 11A). This shows that TDRD3 and TOP3β are stably connected with each other and they might form a separate subunit, namely the "TT unit" of the TTF complex. This result is also in agreement with the finding that TDRD3 and TOP3β directly interact with each other and form a stable hetero-dimer *in vitro* (Figure 6A), as discussed in earlier sections. Furthermore, TDRD3 was also reported to stabilize TOP3β *in vivo* and to prevent its proteasomal degradation (Yang et al., 2014) which might functionally argue for a close connection of both proteins, in addition.

In contrast, FMRP seems to join the TT unit later to form the full TTF complex and/or it might dissociate from the complex earlier, while TDRD3 and TOP3β stay tightly associated together.

Consistent with the hypothesis that FMRP might join TDRD3 and TOP3β at a later step, the interaction of TDRD3 with FMRP occurs via the FIM, but *in vivo* an interaction of the Tudor domain seems to be important before TDRD3 can bind to FMRP. Unlike FMRP, the binding of TOP3β to TDRD3 is not dependent on this interaction and TOP3β might already be associated with TDRD3 at that point in the cell (Stoll et al., 2013). Therefore, it appears likely that FMRP joins TDRD3 and TOP3β to complete the TTF complex when both proteins are already connected as the TT subunit. In this context, it is possible that TDRD3 and TOP3β play a separate role as hetero-dimer, which could be distinct from their function as part of the TTF complex. In agreement with this possibility, it has been reported that TDRD3 recruits TOP3β to TSS via the interaction of its Tudor domain to relax hypernegatively supercoiled DNA to prevent the formation of R-loops during transcription (Yang et al., 2014). FMRP might then join the TT unit afterwards before or upon loading of the TTF complex onto the mRNPs (Figure 17). Moreover, the observation that TDRD3 and TOP3β are both restricted to the pioneer round of translation suggests in this context that TDRD3 and TOP3β might dissociate together as TT subunit from the translation

machinery and FMRP after the first round of translation, but probably still remain connected together as hetero-dimer afterwards.

5.5. TOP3β directly binds to the 80S ribosome and connects also TDRD3 with the ribosome

FMRP takes not only part in the translation associated with mRNPs, but it was also shown to bind directly to the 80S ribosome. Thereby, FMRP binds the 80S ribosome at the inter-subunit space at a region spanning the central protuberance and A-site finger of the 60S subunit to the S12 region in the 40S subunit (Chen et al., 2014). Hence, FMRP was proposed to repress the translation elongation either via synergistically interacting with the mRNA and the 80S ribosome or via interfering with the binding of translation elongation factors and tRNAs to the ribosome. Furthermore, the data presented in this thesis link the full TTF complex which co-sediments with polysomes to the pioneer round of translation. However, the function of this complex is not clear. In this work evidence is provided that apart from FMRP, also TOP3β can directly bind to the 80S ribosome (Figure 12). Although TDRD3 as the third component of the TTF complex failed to bind to the ribosome by itself, TOP3β was capable to mediate the interaction of TDRD3 with the ribosome (Figure 13). However, it is not known yet whether FMRP and TOP3β or the whole TTF complex can bind at the same time to the 80S particle. It is possible that some of the potential interactions among the TTF proteins and the ribosome are mutually exclusive and that a component or components dissociate from the complex at that point. Nevertheless, TDRD3 and TOP3β were found to be tightly connected with each other in the cell. This suggests that TOP3β probably binds at least as a complex with TDRD3 and presumably also with FMRP to the ribosome.

Given that TOP3β binds as part of the TTF complex to the 80S ribosome, the binding site of TOP3β is likely in proximity to the FMRP binding site or their binding sites might even partially overlap. Especially in the case that the components exclude each other at the ribosome, it is rather likely that they bind to the same site. Consistent with both scenarios, TOP3β binds besides the 80S ribosome also to both the 40S and the 60S subunit (Figure 14). Therefore, it is possible that the binding site of TOP3β is also located at the inter-subunit space. Thereby, the binding seems to occur via the RGG box of TOP3β as the deletion of this motif abolished these interactions (Figure 12, Figure 14). Moreover, its RGG box seems to be also responsible for the ability of TOP3β to bind directly to the mRNA (Ahmad et al., 2017). Nevertheless, the RGG deletion mutant associates with polysomes like the wt TOP3β *in vivo* (Figure 15A). This suggests that the interaction of TOP3β with TDRD3 is sufficient to mediate the association of TOP3β with the mRNP during the translation, whereas the direct contact of TOP3β with the mRNA seems to be negligible for this association. Furthermore, both TOP3β and FMRP were not required for

the association of TDRD3 with the translation machinery (Figure 10), although TDRD3 failed to bind the 80S ribosome on its own (Figure 13A). Both results lead to the assumption that the TTF complex is presumably associated with mRNPs via the interaction of TDRD3 with the EJC or with the mRNA directly during the first round of translation. Therefore, it appears likely that the potential interaction of TOP3β with the 80S ribosome occurs when the translating ribosome moves along the mRNA and approaches the EJC occupied with the TTF complex. This would propose a binding at the site for TOP3β on the ribosome at the site where the mRNA entry tunnel is located. This criterion is also met by the binding site of FMRP, which is in rough proximity to the mRNA entry tunnel (Chen et al., 2014).

When the first translating ribosome comes close to the EJC it removes the EJC via the interaction of its associated EJC disassembly factor PYM and the Y14/MAGOH complex (Gehring et al., 2009). It is unknown whether the TTF components dissociate with the EJC from the mRNA or if they remain associated with the mRNP by directly binding to the mRNA at that point. Thus, the interaction of the TTF components with the 80S ribosome can possibly occur before, during or directly after the EJC disassembly. If the complex does not dissociate from the mRNP upon disassembly of the EJC, there are three different scenarios possible: (I) As the translating ribosome moves along the mRNA, the TTF complex could interfere with the motion of the ribosome. This could potentially lead to ribosomal stalling like it was already observed for the translational repressor FMRP (Darnell et al., 2011). However, it is unclear whether FMRP plays a similar role as part of the TTF complex. (II) The complex could fully or partially dissociate when the ribosome moves over the binding site of the complex on the mRNA. Thereby, it is also possible that the contact with the 80S ribosome mediates the dissociation step. (III) The complex could move along with the 80S ribosome and dissociate from the translational machinery at a later point. The dissociation step could then potentially involve the interaction with additional factors like translation termination factors or 3'UTR-associated proteins. Nevertheless, in any case, the connection of TOP3β and TDRD3 with the ribosome is likely to occur rather transiently, as TOP3β and TDRD3 seem to dissociate from the translation machinery after the pioneer round of translation (Figure 11B). In addition, a small reduction in the polysomal association of the TOP3β- and FMRP-binding mutant TDRD3 compared to the wt would be expected if the association with the ribosome was quite stable and occurred for a longer period.

5.6. TOP3β is an RNA topoisomerase bound to ribosomal RNA

TOP3β – a topoisomerase with the ability to catalytically convert DNA and RNA

The catalytical activity of TOP3β on DNA substrates was intensively studied and TOP3β was shown to be capable of relaxing hypernegatively supercoiled DNA (Seki et al., 1998; Yang et al., 2014).

Furthermore, TDRD3 was reported to recruit TOP3β to the chromatin via its Tudor domain. At the chromatin, TOP3β seems to prevent the formation of R-loops during the transcription of the corresponding gene by relaxing the arising hypernegatively supercoiled DNA (Yang et al., 2014). However, TOP3β was shown to associate with TDRD3 and FMRP as part of the TTF complex at early mRNPs and to take part in their first round of translation. This observation strongly suggests, that TOP3β does not only function during the transcription in relaxing DNA but that the enzyme plays a role in the post-transcriptional mRNA metabolism. In agreement with that assumption, I could show that TOP3β is able to form a covalent intermediate not only with single-stranded DNA substrates but also with RNA substrates (Figure 15B, C). As the covalent intermediate is formed upon cleavage of the nucleic acid strand to enable the passage of the other strand, this finding suggests that TOP3β might also be able to topologically convert RNA substrates. Thereby, the same active site tyrosine was used for the formation of the covalent intermediate as for the DNA substrate, since the point-mutation (Y336F) of this active site amino acid abolished the reaction.

Some differences were observed between the TOP3β-catalyzed reaction with DNA and RNA substrates. Although both substrates used in this work share the same sequence, a cleavage site closer to the 3'end was preferred over a second minor site closer to the 5'end when the DNA was offered as substrate. This resulted in the release of a greater portion of the larger 5'end-labeled DNA fragment. On the contrary, upon incubation with the RNA oligonucleotide a cleavage site closer to the 5'end was preferred over the site closer to the 3'end within this nucleic acid. Therefore, a greater portion of the smaller 5'end-labeled fragment was released due to the denaturation of the enzyme (Figure 15C). Furthermore, the formation of the covalent intermediate with the DNA substrate was observed at a pH of 7.0, but not at pH 5.5, whereas the intermediate with the RNA substrate was only observed at pH 5.5, but not at pH 7.0. These results indicate that the activity of TOP3β towards either DNA or RNA might be regulated and that the binding of the nucleic acids might require a different conformation within the enzyme. It is also possible that the interaction with other proteins or factors might modulate the catalytical activity *in vivo* and might contribute to the substrate selection in the cellular context.

It was recently shown that TOP3β can convert RNA circles into RNA knots (Xu et al., 2013) and catalyze the annealing of circular RNAs (Siaw et al., 2016). These results show, that this topoisomerase can indeed completely catalyze the topological conversion of RNA substrates including the passage of the intact strand, as the findings in this work proposed. Therefore, it is possible that TOP3β enzymatically functions in the TTF complex to regulate the topological status of the corresponding mRNA.

TDRD3 regulates the enzymatic activity of TOP3β in the cell

The catalytical activity of TOP3β on both DNA and RNA substrates was shown to be specifically enhanced by the presence of TDRD3 in the reaction (Siaw et al., 2016). Therefore, TDRD3 functions not

only as bridging-factor connecting TOP3β with FMRP into the TTF complex. TDRD3 also seems to directly modulate the activity of TOP3β in two different ways: Besides enhancing the catalytical activity on both DNA and RNA substrates (Siaw et al., 2016), TDRD3 connects TOP3β with its cellular substrates. Thus, TDRD3 was shown to recruit TOP3β to the chromatin, where TOP3β acts on DNA as it prevents the formation of R-loops by relaxing the DNA during the transcription (Yang et al., 2010). TDRD3 recruits TOP3β within the TTF complex to specific mRNPs (Stoll et al., 2013) and the mRNA could then serve as potential RNA substrate for the topoisomerase. In addition, TDRD3 indirectly connects TOP3β also with the translating ribosome as the interaction with TDRD3 is required for the enzyme to reach the translation machinery via the mRNPs (Stoll et al., 2013). Thereby the ribosomal RNA itself could possibly be another RNA substrate or the association with the ribosome at translation might be the process where the activity on the mRNA might be required. In this work, I could show that TOP3β binds to ribosomal RNA at the 80S ribosome as well as at the 40S and the 60S subunit and the binding is abolished by deleting the RGG box (Figure 14C). Interestingly, the RGG box was not required for the formation of the covalent intermediate with a short RNA oligo-nucleotide (Figure 15C). Moreover, the topological conversion of an RNA circle, which requires the full catalytical circle, was reduced upon deletion of the RGG box but not abolished (Xu et al., 2013). Therefore, it is possible that, although TOP3β is bound via its RGG box to the ribosome, it is capable to catalytically convert not only the rRNA itself but that the remaining part of the enzyme is still able to convert the mRNA when the enzyme is bound to the ribosome. As the direct binding to the mRNA *in vivo* was also reported to occur via the RGG box (Ahmad et al., 2017), TDRD3 might assist the enzyme at this point by contributing to the binding and conversion of the potential mRNA substrate. Notably, the pivotal role of the interactions mediated by the RGG box in the neuronal function of TOP3β becomes apparent as the respective mutant failed to rescue the defects in synapse formation of *Drosophila top3β* deletion mutants. Moreover, also the catalytical activity of TOP3β seems to be equally important for its function since the active site mutant was also not able to rescue this phenotype (Ahmad et al., 2017).

As TDRD3 and TOP3β are very stably connected in the cell and participate together at biological processes, the importance of TDRD3 for the coordination of the topological activity of TOP3β in the cellular context is again underlined. However, it is not clear, which role the association with FMRP plays and whether it also might influence the activity of the topoisomerase or might even be required for its function at a certain process. Apart from that, also additional interactions might be important for the correct function of TOP3β in the cellular context which are yet unknown. The point-mutation R472Q within TOP3β was found to cause schizophrenia in a patient like it was frequently observed for the deletion of the whole *TOP3β* gene (Stoll et al., 2013; Xu et al., 2012). However, this mutant of TOP3β formed the covalent intermediate with both DNA and RNA as the wt protein (Figure 15C) and possesses the same catalytical activity on RNA. Also, the association with mRNPs and the ability to bind to mRNA

was not affected by the mutation (Ahmad et al., 2017). The crystal structure of the TOP3β TOPO-Domain suggested that the mutation does not influence the overall structure of the enzyme (Goto-Ito et al., 2017). As the amino acid which is substituted by the mutation resides on the surface of the protein it is likely to account for protein-protein interactions which are assumed to be important for the function of TOP3β in the cell. Although it was reported that the mutation affects the association with FMRP but not with TDRD3 in HeLa cells (Ahmad et al., 2017), it is not clear how this finding could be explained in the cellular context as TDRD3 bridges TOP3β and FMRP and is necessary for their association. Furthermore, I failed to re-produce this observation in HEK 293 cells as TOP3β R472Q still bound similar amounts of FMRP compared to the wt TOP3β at standard IP conditions in my hands (data not shown).

It has become clear that TOP3β is regulated by TDRD3 regarding its interactions, stability and activity in the cell. The findings discussed above provide a complete new perspective for potential functions of this topoisomerase which interact as part of the TTF complex with early mRNPs and the translation machinery in the post-transcriptional metabolism of early mRNPs.

5.7. The TTF components impact the expression of a subset of proteins

The data described so far strongly suggest a role for the TTF complex in the regulation of the post-transcriptional mRNA metabolism and especially a role during the pioneer round of translation becomes very probable for the complex. Therefore, the effect of each single component of the TTF complex on the protein expression was analyzed via pulsed SILAC. These experiments revealed that the knock down of TDRD3, TOP3β or FMRP resulted each in a change of a small subset of proteins, whereas the protein-expression seems not to be affected on a global level (Figure 16). A closer look at the proteins which were regulated by the reduction of each TTF component revealed that some proteins were regulated in the same manner, whereas others differ in their regulation. Some proteins, for example, were found to be up-regulated with the reduction of one TTF protein but down-regulated with the reduction of the other two components. However, as long as the mRNAs associated with the TTF proteins in the HEK 293 cells are yet to be identified, it is not possible to distinguish between direct and indirect effects upon the reduction of the respective TTF protein. It would be very interesting to see, if the mRNPs associated with the TTF complex show a specific regulation pattern in the absence of the TTF components. This knowledge might help to gain a first insight in the functions of the single TTF components in this complex. However, at the moment, it can only be speculated about the effect of the TTF components on the protein-expression. Notably, upon reduction of TOP3β more proteins were down-regulated and only a few proteins were upregulated (Figure 16C). Although the directly

regulated proteins have not been identified yet, the impression is gained by this finding, that TOP3β might possibly rather promote the expression of proteins than repress it. Of course, this assumption would fit to the proposed function of TOP3β in enhancing transcription by preventing R-loop formation (Yang et al., 2014). However, as TDRD3 is needed for the recruitment of TOP3β to the chromatin and has also been described to activate the transcription by that, a similar observation would have been expected upon reduction of TDRD3. On the contrary, TDRD3 affected a slightly smaller subset of proteins, the proteins were both up- and down-regulated and their regulation was also not as strong as with TOP3β and FMRP (Figure 16B-D). This is a little bit surprising as TDRD3 was shown to be the adaptor and recruitment-factor of the TTF complex. On the other hand, FMRP was described to repress the translation of its target mRNAs (Darnell et al., 2011; Laggerbauer et al., 2001), nevertheless the reduction of FMRP resulted equally in up- and down-regulated proteins in the experiments (Figure 16D). This might be explained by secondary or regulatory effects as well as the fact that FMRP might have diverse functions besides translation repression in the cell. As the ectopic expression of FMRP in *Drosophila* eyes with a TOP3β-null background increased the abnormal phenotype observed upon its expression in a wt background, it was proposed that FMRP and TOP3β might at least partially act antagonistically (Xu et al., 2013). Consistent with this presumption, abnormal neuromuscular junctions were observed in *Drosophila* FMRP- or TOP3β-null mutants, whereas a FMRP- and TOP3β double-knock out seemed to suppress this phenotype to some extent (Xu et al., 2013). The hypothetical antagonistic functioning of TOP3β and FMRP would also explain, why the reduction of TDRD3 which recruits both proteins into the complex resulted in only a slight change in the protein-expression. Nevertheless, it can still only be speculated which influence the TTF complex might have on the expression of the mRNPs and how the TTF components might act together. Apart from the potential to reveal the direct effects of the TTF components on the gene expression, the identification of the TTF-associated mRNAs would also enable us to investigate at which step in the mRNA metabolism the regulation takes place: Whether the TTF complex influences the transcription, the processing, the export, the stability or the translation or even several steps in the mRNA metabolism of the respective mRNPs.

5.8. Potential functions of the TTF complex in the mRNA metabolism of early mRNPs

The results obtained as part of this thesis as well as by other laboratories suggest a unifying model for the function of the TTF complex in mRNA metabolism. The TTF complex (or parts thereof) is likely to become loaded onto early mRNPs already in the nucleus, presumably during the course of transcription (Figure 18A). The TTF-containing mRNP is then exported to the cytoplasm. Whether the

TTF complex is involved in the transport process per se is currently unclear (see below). Once in the cytosol, the TTF complex is likely to become displaced from its bound mRNPs during or soon after the pioneer round of translation. Therefore, the TTF complex could potentially function at many steps in the mRNA metabolism (Figure 18). Since the active site tyrosine and the RGG box of TOP3β are required to promote the synapse formation in *Drosophila* (Ahmad et al., 2017), I will mainly focus on situations of the mRNA metabolism which could potentially need a topoisomerase activity in the following discussion.

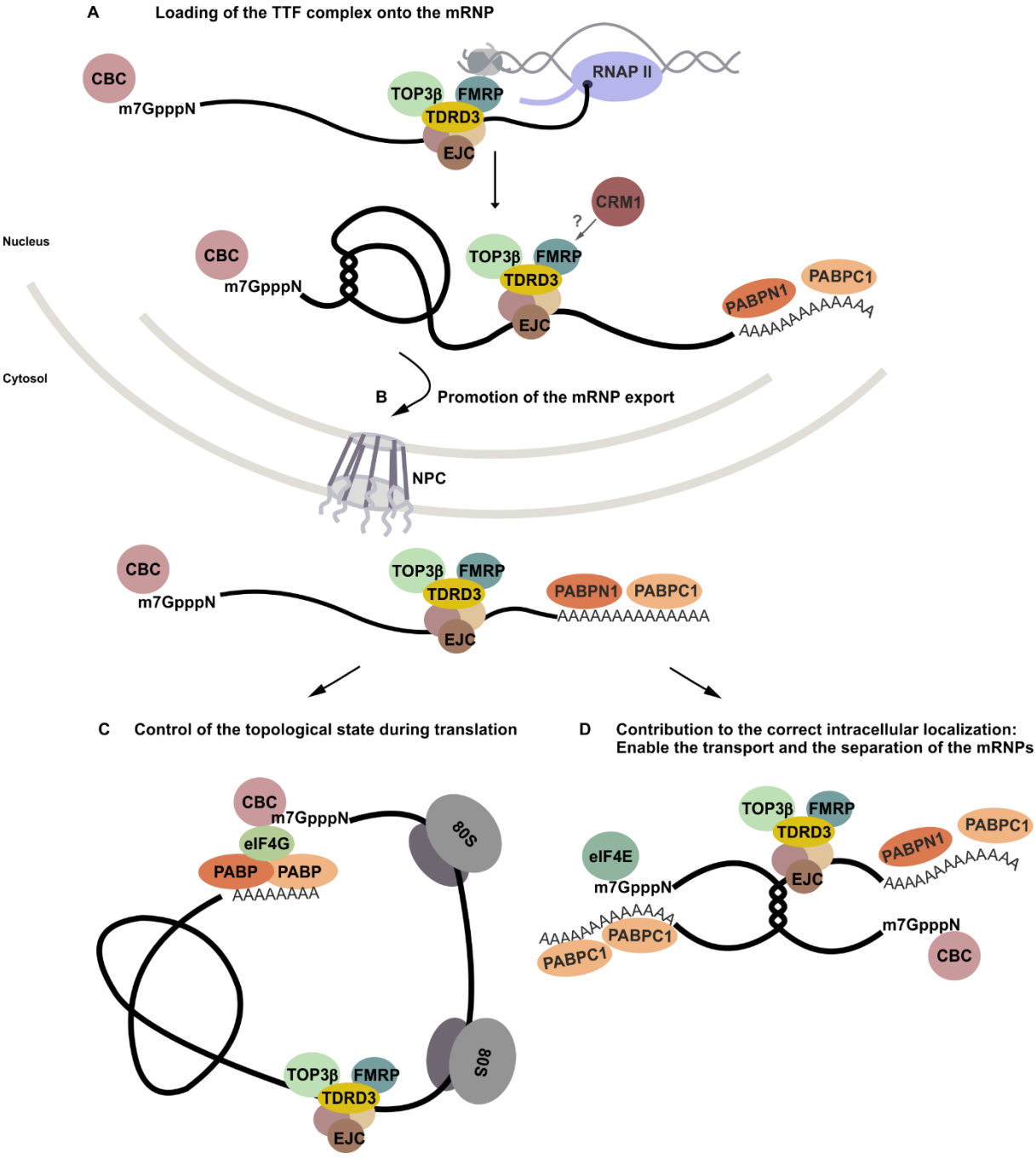

Figure 18: **Hypothetical model of potential functions of the TTF complex in the mRNA metabolism. (A) Co-transcriptional recruitment of the TTF complex.** TDRD3 recruits

TOP3β and FMRP to mRNPs via binding to the EJC. This loading process seems to occur in the nucleus, probably during the transcription. **(B) A role of the TTF complex at the export of the mRNPs.** The TTF complex might function as export adaptor and might mediate a CRM1 dependent export of the mRNPs. In addition, the TTF complex might help to mediate the export of the mRNP via controlling the topological conformation of the mRNP. **(C) Function of the TTF complex during the pioneer round of translation.** The TTF complex might assure that the mRNP adopts a topological arrangement that allows translation of the mRNP. **(D) Contribution of the TTF complex to the correct intracellular localization of the mRNPs.** The TTF complex might be important for the separation of entangled mRNPs. The entanglement could be problematic besides for translation also for the intracellular transport of the mRNPs. The entanglement could possibly occur with an elevated frequency upon stress granule formation where mRNPs are stalled in a high concentration.

The TTF complex might function at the export of mRNPs

It is possible that the TTF complex mediates or enhances the export of the mRNP into the cytoplasm (Figure 18B). All three TTF components are nucleo-cytoplasmic shuttle proteins and each has a CRM1 dependent nuclear export signal (NES) (Eberhart et al., 1996; Stoll et al., 2013). Therefore, they could theoretically recruit the export-factor CRM1 and mediate the export of the mRNPs independently of the general mRNA export pathway via the export factor NXF1-NXT1. In addition, it is also possible that the TTF complex enhances or enables the export of specific mRNPs via its potential remodeling activity. In this scenario the TOP3β subunit would act as RNA topoisomerase that alters the mRNP substrate conformation so that it can be channeled through the nuclear pore. This is likely in the light of the fact that numerous mRNA-binding proteins and protein complexes associate with the mRNP. Therefore, the mRNP might have adopted a secondary structure in the nucleus that interferes with the transit through the NPC and would require the passage of an mRNA strand for its export. In such a case, TOP3β could solve these potential topological problems in the mRNP and thus could ensure the export of the mRNP.

The correct intracellular localization of mRNPs might be assured by the TTF complex

In the cytoplasm, mRNPs usually undergo their first round of translation. However, the translation might not occur immediately and the mRNPs might also be transported within the cell for localized translation at first. It is possible that different mRNP molecules are entangled with each other and require a topoisomerase reaction for their separation to allow a specific cellular localization for the mRNPs.

Upon inhibition of translation initiation due to different stress conditions mRNAs are stalled in SGs in high concentrations (Protter and Parker, 2016). It is easy to imagine that mRNPs might possibly entangle themselves within these condensed foci. In principle, TOP3β which co-localizes with TDRD3

and FMRP to SGs upon arsenite stress (Stoll et al., 2013) could also help to keep the mRNPs separated within the SGs or to separate the mRNPs upon resolution of the SGs (Figure 18D).

The TTF complex might eventually play a role during the pioneer round of translation

Upon initiation of the pioneer round of translation via the CBC, the translation initiation-factor eIF4G binds to the CBC at the 5'end cap (Lejeune et al., 2004; McKendrick et al., 2001) and additionally interacts with PABP at the poly(A) tail (Amrani et al., 2008; Novoa and Carrasco, 1999; Tarun and Sachs, 1996; Tarun et al., 1997; Wells et al., 1998). This interaction between the proteins bound to each end of the mRNA results in the formation of a closed loop of the mRNP molecule. At that point, it is possible once again that the mRNP is arranged due to additional protein-protein interactions or RNA secondary structures in a way that leads to sterical problems for the movement of the ribosome during translation (Figure 18C). Thereby, the topological problems could potentially occur through intra- or inter-molecular interactions, for example due to catenation between different mRNPs. Although helicases could solve certain secondary structures like some stem-loops etc., there might also arise topological formations that would require the strand passage by a topoisomerase. It is conceivable that TOP3β might function as part of the TTF complex at the pioneer round of translation to remove such potential structures and thus ensures efficient translation afterwards.

Different mechanisms of action are possible for the putative topological conversion by TOP3β. The interaction with the ribosome could allow the TTF complex to move along with the first translating ribosome for a certain time until the complex dissociates, for example upon translation termination. During that movement, TOP3β could solve topological obstacles in the mRNA which interfere with the movement of the ribosome. Alternatively, the complex could also solve the topological obstacles during the translation while still being associated with the EJC and the mRNP before the contact with the translating ribosome occurs. The interaction with the 80S ribosome could then serve as dissociation mechanism for the TTF complex.

It is tempting to speculate about the role of FMRP in the complex at both hypothetical scenarios. FMRP could for example help to arrange the complex at the translating 80S ribosome or its action as translational repressor could be required to repress the translation until the topological conversion has been performed by TOP3β.

Unlike the function of FMRP, the role of TDRD3 in the complex appears to be a little more clear: TDRD3 seems to function not only as recruitment-factor for the complex that brings the topoisomerase together with FMRP to the mRNPs and therefore mediates also indirectly the association with the translation machinery (Stoll et al., 2013). Moreover, the tight connection with TDRD3 stabilizes TOP3β

(Yang et al., 2014) and it is likely that TDRD3 also promotes the activity of TOP3β on the mRNA during these processes (Siaw et al., 2016) and thus functions in directly regulating the activity of TOP3β.

The TTF complex might act as a control mechanism for the progress of specific mRNPs through the mRNA metabolism

It is easy to imagine that the TTF complex might function as control unit that alters the topological arrangement of its associated mRNPs during their progression through the mRNA metabolism, if necessary. Thereby, the complex would assure that the requirements for their efficient translation are fulfilled or function in their regulation. However, the function of the TTF complex remains yet unknown and further evidence will be required to confirm these hypotheses.

It is very likely the TTF complex might be necessary for the expression of some proteins, as discussed above, or regulates their expression, especially during the pioneer round of translation. Thus, the reduction of the TTF components resulted in small but reproducible change in protein-levels (Figure 16). Nevertheless, the complex seems not to have an impact on the global gene expression per se as only a small subset was affected in the experiments, respectively. In consistence with this, it was recently reported that the translation of some mRNAs to which TDRD3 was bound was decreased upon reduction of TDRD3 levels in the cell whereas non-target mRNAs were not affected (Morettin et al., 2017). As TDRD3 recruits the TTF complex to the mRNPs, a similar effect would be also expected upon depletion of the whole TTF complex.

The TTF complex in the context of neuronal protein expression

In the light of these findings and the potential functions of the TTF complex in the mRNA metabolism, the question raises which targets in particular might require the TTF complex for their expression or which targets might be regulated by this complex. As neuropsychiatric disorders are associated with the absence of functional FMRP and TOP3β, neurons seem to be the cell type which depends the most on the function of the TTF complex.

Notably, in neurons generally longer transcripts are expressed as compared to other cell types (Zylka et al., 2015). Statistically, longer transcripts could adopt structures containing topological problems with a higher probability than shorter transcripts. Interestingly, a HITS-CLIP-experiment revealed that TOP3β seems to be mainly associated with longer mRNA also in HeLa cells (Xu et al., 2013).

Moreover, neurons build neuronal circuits that can dynamically respond to sensory, cognitive or emotional experiences. For this, neurons require a localized expression of proteins which depends on neuronal activity and regulates the function of synapses. This activity-dependent protein expression is regulated via signaling networks that induce the transcription of genes, lead to post-translational modifications and promote localized protein synthesis at the synapse (Ebert and Greenberg, 2013).

Thereby, one function of FMRP is thought to be the negative regulation of the translation of specific mRNAs at the synapse (Zalfa et al., 2003). This repression by FMRP was shown to be controlled via its phosphorylation (Ceman et al., 2003; Narayanan et al., 2007). Therefore, it is suggested that FMRP is rapidly dephosphorylated upon glutamate receptor signaling to stop the translation repression and is re-phosphorylated after a short time, which restores the translation inhibition (Bassell and Warren, 2008; Ceman et al., 2003; Ebert and Greenberg, 2013; Narayanan et al., 2007; Niere et al., 2012). Consistent with this, the absence of FMRP in knock out mice results in an increased basal protein level and the loss of the stimulus-dependent induction of translation for FMRP-regulated mRNAs (Ebert and Greenberg, 2013; Niere et al., 2012). Due to the short release of FMRP-mediated repression upon neuronal signaling, these mRNAs are translated for a very short period and only a few rounds of translation can occur. It appears to be a logic consequence thereof that this rapid and dynamic regulation of the protein synthesis must rely on an equally and solidly efficient translation. Therefore, it is possible that the TTF complex is particularly important in neurons to guarantee a constantly efficient translation of the mRNAs after it has controlled and potentially corrected the topological status of the mRNPs during the first round of translation.

However, at the moment, it can only be speculated about the potential role of the TTF complex as a functional unit and further investigations are crucial to shed some light into its cellular functions. Thereby, the knowledge of the TTF-associated mRNP subset will enable us to functionally analyze the complex and the role of each of its components. As the TTF complex connects schizophrenia and the fragile X syndrome on a molecular level, this complex represents a unique biochemical tool to study the functional relation between these two neuropsychiatric diseases.

6. Material and methods

6.1. Material

All chemicals, which were used in this work, were purchased from BD Biosciences, Boehringer Ingelheim, Merck, Riedel-de Haen, Roth, Serva and Sigma-Aldrich. Radiochemicals were obtained from Hartmann Analytic. Laboratory consumable supplies were purchased from Eppendorf, Dispomed, Greiner, Hartenstein, Macherey-Nagel, Sarstedt and Sartorius Stedim.

6.1.1. Protein and nucleotide ladders

PageRuler™ Unstained Protein Ladder	Thermo Fisher scientific
PageRuler™ Prestained Protein Ladder	Thermo Fisher scientific
GeneRuler™ DNA Ladder Mix	Thermo Fisher scientific
GeneRuler™ DNA 100bp Plus Ladder	Thermo Fisher scientific

6.1.2. Standard buffers

1x TBT	150 mM NaCl
	6 mM Tris Base
	15 mM Tris-HCl
	0.5% (v/v) Tween
	pH 7.5
10x Laemmli	250 mM Tris
	1.92 M Glycine
	1% (w/v) SDS
5x TBE	445 mM Tris-HCl, pH 8.3
	445 mM boric acid
	10 mM Na2EDTA

6x Protein loading dye	300 mM Tris-HCl, pH 6.8
	12% (w/v) SDS
	30% (v/v) Glycerol
5x DNA loading dye	5 mM Tris-HCl
	0.05 mM EDTA
	0.04% (w/v) Bromphenol blue
	0.04% (w/v) xylene cyanol
2x RNA loading dye	95% (v/v) formamide
	0.025% (w/v) SDS
	0.025% (w/v) bromophenol blue
	0.025% (w/v) xylene cyanol
	0.5 mM EDTA
10x PBS	1.4 M NaCl
	27 mM KCl
	32 mM Na_2HPO_4
	15 mM KH_2PO_4
	pH 7.4
10x NET buffer	1.5 M NaCl
	50 mM EDTA
	500 mM Tris
	0.5% Triton X-100
	pH 7.5
Coomassie-staining solution	0.15% (w/v) Serva Blue R
	15% (v/v) Acetic acid
	45% (v/v) Methanol

Coomassie-destaining solution	30% (v/v) Methanol
	10% (v/v) Acetic acid
Amido black staining solution	0.3% (w/v) Amido black
	10% (v/v) Methanol
	2% (v/v) Acetic acid
Amido black de-staining solution	90% (v/v) Methanol
	3% (v/v) Acetic acid

6.1.3. Cell culture

6.1.3.1. organisms and strains

Bacterial cells

Strain	Chromosomal genotype	Supplier
E. coli DH5α	F-Φ80*lac*ZΔM15 Δ(*lac*ZYA-*arg*F) U169 *rec*A1 *end*A1 *hsd*R17 (rk-, mk+) *pho*A *sup*E44λ- *thi*-1 *gyr*A96 *rel*A1λ-	Invitrogen
E. coli DH10EMBacY		Geneva Biotech
E. coli BL-21-Rosetta	F- *ompT hsdSB*(rB-mB-) *gal dcm* pRARE (CamR)	GE Healthcare

Eukaryotic cell lines

Cell type	Description	Supplier
Sf21	Sf21 (Spodoptera frugiperda) insect cells, derivative of Sf9 cells	ECACC
HeLa S3	Human cervix carcinoma cell line	ECACC
HEK 293	Human embryonic kidney cell line	DSMZ (ACC 035)
Flp-In™ T-REx™ 293	Human embryonic kidney cell line	Invitrogen (R780-07)
Flp-In™ T-REx™ 293 TDRD3 wt		(Stoll, 2015)
Flp-In™ T-REx™ 293 TDRD3 EBM mutant		(Stoll, 2015)
Flp-In™ T-REx™ 293 TDRD3 Tudor mutant		(Stoll, 2015)
Flp-In™ T-REx™ 293 TDRD3 ΔNTD mutant		This work
Flp-In™ T-REx™ 293 TDRD3 ΔFIM mutant		(Stoll, 2015)
Flp-In™ T-REx™ 293 TDRD3 ΔNTD ΔFIM mutant		This work
Flp-In™ T-REx™ 293 TOP3β wt		(Stoll, 2015)
Flp-In™ T-REx™ 293 TOP3β Y336F mutant		This work
Flp-In™ T-REx™ 293 TOP3β ΔRGG mutant		This work
Flp-In™ T-REx™ 293 FMRP wt		This work

6.1.3.2. Cell culture media

Bacterial cell media

Luria broth (LB)	1.0% (w/v) Bacto™ Tryptone
	1.0% (w/v) NaCl
	0.5% (w/v) Bacto™ Yeast Extract
Terrific broth (TB)	1.2% (w/v) Bacto™ Tryptone
	2.4% (w/v) Bacto™ Yeast Extract
	0.4% (v/v) Glycerol
	17 mM KH2PO4
	72 mM K2HPO4

For the generation of LB agar plates, 2% (w/v) Bacto™ Agar was added to the LB medium. Selection media were generated by addition of the respective antibiotics. For this, Ampicillin was added to a final concentration of 100 µg/ml. Kanamycin and Chloramphenicol were used at a concentration of 50 µg/ml and Tetracycline and Gentamycine at 10 µg/ml. For blue/white screening 2 mM ITPG and 2 mM X-Gal was added.

Eukaryotic cell media

Cell line	
Sf21	EX-CELL® TiterHigh™
HEK 293	DMEM
	10% FBS
	1% (v/v) Pen Strep
Flp-In™ T-REx™ 293	DMEM
	10% (v/v) FBS
	10 µg/ml Blasticidin
	100 µg/ml Zeocin

HeLa S3	DMEM
	5-10% FBS
	1% (v/v) Pen Strep
Cryo medium for Sf21 cells	45% EX-CELL® TiterHigh™
	45% culture supernatant
	10% DMSO
Cryo medium adherent cell lines	70% medium
	20% FBS
	10% DMSO
SILAC label medium	DMEM (Invitrogen A14431-01) without glutamine, arginine and lysine
	10% (v/v) FBS dialyzed (Invitrogen 26400-036)
	4 mM glutamine
	antibiotics for labeling over several passages
Light	1.74 mM L-proline (Sigma)
	0.8 mM L-lysine monohydrochloride (Sigma)
	0.4 mM L-arginine monohydrochloride (Sigma)
heavy	1.74 mM L-proline (Sigma)
	0.8 mM L-lysine 2HCl (U-13C6 99%, 15N2 99%, Cambridge Isotope Laboratories)
	0.4 mM L-arginine HCl (U-13C6 99%, 15N4 99%, Cambridge Isotope Laboratories)
medium-heavy	1.74 mM L-proline (Sigma)
	0.8 mM L-lysine 2HCl (4,4,5,5,-D4 96-98%, Cambridge Isotope Laboratories)

0.4 mM L-arginine HCl (U-13C6, Cambridge Isotope Laboratories)

6.1.4. Antibodies

Primary Antibodies

Antibody	Supplier	Dilution (WB)
HA	HISS (MMS-101R)	1:1000
TDRD3	Bethyl (A310-983A)	1:500
TOP3β	Abcam (ab56445)	1:200
FMRP	Linder, et al. 2008	1:500
PABP-C1	Abcam (ab21060)	1:500
LARP1	Abcam (ab86359)	1:500
LARP4	Bethyl (303-900A)	1:1000
CBP20	Santa Cruz (sc-48793)	1:500
MAGOH	Santa Cruz (sc-271405)	1:500
eIF4E	Abcam (ab1126	1:500
rpS6	Abcam (ab59261)	1:1000
rpL7	Abcam (ab72550)	1:1000
β-ACTIN	Sigma-Aldrich	1:1000
α-TUBULIN	Sigma-Aldrich	1:1000
PGD	Abcam (ab129199)	1:2000
TOP2α	Abcam (ab52934)	1:500

Secondary antibodies

Antibody	Supplier	Dilution (WB)
α-mouse gIgG (whole molecule) peroxidase conjugate	Sigma-Aldrich (A4416)	1:5000
α-rabbit gIgG (whole molecule) peroxidase conjugate	Sigma-Aldrich (A6154)	1:5000

6.1.5. Plasmid vectors

Plasmid	Description	Cloning	Reference/Supplier
pFRT/TO/MCS Mammalian expression vector	5'-FLAG/HA-tag insertion into pcDNA5/FRT/TO		(Küspert, 2014)
pFRT/TO/MCS::TOP3β wt	TOP3β-ORF insertion	BamHI/XhoI	(Stoll, 2015)
pFRT/TO/MCS::TOP3β Y336F	Point mutation active site	Mutagenesis	This work
pFRT/TO/MCS::TOP3β ΔRGG	Deletion of RGG box	Mutagenesis	This work
pFRT/TO/MCS::TDRD3 wt	TDRD3-ORF insertion	BamHI/XhoI	(Stoll, 2015)
pFRT/TO/MCS::TDRD3 Tudor mutant	point mutation in Tudor domain	Mutagenesis	(Stoll, 2015)
pFRT/TO/MCS::TDRD3 EBM mutant	point mutations in EBM	Mutagenesis	(Stoll, 2015)
pFRT/TO/MCS::TDRD3 ΔNTD	Deletion of N-terminal domain	Truncation	This work

pFRT/TO/MCS::TDRD3 ΔFIM	Deletion of FIM	Mutagenesis	(Stoll, 2015)
pFRT/TO/MCS::TDRD3 ΔNTD ΔFIM	Deletion of N-terminal domain and FIM	Truncation, mutagenesis	This work
pFRT/TO/MCS::FMRP	FMRP-ORF Insertion, (Q06787-7)	NheI/ApaI	This work
pGEX-6P-1 Bacterial expression vector			GE-Healthcare
pGEX-6P-1 dTag Bacterial expression vector	3'-insertion of a 6xHis-tag into pGEX-6P-1	XhoI	(Stoll, 2015)
pGEX-6P-1 dTag::TOP3β	TOP3β ORF insertion	BamHI/XhoI	(Stoll, 2015)
pGEX-6P-1 dTag::TDRD3	TDRD3 ORF insertion	BamHI/XhoI	(Stoll, 2015)
pACEBac1 Insect cell expression vector			Geneva Biotech
pACEBac1-GST::TOP3β wt	GST-TOP3β ORF insertion	EcoRI/HindIII	This Work
pACEBac1-GST::TOP3β ΔRGG	Deletion	Mutagenesis	This Work
pACEBac1-GST::TOP3β R472Q	Point mutation	Mutagenesis	This Work
pACEBac1-GST::TOP3β Y336F	Point mutation	Muatgenesis	This Work
pACEBac1::FMRP wt-6xHis	FMRP-6xHis-ORF insertion	EcoRI/SalI	This Work
pACEBac1::TDRD3 wt	TDRD3-ORF insertion	BamHI/XhoI	This work

6.1.6. DNA and RNA oligonucleotides

DNA oligonucleotides for cloning and mutagenesis

Primer name	Sequence
GST (EcoRI) forward	AATAGAATTCATGTCCCCTATACTAGG
TOP3β Stop (HindIII) reverse	AATAAAGCTTTCATACAAAGTAGGCGGCC
TOP3β QC Y336F sense	CGCAAGGCTACATCAGCTTCCCACGGACA
TOP3β QC Y336F antisense	TGTCCGTGGGAAGCTGATGTAGCCTTGCG
TOP3β QC R472Q sense	CCCACTTGCCAGCAGGGTGATGCCTTC
TOP3β QC R472Q antisense	GAAGGCATCACCCTGCTGGCAAGTGGG
TOP3β QC ΔRGG (824-840) sense	CCACCCCATGCACCCCCCTGGGAAGC
TOP3β QC ΔRGG (824-840) antisense	GCTTCCCAGGGGGGTGCATGGGGTGG
TDRD3 dNTD (BamHI) forward	AATAGGATCCCCTTTTGGACAGAAGTG
TDRD3 Stop (XhoI) reverse	TATGATCAGCTCGAGTTAGTTCCGAGCCCGGGGTG
FMRP (EcoRI) forward	AATAGAATTCATGGAGGAGCTGGTGGTGG
6xHis Stop (SalI) reverse	AATAGTCGACTCAGTGGTGGTGGTGGTGG
TDRD3 (BamHI) forward	AATAGGATCCATGGCCCAGGTGGCCG
FMRP (NheI) forward	AATAGCTAGCATGGAGGAGCTGGTGG
FMRP (ApaI) reverse	AATAGGGCCCTTAGGGTACTCCATTC

DNA and RNA oligonucleotide substrates for topoisomerase activity

Name	Sequence
R3+ (RNA)	GGGAUUAUUGAACUGUUGUUCAAGCGUGGU
D3+ (DNA)	GGGATTATTGAACTGTTGTTCAAGCGTGGT

6.2. Methods

6.2.1. Molecular biological methods

Polymerase chain reaction (PCR)

PCR was used to amplify DNA for cloning purposes. For this, 50 ng DNA template was mixed with a forward and a reverse primer (0.5 µM each) and a 2x Phusion High fidelity polymerase mastermix (Thermo Fisher scientific) in a 1x final concentration. The reaction was initially denatured at 98 °C for 90 sec. followed by 28 cycles of 30 sec. at 98 °C, 30 sec. at annealing temperature which was determined by the melting temperature of the primers and elongation at 72 °C for a period which depends on the length of the desired amplicon (15-30 sec. per kb). The reaction was ended with a final elongation time span of 7 min at 72 °C and stored at 4 °C till further purification. 2 µl of the reaction were checked by electrophoresis on an agarose gel to confirm the correct size of the product.

Agarose gel electrophoresis

To separate longer DNA products by size agarose gel electrophoresis was performed. Therefore 0.7-2% agarose (dependent on the size of the DNA) was dissolved in 1x TBE buffer by heating. Before pouring the gel in a gel chamber ethidium bromide was added to a final concentration of 5 µg/ml. The electrophoresis was carried out at 140 Volt for 30-60 min. (dependent on the size of the DNA).

Purification of DNA from gels or reactions

DNA products were purified either from reactions (PCR-reaction or restriction digest) directly or from excised gel pieces using the respective clean-up kit from Macherey-Nagel.

Restriction digest of DNA

DNA products were specifically cleaved by restriction endonucleases for cloning purposes. For this PCR products or plasmid vectors (4-8 µg) were digested with 1.5-3 U of the respective restriction enzyme (Fermentas) in the corresponding reaction buffer at 37 °C for 4 h. After 3 h of digestion 1 U Thermosensitive alkaline phosphatase (FastAP, Thermo Fisher Scientific) was added to plasmid vectors to avoid re-ligation after the digestion reaction.

Ligation of DNA fragments

To generate vectors containing a desired fragment, digested vector plasmids were ligated with the respective DNA fragment. For the ligation reaction a 10-fold excess of insert were mixed with the plasmid, and 1 U of T4 DNA ligase (Thermo Fisher scientific) was added in 1x reaction buffer. The ligation was then incubated at 14 °C overnight. After ligation, the entire reaction was used for transformation of competent DH5α *E. coli* cells.

Preparation of competent *E. coli* cells

The desired *E. coli* strains were grown in 50 ml LB medium at 180 rpm and 37 °C overnight. The next day, 4 ml of this culture were used to inoculate a 400 ml LB medium culture . This culture was incubated at the same conditions until an OD^{600} of 0.375 was reached. Then the culture was incubated on ice for 10 min. followed by pelleting of the bacterial cells via centrifugation at 2 °C and 1600 xg for 7 min. The pellet was resuspended in 80 ml buffer containing 60 mM $CaCl_2$, 15% glycerol, 10 mM PIPES pH 7.0. After the resuspension, the cells were collected again by centrifugation and resuspended in 16 ml of the $CaCl_2$-Buffer described before. Finally, 100 µl aliquots were prepared and stored at -80 °C after snap-freezing.

Transformation of chemically competent *E. coli* cells

100 ng of DNA plasmid or a ligation reaction was added to a 100 µl aliquot of competent *E. coli* cells. After gentle mixing, the cap was incubated on ice for 20 min. followed by a heat shock at 42 °C for 45 sec. and subsequent incubation of 2 min. on ice. After that, 500 µl LB medium without antibiotics was added to the cells and they were incubated at 37 °C and 1400 rpm for 1 h in an Eppendorf shaker. Finally, 10% and 90% of the bacteria cells were plated on separate LB agar plates containing the respective antibiotics for selection.

For the transformation of competent DH10EMBacY to generate recombinant bacmid DNA, 2 µg of the desired acceptor plasmid (e.g. pACEBac1) was used. After LB medium was added, the cells were incubated at 37 °C and 1400 rpm for at least 8 h before they were plated on a blue-white screening plate.

Colony-screening

To check the transformed *E. coli* cells for a positive cloning result a colony-screening via PCR was performed. For this, clones from the selection plate were picked using a pipette tip and transferred to a 10 µl PCR reaction. The PCR reaction mix contained the PCR mastermix (Promega) at a 1x concentration, a forward and a reverse primer. Thereby, one of the primers pairs typically with the insert, whereas the other pairs with the plasmid vector of the desired cloning product. After this, a new LB agar plate was inoculated with the respective clone at a marked position, to enable the identification of the clones which were tested the screening so that they can be selectively used for inoculation of a small culture for DNA preparation afterwards. The colony PCR reaction was initially denatured for 5 min. at 95 °C, followed by 27 cycles of 30 sec. at 95 °C, 30 sec. annealing at 47 °C and a elongation period at 72 °C, followed by final elongation at 72 °C for 7 min. and storing at 4 °C. The PCR reaction was then loaded on an agarose gel to check for the amplified product.

The DH10EMBacY cells were checked for positive clones by plating on a X-Gal- and IPTG-containing plate with the respective antibiotics. On this plate, negative colonies appear blue, whereas recombination positive clones are white.

Site-directed mutagenesis

Site directed mutagenesis was used to generate mutations or deletions in pre-existing vector plasmids. For this, two different reaction mixtures were prepared in the first step: Both reactions contained 100 ng DNA template in 1x Phusion polymerase High Fidelity master mix, but to one of the mixtures 0.5 µM forward primer was added and to the other reaction 0.5 µM of the reverse primer. The reactions were incubated for 90 sec. at 98 °C followed by 10 cycles each 30 sec. at 98 °C, 1 min. at 55 °C and 30 sec. per kb of the entire vector size at 72 °C. After a final elongation at 72 °C for 7 min., the reactions were stored at 4 °C. In the second step, these reactions were mixed equally, and 200 µM dNTP-mix and 1 U of Phusion polymerase is added. The reaction mixture was incubated in the thermocycler using the same program as in the first step, but for 18 instead of 10 cycles. Afterwards 1 U Dpn1 restriction enzyme (Fermentas) was added to the reaction and it was incubated at 37 °C for 1 hour to digest the DNA template strand. After the restriction digest, the reaction was used for transformation into competent *E. coli* DH5α cells. The clones were tested for the desired mutation by sequencing.

Purification of bacteria amplified plasmid vectors

After identification of positive clones, they were used to inoculate 5 ml LB cultures for a small-scale preparation of the plasmid DNA. The cultures containing the respective antibiotics were incubated at 180 rpm and 37 °C overnight. The purification was then performed with a mini preparation kit from Macherey-Nagel. For large-scale preparations, a clone was used to inoculate a 2 ml LB pre-culture. After incubation at 180 rpm and 37 °C overnight, the culture was then added to 250 ml LB medium, which was subsequently incubated overnight at 180 rpm at 37 °C. The large-scale plasmid purification was performed using the maxi preparation kit from Macherey-Nagel.

For the purification of bacmid DNA from DH10EMBacY cells, a white colony was used to inoculate 25 ml LB culture containing the respective antibiotics. The cells were grown at 180 rpm at 37 °C overnight and the bacmid DNA was then purified according to the Multibac-manual instructions and was stored at 4 °C in the dark for a maximum of 6 months. This bacmid DNA was used to transfect Sf21 cells to generate a recombinant baculovirus strain for protein expression.

Preparation of glycerol stocks of bacterial cells

For the preparation of glycerol stocks 500 µl of the respective bacterial culture which was grown at 180 rpm and 37 °C overnight were mixed with 750 µl glycerol (86%). Thereof, 100 µl aliquots were

prepared and stored at -80 °C. For the inoculation of a new culture 10 µl of the glycerol stock were used.

6.2.2. Eukaryotic cell culture

Culture and maintenance of adherent cells

Cells were grown at 5% CO_2 at 37 °C and 100% humidity in the appropriate medium. After growing to 100% confluency, the cells were split 1:10 or to the experimental specified confluency. For this, cells were washed once with cold PBS before 0.25% Trypsin-EDTA (life technologies) was added. After the cells started to detach, pre-warmed fresh medium was added to 10 ml and the cells were separated by pipetting up and down. 1 ml of this cell-dilution was then added to a new plate with the appropriate medium.

Culture and maintenance of Sf21 cells

Sf21 cells were grown in flasks with Ex-cell Titer high medium at 27 °C and 100 rpm. Cells were counted, and at a density of 1.5-4 million cells per ml, they were diluted in pre-warmed fresh medium in a new flask to a density of 0.5 million cells per ml.

Preparation of cryo stocks of the eukaryotic cell lines

To preserve the adherent cell lines cryo-stocks were prepared. For this, the cells were detached from the plate surface by Trypsin-EDTA and diluted in fresh medium. After pelleting the cells (5 min. at 400 xg), the supernatant was removed and the cells were resuspended in the cryo medium. The cells were then kept at -20 °C for 4 h and then at -80 °C overnight before they were transferred into liquid nitrogen.

For starting a new culture, one cryo vial was thawed in a 37 °C water bath and the cells were diluted in 10 ml pre-warmed fresh medium. After pelleting, the supernatant was removed, and the cells were transferred with fresh medium into a plate containing fresh pre-warmed medium.

Preparation of cryo stocks of Sf21 cells

For the preparation of cryo stocks, Sf21 cells with 95-100% viability were pelleted and resuspended in cryo-medium for insect cells to 5x 10^7 cells per ml and 1 ml aliquots were prepared thereof in cryo-vials. The cells were then kept for at -20 °C 4 h and then at -80 °C overnight before they were transferred into liquid nitrogen.

For a new culture, one cryo vial was thawed in a 37 °C water bath and the cells were then diluted in 10 ml fresh pre-warmed medium. After pelleting, the cells were diluted in 10 ml medium for a second

time and then collected again. The cells were resuspended and added to 50 ml fresh pre-warmed medium in a 500 ml flask.

Generation of stable Flp-In T-REx 293 cell lines

For the generation of stable Flp-In T-REx 293 cell lines expressing the ORF of the protein of interest upon induction with tetracycline, the cells were grown to 30-40% confluency in antibiotic-free medium. Then the cells were co-transfected with the POG44 plasmid and the pFRT-vector containing the ORF of the protein of interest using Lipofectin (Thermo Fisher scientific). 24 h after the transfection, fresh medium was added and after 48 h, the medium was exchanged with the selection medium containing 10 µg/ml blasticidin and 100 µg/ml hygromycin. The selection medium was exchanged with fresh medium every couple of days until single colonies were clearly visible on the plate. Colonies were picked with Trypsin-EDTA and transferred to a new plate and cultivated. To confirm the expression of the protein of interest the cells were induced for expression with tetracycline (1:2000) and the expression of the protein was checked via immunoblotting.

siRNA transfection of HEK 293 cells

For knock down of the protein of interest HEK 293 cells were grown on a 6-well to 10% confluency in antibiotic-free medium and were transfected with an siRNA either against Firefly luciferase as control or against TDRD3, TOP3β or FMRP (Firefly: eurofins 12US-N200DT and GE healthcare: SMART pool ON-TARGET plus TDRD3 siRNA, TOP3β siRNA, FMR1 siRNA), respectively, using Lipofectamin RNAi-MAX (Thermo Fisher Scientific) as follows:

Target	siRNA (100 µM)	Optimem	Lipofectamin	0ptimem
TOP3β	2 µl	250 µl	4 µl	250 µl
FMRP	2 µl	250 µl	4 µl	250 µl
TDRD3	2 µl	150 µl	12 µl	150 µl

The Firefly control was transfected accordingly. After 24 h the cells were washed with PBS and cells of one well of the 6-well plate were detached with 0.25% Trypsin-EDTA and transferred to a 10 cm plate with pre-warmed medium containing light amino acids.

For the pulsed SILAC experiment, cells were washed twice with PBS and the medium was exchanged 48 h after the transfection. For the control the medium containing heavy amino acids was used and for the knock down of TDRD3, TOP3β or FMRP the medium contained medium-heavy amino acids.

72 h after the transfection, cells were washed with PBS and lysed in 150 mM NaCl, 50 mM TrisHCl pH 7.5, 2.5 mM $MgCl_2$, 0.5% (v/v) NP-40. After incubation on ice for 10 min., the lysates were centrifuged

at 11,000 rpm and 4 °C in a tabletop centrifuge for 10 min. The protein concentration was determined using Bradford assay and for pulsed SILAC 100 µg of the knock down lysate and 100 µg of the respective control lysate were mixed and analyzed via mass spectrometry by Dr. Jens Vanselow, Arbeitsgruppe Schlosser, Rudolf-Virchow Zentrum, Würzburg. For confirmation an analysis of the lysates was carried out also via WB.

Generation of a recombinant baculovirus

For protein expression in eukaryotic insect cells, a recombinant baculovirus was generated. For this Sf21 cells were cultivated at a viability of 95-100% at 100 rpm and 27 °C. For the transfection with bacmid DNA, 1x 10^6 cells in a volume of 2 ml were transferred into one well of a 6-Well plate. The plate was incubated at 27 °C for about 45 min. until the cells attached to the surface of the plate. Then 2 µg of bacmid DNA from DH10EMBacY cells in which the ORF of the protein of interest was inserted via recombination were transfected via Cellfectin II (Thermo Fisher Scientific) according to manufacturer`s instructions. The cells were incubated at 27 °C and after 5 h, the medium was exchanged. After 10 days at 27 °C, the transfection efficiency was monitored via fluorescence microscopy (Zeiss) of the cells, since the backbone of the bacmid encodes for the yellow fluorescent protein YFP. Then the cells were collected, and the supernatant was kept as the initial virus generation V_0. To further amplify the virus, 500 µl of the V_0-virus was used to infect 1 x10^6 fresh cells in 2 ml medium, which were attached on one well in a 6-Well plate. After 6 days incubation at 27 °C the cells were collected again, and the supernatant was kept as second virus generation V_1. The entire V_1-virus corresponding to one well of the plate was used to infect a culture with 100 ml of 1 x10^6 cells per ml. This culture was then incubated at 100 rpm and 27 °C for 72 h followed by collection of the cells (3000 rpm 3 min.). The supernatant was transferred to a falcon and kept as V_2-virus generation which was stored for a maximum of 6 months at 4 °C in the dark. After confirming of the expression of the protein of interest in the infected cells via Western blot and Coomassie staining, the V_2-virus was used to infect Sf21 cells for protein expression.

To determine the number of infective particles for each virus, end-point dilution was used. For this 100 µl of cells with a concentration of 0.2x 10^6 cells/ml were pipetted in the wells of a 96-Well plate. After the cells have attached to the surface, the Virus was diluted to 10^{-4}-10^{-9} and of each dilution 10 µl virus was pipetted into 12 wells of this plate. After 10 days the transfection was monitored via fluorescence microscopy and every well containing fluorescent cells was counted as transfected.

6.2.3. Biochemical methods

Bradford assay

The concentration of proteins in solution was determined using Bradford 1976. For this, a blank and the samples were prepared as follows: 1 µl sample or buffer in 200 µl Bradford reagent (BioRad) and 799 µl H_2O. The blank and the samples were then measured and calculated based on a standard curve in a spectrometer (Eppendorf) at 595 nm.

SDS-PAGE

Proteins were separated by their size using denaturing polyacrylamide gel electrophoresis (SDS-PAGE). The SDS-PAGE was performed in 1x Laemmli buffer at a constant current of 65 mA until the loading dye reached the bottom of the gel.

The typical 11% gel was composed as follows:

Separating gel:

11 ml	Rotiphorese gel 30 (37.5:1 Acrylamid:Bisacrylamid)
5.5 ml	1.5 M TrisHCl pH 8.8
13.5 ml	H_2O
100 µl	APS
100 µl	TEMED

Stacking gel:

1.65 ml	Rotiphorese gel 30 (37.5:1 Acrylamid:Bisacrylamid)
2.45 ml	0.5 M TrisHCl pH 6.8
5.9 ml	H_2O
50 µl	APS
12.5 µl	TEMED

Coomassie-staining of SDS-gels

The gel was incubated for 20 min. in the Coomassie-staining solution while shaking slowly at room temperature (RT). After that, the gel was rinsed with water followed by incubation with destaining solution. The destaining solution is exchanged three or four times until the background is destained and the protein bands are clearly visible.

Silver-staining of SDS-gels

After fixation of the gel in 50% (v/v) methanol, 12% (v/v) acetic acid and 0.5 ml/l formaldehyde (37%) for 2 h, the gel was washed three times in 50% (v/v) ethanol for 15 min. and was incubated in 0.2 g/l sodium thiosulfate for 60 sec. The gel was then washed three times with water for 20 sec. and is then incubated with 2 g/l $AgNO_3$ and 0.75 ml/l formaldehyde (37%) for 25 min. After washing two times with water for 20 sec., the gel is developed with 60 g/l Na_2CO_3 and 0.5 ml/l formaldehyde (37%) until the bands are clearly visible. The staining reaction is then stopped by the addition of 50% methanol and 12% acetic acid.

Expression and purification of recombinant protein in *E. coli*

For the pull down experiment, recombinant GST-TDRD3-6xHis wt or EBM mutant or GST-TOP3β-6xHis were expressed from the pGEX-6-p-1 dtag vector plasmid in *E. coli* BL21 Rosetta II cells. For this, a pre-culture with 200 ml TB medium containing 1:1000 Ampicillin and Chloramphenicol was inoculated with 10 µl of the respective glycerol-stock. The pre-culture was then incubated overnight at 37 °C and 180 rpm.

On the next day, the expression culture was started and 500 ml TB medium in a 2 l baffled flask was supplemented with 10 g glucose and 22.5 g D-Sorbitol as well as with 1:1000 ampicillin and chloramphenicol. This culture was then inoculated with 5 ml of the pre-culture and the bacterial cells were grown at 37 °C and 180 rpm until an OD^{600} of ca. 0.4 was measured. At that point, the cells were induced by the addition of 250 µl IPTG (1M) and 10 ml ethanol (99,9% p.A.) was added. The cells were then incubated for the expression of the protein for 4 h at 15 °C and 180 rpm before they were collected (2.800 xg for 15 min. at 4°C). The pellets were stored at -20 °C until the lysis and purification occurred. The expression was checked on an SDS-PAGE.

For the protein purification, all steps were performed on ice or at 4 °C. The bacterial pellet was resuspended in 50 ml high salt buffer (500 mM KCl, 20 mM HEPES pH 8.0, 10% (v/v) glycerol, 5 mM 2-mercaptoethanol) with additional 5 mM EDTA and 1:1000 protease inhibitors. After resuspension, the lysate was sonicated (Branson sonifier, Duty cycle 50%, Output control 8, 1x 1 min., 1x 45 sec., 1x 30 sec., with at least 1 min. break between each sonication step) followed by centrifugation in a 45Ti Rotor (Beckman Coulter) for 45 min. at 30,000 rpm. The cleared lysate was then incubated with 200 µl

glutathione Sepharose beads for 2 h on a head-over-tail shaker. After collecting, the beads were subsequently washed with 10 ml high salt buffer.

The GST-TDRD3-6xHis protein which was used as prey for the pull down assay with GST-immobilized GST-TOP3β-6xHis, was digested directly on the beads via preScission protease in 1 ml high salt buffer on a head-over-tail shaker overnight to remove the GST-tag. After collection of the beads, the supernatant containing the 6xHis-tagged protein was transferred to 200 µl Ni-NTA for further purification.

The GST-TDRD3-6xHis and the GST-TOP3β-6xHis proteins, which were later immobilized as bait on a glutathione Sepharose column in the pull down assay, were eluted with high salt buffer containing 50 mM reduced L-glutathione in 2 ml. The eluate was then incubated with 200 µl Ni-NTA for 2 h on a head-over-tail shaker. After collecting the Ni-NTA beads, the matrix was washed with 4 ml high salt buffer and with 10 ml low salt buffer (100 mM KCl, 20 mM HEPES pH 8.0, 10% (v/v) glycerol, 5 mM 2-mercaptoethanol), both containing 10 mM imidazole. After washing, the protein was eluted from the column in 10x 200 µl fractions using low salt buffer with 500 mM imidazole. The fractions were analyzed via SDS-PAGE and the peak fractions were used for the pull down experiment, respectively.

Expression and purification of recombinant catalytically active GST-TOP3β in Sf21 cells

For the expression of recombinant GST-TOP3β in Sf21 cells a 200 ml culture with 1x 10^6 cells/ml in fresh Ex-cell Titer high medium was infected with the baculovirus (V_2 generation) containing the GST-TOP3β ORF at a MOI of 1. The culture was incubated for 72h at 27 °C and 100 rpm. After expression, the cells were collected via centrifugation (4 °C 1377 xg for 15 min.) and stored at -20 °C until purification.

All purification steps were performed on ice or at 4 °C. The cell pellet was resuspended in 35 ml high salt buffer (750 mM KOAc, 20 mM HEPES pH 7.5, 10% (v/v) glycerol, 5 mM 2-mercaptoethanol) with 1:1000 protease inhibitors. The lysate was sonicated (Branson sonifier, Duty cycle 50%, Output control 8, 5x 30 sec. with at least 1 min. break between each sonication step) and subsequently centrifuged in a 45Ti rotor (Beckman Coulter) at 25,000 rpm for 45 min. The cleared lysate was then incubated with 200 µl glutathione Sepharose beads for 2 h on a head-over-tail shaker. After collecting, the beads were washed with 4 ml high salt buffer and with 10 ml low salt buffer (100 mM KOAc, 20 mM HEPES pH 7.5, 10% (v/v) glycerol, 5 mM 2-mercaptoethanol). The GST-tagged protein was then eluted in 10x 200 µl fractions using 50 mM reduced L-glutathione in low salt buffer. The peak fractions were collected and either were used immediately or stored at -80 °C after snap freezing.

Co-expression and -purification of GST-TOP3β and TDRD3 or the TTF complex

To co-express proteins in Sf21 cells a 200 ml culture with 1x 10^6 cells/ml was infected with both a virus containing the GST-TOP3β ORF and a virus containing the TDRD3 ORF or with both and a third virus

containing FMRP-6xHis. The expression occurred at 27 °C and 100 rpm for 72 h. The cells were collected as described above and stored at -20 °C.

For the purification the pellet was resuspended in 15 ml high salt buffer (400 mM KOAc, 28 mM HEPES pH 7.5, 4% (v/v) glycerol, 5 mM MgOAc, 5 mM 2-mercaptoethanol) with 1:1000 protease inhibitors, respectively. The lysate was sonicated (Branson sonifier, Duty cycle 50%, Output control 8, 4x 40 sec. with at least 1 min. break between each sonication step) followed by centrifugation in a 45Ti rotor (Beckman Coulter) at 25,000 rpm for 45 min. The cleared lysate was then incubated with 200 µl glutathione Sepharose on a head-over-tail shaker for 2 h. The matrix was washed with 4 ml high salt buffer and 10 ml low salt buffer (100 mM KOAc, 20 mM HEPES pH 7.5, 5 mM MgOAc) followed by elution in 10x 200 µl fractions via low salt buffer containing 50 mM L-glutathione. The fractions were analyzed via Coomassie-staining after SDS-PAGE.

The peak fractions containing co-purified GST-TOP3β and TDRD3 were pooled and used for testing the interaction with the 80S ribosome.

For the co-purification of GST-TOP3β, TDRD3 and FMRP-6xHis the peak fractions were pooled and incubated with 200 µl Ni-NTA on a head-over-tail shaker for 2 h. After collecting the beads, the matrix was washed with low salt buffer containing 10 mM imidazole and eluted in 10x 200 µl fractions using 500 mM imidazole in low salt buffer. The fractions were analyzed via Coomassie staining of a SDS-PAGE.

Pull down assay with immobilized GST-TOP3β-6xHis and TDRD3-6xHis

GST-TOP3β-6xHis was immobilized on glutathione Sepharose and was incubated with equal amounts of TDRD3-6xHis at 4 °C for 1 h. The matrix was then washed with 3x buffer containing 300 mM KCl, 20 mM HEPES pH 8.0 and 0.5% (v/v) NP-40 followed by elution with 1x protein sample buffer at 95 °C for 5 min. The proteins were then analyzed via SDS-PAGE followed by Coomassie staining.

Pull down assay with immobilized GST-TDRD3-6xHis and the EJC core

Either GST-TDRD3-6xHis wt or EBM mutant was immobilized on glutathione Sepharose and incubated with equal amounts of the EJC core (a generous gift from Prof. Elena Conti) consisting of Y14, MAGOH, BTZ and eIF4AIII on U15 RNA for 1 h at 4 °C in a buffer containing 20 mM TrisHCl pH 7.5, 250 mM NaCl, 2 mM MgOAc, 10% (v/v) glycerol, 0.5% NP-40 and 1 mM DTT. After intensive washing with this buffer, the proteins were eluted in 1x protein sample buffer for 5 min. at 95 °C and analyzed on a 4-20% NuPAGE SDS gel via Coomassie staining.

Purification of the 80S ribosome from HeLa S3 pellets

HeLa S3 cells were cultivated in a bioreactor and cells were collected at 6-9x 10^5 cells/ml via centrifugation at 800 xg for 15 min. at 4 °C. After washing with cold PBS, the cell pellets were snap frozen and stored at -80 °C.

All purification steps are carried out on ice or at 4 °C.

The pellet was thawed on ice and incubated with hypotonic lysis buffer (3x volume) containing 10 mM KOAc, 20 mM HEPES pH 7.5, 5 mM MgOAc, 2 mM DTT and 1:1000 protease inhibitors for 20 min. The cells were lysed in a 40 ml B-tight douncer. The lysate was cleared via centrifugation at 22,000 xg for 30 min. and was loaded on a high salt sucrose cushion in a low salt buffer (1 M sucrose, 100 mM KOAc, 20 mM HEPES pH 7.5, 5 mM MgOAc, 2 mM DTT). After centrifugation in a 45Ti rotor at 40,000 rpm for 4 h, the crude ribosomal pellet was washed once with 7 ml resuspension buffer 1 (500 mM KOAc, 20 mM HEPES pH 7.5, 5 mM MgOAc, 2 mM DTT and 1:1000 protease inhibitors) followed by resuspension in 2 ml resuspension buffer 1 overnight. After spinning down shortly, the ribosomes were then loaded on a second sucrose cushion (composition as described before but 500 mM KOAc) followed by centrifugation. The pellet was again resuspended in resuspension buffer 1 and loaded on a 10-30% (w/v) sucrose gradient in resuspension buffer 1 and was centrifuged for 12 h at 22,000 rpm in an SW32Ti rotor (Beckman Coulter). The gradient was harvested by hand in 19x 2 ml fractions and the RNA profile was measured. The fractions containing the 80S peak were pooled and pelleted in a 70Ti rotor (Beckman Coulter) at 35,500 rpm for 4 h. The ribosomal pellet was then resuspended in resuspension buffer 2 (100 mM KOAc, 50 mM HEPES pH 7.5, 15 mM MgOAc, 2 mM DTT).

Purification of the 40S and 60S ribosomal subunits from HeLa S3 cells

HeLa S3 pellets were resuspended in hypotonic lysis buffer (10 mM KCl, 20 mM TrisHCl pH 7.5, 5 mM $MgCl_2$, 2 mM DTT and 1:1000 protease inhibitors) and lysed as described above. After centrifugation at 22,000 xg for 30 min., the lysate was loaded on a sucrose cushion (1 M sucrose, 100 mM KCl, 20 mM TrisHCl pH 7.5, 5 mM $MgCl_2$, 2 mM DTT) and was resuspended after centrifugation in a 45Ti rotor at 40,000 rpm for 4 h, in resuspension buffer 1 (50 mM KCl, 20 mM TrisHCl pH 7.5, 4 mM $MgCl_2$ and 2 mM DTT). After spinning down quickly, the RNA concentration was measured in a photometer and the crude 80S was diluted to 0.150 units of absorption at 260 nm in a volume of 13 ml. To this solution 131.3 µl puromycin-HCl (0.1 M) was added followed by incubation for 10 min. on ice and 10 min. at 30 °C. Next, 1.69 ml 4 M KCl in resuspension buffer 1 was added dropwise under constant shaking. The solution is then loaded on a 10-30% (w/v) sucrose gradient in 500 mM KCl, 20 mM TrisHCl, 4 mM $MgCl_2$ and 2 mM DTT followed by centrifugation in an SW32Ti rotor at 22,000 rpm for 17 h at 4 °C. The gradient is then fractionated in 40x 1 ml fractions and the RNA concentration of each fraction is measured.

The peak fractions of the 40S peak were pooled and diluted with the 3-fold volume of 100 mM KCl, 20 mM TrisHCl pH 7.5, 2 mM $MgCl_2$ and 2 mM DTT and the 60S subunits were pooled and diluted with the 2-fold volume of the same buffer. The ribosomal subunits were pelleted in a 45Ti rotor for 15 h at 38,600 rpm at 4 °C and 40S was directly resuspended in resuspension buffer 2 (100 mM KCl, 20 mM TrisHCl, 2 mM $MgCl_2$, 0.25 M sucrose, 2 mM DTT) and 60S was resuspended after washing in the same buffer. The 40S subunits were stored at -80 °C after snap freezing, whereas the 60S subunits were diluted to 50 mM KCl and loaded on a second 10-30% (w/v) sucrose gradient in 50 mM KCl, 20 mM TrisHCl pH 7.5, 2 mM $MgCl_2$ and 2 mM DTT. The gradient is centrifuged in a SW32Ti rotor at 22,000 xg for 17 h at 4 °C and fractionated in 40x 1 ml fractions. The RNA concentration of each fraction was measured, and the peak fractions were pooled and diluted as described above. The diluted 60S subunits were pelleted via centrifugation in a 70Ti rotor at 35,500 rpm for 15.5 h at 4 °C and resuspended in resuspension buffer 2. After snap freezing, the 60S subunits were stored at -80 °C.

Test for direct interaction with ribosomal particles

To test for direct interaction of recombinant proteins with 80S or 40S and 60S, purified recombinant protein was incubated with the equimolar amount (typically 700 pmol were used) of the respective ribosomal particle and incubated for 7 min. at 30 °C, followed by 5 min. on ice. The solution was centrifuged for 5 min. at 10,000 rpm in a tabletop centrifuge (Eppendorf) and was loaded on a sucrose gradient.

For the interaction with 40S and 60S subunits a 5-30% (w/v) sucrose gradient in 100 mM KCl, 20 mM TrisHCl pH 7.5, 10 mM $MgCl_2$ and 2 mM DTT was used, which was centrifuged in a SW60Ti rotor (Beckman Coulter) at 34,500 rpm at 4 °C for 4 h.

For the interaction with the 80S ribosome a 10-30% (w/v) sucrose gradient in 100 mM KOAc, 50 mM HEPES pH 7.5, 15 mM MgOAc and 2 mM DTT was used and was centrifuged in a SW60Ti rotor (Beckman Coulter) at 34,500 rpm at 4 °C for 2 h 15 min.

After centrifugation, the gradients were manually fractionated in 20x 200 µl fractions and 50 µl of each fraction was analyzed via SDS-PAGE followed by Coomassie-staining or WB.

Pull down and 5' end labeling of rRNA bound by TOP3β

To check for rRNA binding the interaction of recombinant GST-TOP3β wt or ΔRGG mutant with 80S and 40S and 60S was analyzed as described above. The gradient fractions containing the ribosomal particles and the ribosome bound GST-TOP3β fraction were pooled and transferred to a small cell culture dish. After crosslinking twice at 254 nm with 240 mJ/cm^2 (CL-1000 Ultraviolet Crosslinker), the RNA was partially digested with 1:10000 RNase T1 for 7 min. at 22 °C. After incubation for 5 min. on ice, 70 µl glutathione Sepharose beads were added and this was incubated on a head-over-tail wheel at 4 °C for

1 h. The beads were then washed three times with IP buffer (300 mM KCl, 50 mM HEPES pH 7.5, 0.05% (v/v) NP-40, 0.5 mM DTT) followed by a second RNase T1 (1:100) digestion for 15 min. at 22 °C. After incubation for 5 min. on ice, the beads were washed 3 times with high salt buffer (500 mM KCl, 50 mM HEPES pH 7.5, 0.05% (v/v) NP-40, 0.5 mM DTT) and 3 times with FastAP buffer (100 mM NaCl, 50 mM TrisHCl pH 7.9, 10 mM $MgCl_2$, 1 mM DTT). The dephosphorylation was carried out on the matrix and 16 U FastAP in 100 µl FastAP buffer was added to the beads. After incubation at 37 °C for 30 min. at 800 rpm, the beads were washed twice with phosphatase buffer (50 mM TrisHCl pH 7.5, 20 mM EGTA, 0.5% (v/v) NP-40) and twice with PNK buffer (50 mM NaCl, 50 mM TrisHCl pH 7.5, 10 mM $MgCl_2$, 0.5% (v/v) NP-40) followed by 5' end labeling with 4 µl γ-[^{32}P]-ATP (10 mCi/ml, 6000 Ci/mmol) with 1 U/µl PNK in 70 µl 1x reaction buffer A (Fermentas) for 30 min. at 37 °C. Then the beads were washed four times with PNK buffer followed by elution in protein sample buffer for 5 min. at 95 °C. The samples were analyzed via SDS-PAGE which was blotted on nitrocellulose and monitored via autoradiography (Amersham, Hyperfilm).

5' end labeling of DNA and RNA oligonucleotides

To label the 5' end of a DNA or RNA oligonucleotide 2 µl of the oligonucleotide (10 µM) were incubated in a 20 µl reaction with 2 µl T4 polynucleotide kinase (PNK, Thermo Fisher Scientific) and 3 µl γ-[^{32}P]-ATP (10 mCi/ml, 6000 Ci/mmol) in the reaction buffer A for 30 min. at 37 °C. The reaction was mixed with the equal volume of 2x RNA sample buffer and the labeled product was purified via denaturing gel electrophoresis.

Denaturing gel electrophoresis of nucleic acids

For the purification of the 30 nt oligonucleotides after the labeling reaction or analysis of the products of the cleavage assay, gel electrophoresis using a denaturing polyacrylamide urea gel. Therefore, a 12% acrylamide gel was made by dissolving 24 g urea in 10 ml 5x TBE buffer, 15 ml Rotiphorese Gel 40 (19:1 Acrylamide/bisacrylamide) and 7.7 ml water and adding 300 µl APS and 30 µl TEMED. The electrophoresis was then performed at 450 Volt for 60-90 min. in 1x TBE buffer after short boiling and snap freezing of the samples. The gel was then wrapped in saran wrap and was exposed to a film (Amersham) for autoradiography.

For the purification of the labeled oligonucleotides the respective bands were excised and shortly frozen at -80 °C. Then 350 µl elution buffer (0.5 M NH_4OAc, 2 mM $MgCl_2$, 0.1 mM Na_2EDTA, 0.04% (w/v) SDS) was added and the nucleic acids were eluted by shaking at RT overnight. The eluate was transferred into a new reaction cap and 1 µl glycogen and 1 ml cold ethanol (99% p.A.) was added and the cap was put for precipitation for at least 2 h at -20 °C. After centrifugation for 1 h at 13,200 rpm and 4 °C, the supernatant is removed and 800 µl 70% (v/v) is added. After centrifugation for 10 min. at

13,200 rpm and RT, the supernatant was removed completely, and the pellet was dried for up to 5 min. at RT. Finally, the pellet was resuspended in the desired volume of water.

Cleavage assay

To monitor the formation of an intermediate of the topoisomerase with the substrate the cleavage assay was used. For the cleavage reaction with the 30 nt DNA substrate, ca. 20 fmol of the 5' end labeled DNA oligonucleotide were added to 2 pmol GST-TOP3β (wt or mutant) in 40 mM HEPES pH 7.5, 10% (v/v) PEG 400, 40% (v/v) glycerol, 1 mM $MgCl_2$, 1 mM DTT, 10 µg/ml BSA at 42 °C, whereas for the reaction with the RNA substrate, ca. 20 fmol of the 5' end labeled RNA oligonucleotide were added to 2 pmol GST-TOP3β in 40 mM HEPES pH 5.5, 10% (v/v) PEG 400, 40% (v/v) glycerol, 1 mM $MgCl_2$, 1 mM DTT, 10 µg/ml BSA at 42 °C. After incubation for 2 min., SDS was added to a final concentration of 0.2% (w/v) and the reaction was incubated at 42 °C for one more min. The reaction was then put on ice and 2x RNA sample buffer is added. After shortly boiling at 95 °C and subsequently placing on ice, the oligo nucleotides were analyzed on a 12% urea gel.

Polysomal gradient centrifugation

Cells were treated with 25 µg/ml cycloheximide for 10 min. before they were washed with cold PBS and lysed in 100 mM KCl, 20 mM TrisHCl pH 7.5, 5 mM $MgCl_2$, 1 mM DTT, 1:1000 protease inhibitors, 4 U/ml RNase inhibitor murine (New England Biolabs). After incubation for 10 min. on ice, the lysate was centrifuged at 11,000 rpm for 10 min. at 4 °C in a tabletop centrifuge (Eppendorf). The cleared lysate was loaded on a 5-45% (w/v) sucrose gradient in the respective buffer and was centrifuged for 1 h at 38,000 rpm in a SW60Ti rotor. The UV-profile of the gradient was measured and the gradient was fractionated using a gradient fractionator (Biocomp, Piston Gradient Fractionator and BioRad, UV-lamp and Fraction Collector). The fractions of the gradient were then analyzed via SDS-PAGE followed by WB.

Treatment	Concentration	Step	Incubation
Actinomycin D	5 µg/ml	In the medium prior to the cycloheximide treatment	2 h at 37 °C, 5% CO_2, 100% humidity
RNase A	100 µg/ml	After lysis in the cleared lysate	10 min. at 22 °C

6.2.4. Immunobiochemical methods

Western blot (WB)

To transfer proteins separated via SDS-PAGE to a membrane for immunoblotting, semi dry Western blot was used. For this, three layers of Whatman paper were soaked with 1x Towbin blot buffer consisting of 1x Laemmli buffer in 10% methanol. Next, PVDF membrane (0.45 µm, Millipore, Merck) was incubated for 1 min. in methanol and is then laid on top of the Whatman layers. The gel was then carefully placed on the membrane and 3 wetted layers of Whatman paper were put on top of the gel. The transfer occurred in the blotting chamber at 0.8 mA/cm^2 of the gel for 2 h. After blotting, the pre-stained marker was marked with a pencil on the membrane and the membrane was stained with amido black for 1 min. to check the transfer. After de-staining of the membrane by washing two times with amido black de-staining solution, the membrane was washed once with TBT buffer and was then blocked with 5% (w/v) milk powder in TBT for at least 30 min. After blocking, the membrane was washed several times with TBT and was then incubated with the first antibody dilution in 0.025% gelatin in 1x NET buffer and 1:1000 sodium azide overnight at 4 °C. After three times washing for 4 min. with TBT, the membrane was incubated with the secondary antibody diluted in TBT for 2 h at RT. The membrane was washed again for three times for 4 min. with TBT, before the blot was developed using enhanced chemical luminescence (ECL). For this 10 ml of 0.222 g/l luminol in TrisHCl pH 8.5 were mixed with 100 µl of 6.8 mM coumaric acid in DMSO and 8 µl H_2O_2 (30%) and the membrane was incubated with this solution for 1 min. before the membrane was wrapped in a plastic foil and an x-ray film (CEA RP NEW Medical X-Ray, Christiansen and Linhard) was exposed to the signal.

Quantification of WB signals

For the quantification of the ECL signal of Western blots, ImageJ was used (Rasband, W.S., ImageJ, U. S. National Institutes of Health, Bethesda, Maryland, USA, https://imagej.nih.gov/ij/, 1997-2016).

Immunoprecipitation (IP)

Cells were grown to a confluency of 50% and were then induced with 1:2000 tetracycline overnight. On the next day, cells were washed with cold PBS and scraped in IP buffer (150 mM NaCl, 50 mM TrisHCl pH 7.5, 2.5 mM $MgCl_2$, 0.5 mM DTT, 1:1000 protease inhibitors and 4 U/ml RNase inhibitor murine). The lysate was incubated for 10 min. on ice followed by centrifugation for 10 min. at 11,000 rpm at 4 °C in a tabletop centrifuge. The protein concentration was determined via Bradford assay and equal amounts of each lysate was incubated for 1 h with anti-FLAG M2 agarose beads (sigma) on a head-over-tail shaker at 4 °C. The beads were collected, and after washing five times with the IP buffer, elution was carried out with 200 µg/ml 3x FLAG peptide at 550 rpm and 30 °C for 30 min. The eluate was either analyzed via mass spectrometry or on a SDS-PAGE followed by silver-staining or WB.

For the anti-FLAG IP of heavy-labeled FLAG/HA-TDRD3 cells and light-labeled Flp-In T-REx 293 control cells, the cells were grown over 6 passages in the respective medium containing heavy or light amino acids. The lysis was performed as described above, but lysates were divided in two parts. For the first sample, the anti-FLAG IPs were performed separately, along the same lines as described above, and after both IPs were performed, the FLAG-peptide eluates of the control and the FLAG/HA-TDRD3 IPs were mixed equally and analyzed via mass spectrometry. For the second sample, both the control and the FLAG/HA-TDRD3 containing lysates were equally mixed together before the IP was carried out. Then, one anti-FLAG IP is performed of the lysate mix and the eluate of this IP was also analyzed via mass spectrometry.

The mass spectrometry measurement of the IP experiments and the analysis of the data was performed by Dr. Jens Vanselow (AG Schlosser, Rudolf-Virchow Center of Würzburg, Proteomics unit).

7. Supplementary information

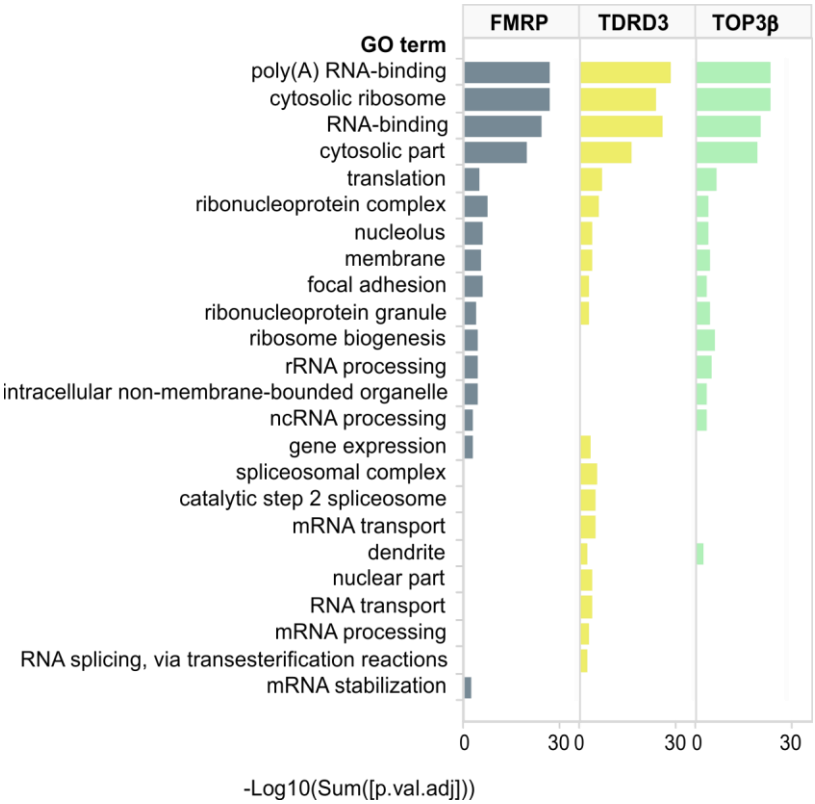

Figure 19: **GO term analysis of the proteins which were significantly associated with the respective TTF protein in the IP experiments.** The significant interactors of the individual TTF proteins are mainly poly(A)RNA-binding proteins, ribosomal proteins and proteins located in the cytoplasm, respectively. Only the most enriched GO terms are depicted in the diagram.

Table 1: **Significant interactors of the TTF proteins TDRD3, TOP3β and FMRP.** The listed proteins were significantly enriched in the individual anti-FLAG IP experiments of the FLAG/HA-tagged TTF component(s) as specified in the headline (bold). The classification is based on the mass spectrometry measurements of the respective IP experiments (Note: The listed proteins correspond to the columns displayed in Figure 8D).

TTF	**TDRD3, TOP3β**	**TDRD3, FMRP**	**TOP3β, FMRP**	**TDRD3**	**TOP3β**	**FMRP**
TOP3B	TDRD3	RPSA	RIOK1	EEF1A1; EEF1A1P5	MMS19	XRCC6
FMR1	EIF4A3	HNRNPC		GNB2L1	HSPH1	NPM1
FXR2	EIF3A	NCL		NCOA5	PDCD6IP	UBAP2L
PRRC2A	RBM8A	ERH		HNRNPA2B1	CIAO1	SDCCAG3
FXR1	ZC3H14	G3BP1		SNRNP200	U2SURP	LGALS3BP

IGF2BP1	CASC3	PRMT1		XRCC5	UBE2O	PRPSAP1
PABPC1	CCDC9	DDX17		HNRNPL	CDKAL1	PPHLN1
PABPC4	EFTUD2	RPL31		PRPF8	ERC1	FBL
YBX1	C17orf85	ILF2		PCBP2	PTPN13	MMTAG2
BCLAF1	ZC3H11A	RPL9		EIF3E		H1FX
RPS3	CPSF1	SRSF4		HNRNPD		TRMT1L
HNRNPU		RPS25		SF3A1		KRI1
RPS8		PRPF19		PGAM5		BLM
THRAP3		SRRM1		HNRNPA3		DNAJC13
HNRNPM		RPL23		ALYREF		
RPL7		HNRNPAB		TRIM27		
RPS11		SSB		EIF3F		
RPL4		TRA2B		CDC5L		
RPS3A		SRSF6		RPL29		
ILF3		SRSF9		ASCC3		
IGF2BP3		RPLP2		EIF3H		
RPS4X		RPL34		HADHA		
CHTOP		RPL35		HNRNPF		
DDX21		NCBP1		EIF3G		
RPL13		TOP1		DDX1		
YBX3		HIST1H1E		RTCB		
RPL3		DDX5		SNW1		
RPL10A		MYCBP2		SF3A3		
RPS2		RPL36		RPS24		
TRIM28		PURA		BCL2L2		
RPS18		SNRNP70		EIF3M		
RPLP0; RPLP0P6		DDX6		RNPS1		
RPS13		XRN2		XAB2		
RPS9		ZNF326		RALY		
DHX9		GTPBP4		SAP18		

RPS6		SRPK1		SRSF3		
RPL5		ATXN2L		PRPF6		
RPS14		NUFIP2		CRNKL1		
RPS19		NOP2		G3BP2		
RPL8		SRSF10		ADAR		
LARP1		SART3		HADHB		
MOV10		RBM14		C19orf47		
SYNCRIP		RPL36A; RPL36A-HNRNPH2		IK		
SRRM2		YTHDF2		AQR		
RPS20		ZC3H18		SNRNP40		
RPL11		TRA2A		ASCC2		
RBMX		YTHDC1		DDX23		
RPS16; ZNF90		STAU2		RBM39		
RPS5		AGO2		HNRNPDL		
DDX39B		SRPK2		SART1		
RPL15		ELAVL2; ELAVL4		USP9X		
UPF1		SMU1		STRBP		
ACIN1		NOP56		RPS21		
SERBP1		ZCCHC3		PLOD1		
RPL12		POP1		MYBBP1A		
RPL7A		FIP1L1		SON		
CAPRIN1		DDX27		RBM22		
PNN		MKI67		ZC3H13		
RPL13A; RPL13a				PPIG		
RPL23A				PRPF3		
RPL17-C18orf32				DDX50		

DHX30				FYTTD1		
RPS15A				CDC40		
RPL18				PLRG1		
RPL19				RBM15		
PRRC2C				USP10		
HNRNPA1; HNRNPA1L2				PRKRA		
IGF2BP2				GLB1		
RPL6				KIAA1429		
RPL10				CPVL		
MATR3				MFAP1		
RPL14				USP7		
RPL26				PEG10		
SF3B2				NKTR		
RPL27				RSL1D1		
RPL28				PRPF4		
RPL22				DDX24		
RPS12				ZNF768		
HNRNPR				CWC22		
SRSF1				L1RE1		
RPS27				DHX57		
HNRNPUL1				TP53		
SRSF7				SAFB		
RPS10				DHX8		
RPL24				SLU7		
RPS17				TNKS		
RPS7						
RPL30						
RPL27A						
STAU1						

DHX15						
FAM120A						
RPL35A						
ELAVL1						
RPL18A						
HNRNPUL2-BSCL2						
MAGOHB						
RPL32						
RPL21						
RPS23						
LARP4B						
ZC3HAV1						
RRP1B						
LARP4						
ZFR						
GNL3						
NKRF						
PURB						
RBM28						
LAS1L						

8. Bibliography

Addington, A.M., Gauthier, J., Piton, A., Hamdan, F.F., Raymond, A., Gogtay, N., Miller, R., Tossell, J., Bakalar, J., Germain, G., et al. (2011). A novel frameshift mutation in UPF3B identified in brothers affected with childhood onset schizophrenia and autism spectrum disorders. Mol. Psychiatry *16*, 238–239.

Ahmad, M., Xue, Y., Lee, S.K., Martindale, J.L., Shen, W., Li, W., Zou, S., Ciaramella, M., Debat, H., Nadal, M., et al. (2016). RNA topoisomerase is prevalent in all domains of life and associates with polyribosomes in animals. Nucleic Acids Res. *44*, 6335–6349.

Ahmad, M., Shen, W., Li, W., Xue, Y., Zou, S., Xu, D., and Wang, W. (2017). Topoisomerase 3β is the major topoisomerase for mRNAs and linked to neurodevelopment and mental dysfunction. Nucleic Acids Res. *45*, 2704–2713.

Alpatov, R., Lesch, B.J., Nakamoto-Kinoshita, M., Blanco, A., Chen, S., Stützer, A., Armache, K.J., Simon, M.D., Xu, C., Ali, M., et al. (2014). A Chromatin-Dependent Role of the Fragile X Mental Retardation Protein FMRP in the DNA Damage Response. Cell *157*, 869–881.

Amrani, N., Ghosh, S., Mangus, D.A., and Jacobson, A. (2008). Translation factors promote the formation of two states of the closed-loop mRNP. Nature *453*, 1276–1280.

Ascano, M., Mukherjee, N., Bandaru, P., Miller, J.B., Nusbaum, J.D., Corcoran, D.L., Langlois, C., Munschauer, M., Dewell, S., Hafner, M., et al. (2012). FMRP targets distinct mRNA sequence elements to regulate protein expression. Nature *492*, 382–386.

Ballut, L., Marchadier, B., Baguet, A., Tomasetto, C., Séraphin, B., and Le Hir, H. (2005). The exon junction core complex is locked onto RNA by inhibition of eIF4AIII ATPase activity. Nat. Struct. Mol. Biol. *12*, 861–869.

Bardoni, B., Schenck, A., and Mandel, J.L. (1999). A novel RNA-binding nuclear protein that interacts with the fragile X mental retardation (FMR1) protein. Hum. Mol. Genet. *8*, 2557–2566.

Bassell, G.J., and Warren, S.T. (2008). Fragile X Syndrome: Loss of Local mRNA Regulation Alters Synaptic Development and Function. Neuron *60*, 201–214.

Beckmann, B.M., Castello, A., and Medenbach, J. (2016). The expanding universe of ribonucleoproteins: of novel RNA-binding proteins and unconventional interactions. Pflüg. Arch. - Eur. J. Physiol. *468*, 1029–1040.

Björk, P., and Wieslander, L. (2017). Integration of mRNP formation and export. Cell. Mol. Life Sci. 1–23.

Brahms, H., Meheus, L., Brabandere, V. de, Fischer, U., and Lührmann, R. (2001). Symmetrical dimethylation of arginine residues in spliceosomal Sm protein B/B' and the Sm-like protein LSm4, and their interaction with the SMN protein. RNA *7*, 1531–1542.

Bugreev, D.V., and Nevinsky, G.A. (2009). Structure and mechanism of action of type IA DNA topoisomerases. Biochem. Mosc. *74*, 1467–1481.

Cao, A., and Galanello, R. (2010). Beta-thalassemia. Genet. Med. *12*, 61–76.

Castello, A., Fischer, B., Eichelbaum, K., Horos, R., Beckmann, B.M., Strein, C., Davey, N.E., Humphreys, D.T., Preiss, T., Steinmetz, L.M., et al. (2012). Insights into RNA Biology from an Atlas of Mammalian mRNA-Binding Proteins. Cell *149*, 1393–1406.

Ceman, S., Brown, V., and Warren, S.T. (1999). Isolation of an FMRP-Associated Messenger Ribonucleoprotein Particle and Identification of Nucleolin and the Fragile X-Related Proteins as Components of the Complex. Mol. Cell. Biol. *19*, 7925–7932.

Ceman, S., O'Donnell, W.T., Reed, M., Patton, S., Pohl, J., and Warren, S.T. (2003). Phosphorylation influences the translation state of FMRP-associated polyribosomes. Hum. Mol. Genet. *12*, 3295–3305.

Champoux, J.J. (2001). DNA Topoisomerases: Structure, Function, and Mechanism. Annu. Rev. Biochem. *70*, 369–413.

Chari, A., Golas, M.M., Klingenhäger, M., Neuenkirchen, N., Sander, B., Englbrecht, C., Sickmann, A., Stark, H., and Fischer, U. (2008). An Assembly Chaperone Collaborates with the SMN Complex to Generate Spliceosomal SnRNPs. Cell *135*, 497–509.

Chen, E., Sharma, M.R., Shi, X., Agrawal, R.K., and Joseph, S. (2014). Fragile X Mental Retardation Protein Regulates Translation by Binding Directly to the Ribosome. Mol. Cell *54*, 407–417.

Chonchaiya, W., Schneider, A., and Hagerman, R.J. (2009). Fragile X: A Family of Disorders. Adv. Pediatr. *56*, 165–186.

Coffee, R.L., Tessier, C.R., Woodruff, E.A., and Broadie, K. (2010). Fragile X mental retardation protein has a unique, evolutionarily conserved neuronal function not shared with FXR1P or FXR2P. Dis. Model. Mech. *3*, 471–485.

Comery, T.A., Harris, J.B., Willems, P.J., Oostra, B.A., Irwin, S.A., Weiler, I.J., and Greenough, W.T. (1997). Abnormal dendritic spines in fragile X knockout mice: Maturation and pruning deficits. Proc. Natl. Acad. Sci. U. S. A. *94*, 5401–5404.

Côté, J., and Richard, S. (2005). Tudor Domains Bind Symmetrical Dimethylated Arginines. J. Biol. Chem. *280*, 28476–28483.

Darnell, J.C., Van Driesche, S.J., Zhang, C., Hung, K.Y.S., Mele, A., Fraser, C.E., Stone, E.F., Chen, C., Fak, J.J., Chi, S.W., et al. (2011). FMRP stalls ribosomal translocation on mRNAs linked to synaptic function and autism. Cell *146*, 247–261.

De Boulle, K., Verkerk, A.J.M.H., Reyniers, E., Vits, L., Hendrickx, J., Van Roy, B., Van Den Bos, F., de Graaff, E., Oostra, B.A., and Willems, P.J. (1993). A point mutation in the FMR-1 gene associated with fragile X mental retardation. Nat. Genet. *3*, 31–35.

Delaleau, M., and Borden, K.L.B. (2015). Multiple Export Mechanisms for mRNAs. Cells *4*, 452–473.

Douglas L. Theobald, Rachel M. Mitton-Fry, and Wuttke, and D.S. (2003). Nucleic Acid Recognition by OB-Fold Proteins. Annu. Rev. Biophys. Biomol. Struct. *32*, 115–133.

Eberhart, D.E., Malter, H.E., Feng, Y., and Warren, S.T. (1996). The Fragile X Mental Retardation Protein is a Ribonucleoprotein Containing Both Nuclear Localization and Nuclear Export Signals. Hum. Mol. Genet. *5*, 1083–1091.

Ebert, D.H., and Greenberg, M.E. (2013). Activity-dependent neuronal signalling and autism spectrum disorder. Nature *493*, nature11860.

Fagerberg, L., Hallström, B.M., Oksvold, P., Kampf, C., Djureinovic, D., Odeberg, J., Habuka, M., Tahmasebpoor, S., Danielsson, A., Edlund, K., et al. (2014). Analysis of the Human Tissue-specific Expression by Genome-wide Integration of Transcriptomics and Antibody-based Proteomics. Mol. Cell. Proteomics *13*, 397–406.

Fatemi, S.H., Kneeland, R.E., Liesch, S.B., and Folsom, T.D. (2010). Fragile X mental retardation protein levels are decreased in major psychiatric disorders. Schizophr. Res. *124*, 246–247.

Feng, Y., Lakkis, L., Devys, D., and Warren, S.T. (1995). Quantitative comparison of FMR1 gene expression in normal and premutation alleles. Am. J. Hum. Genet. *56*, 106–113.

Feng, Y., Absher, D., Eberhart, D.E., Brown, V., Malter, H.E., and Warren, S.T. (1997). FMRP Associates with Polyribosomes as an mRNP, and the I304N Mutation of Severe Fragile X Syndrome Abolishes This Association. Mol. Cell *1*, 109–118.

Fischer, U., Liu, Q., and Dreyfuss, G. (1997). The SMN–SIP1 Complex Has an Essential Role in Spliceosomal snRNP Biogenesis. Cell *90*, 1023–1029.

Fridell, R.A., Benson, R.E., Hua, J., Bogerd, H.P., and Cullen, B.R. (1996). A nuclear role for the Fragile X mental retardation protein. EMBO J. *15*, 5408–5414.

Gatto, C.L., and Broadie, K. (2009). The Fragile X Mental Retardation Protein in Circadian Rhythmicity and Memory Consolidation. Mol. Neurobiol. *39*.

Gebhardt, A., Habjan, M., Benda, C., Meiler, A., Haas, D.A., Hein, M.Y., Mann, A., Mann, M., Habermann, B., and Pichlmair, A. (2015). mRNA export through an additional cap-binding complex consisting of NCBP1 and NCBP3. Nat. Commun. *6*, ncomms9192.

Gehring, N.H., Lamprinaki, S., Kulozik, A.E., and Hentze, M.W. (2009). Disassembly of Exon Junction Complexes by PYM. Cell *137*, 536–548.

Gehring, N.H., Wahle, E., and Fischer, U. (2017). Deciphering the mRNP Code: RNA-Bound Determinants of Post-Transcriptional Gene Regulation. Trends Biochem. Sci. *42*, 369–382.

Gonatopoulos-Pournatzis, T., and Cowling, V.H. (2014). Cap-binding complex (CBC). Biochem. J. *457*, 231–242.

Goto-Ito, S., Yamagata, A., Takahashi, T.S., Sato, Y., and Fukai, S. (2017). Structural basis of the interaction between Topoisomerase IIIβ and the TDRD3 auxiliary factor. Sci. Rep. *7*, srep42123.

Goulet, I., Boisvenue, S., Mokas, S., Mazroui, R., and Côté, J. (2008). TDRD3, a novel Tudor domain-containing protein, localizes to cytoplasmic stress granules. Hum. Mol. Genet. *17*, 3055–3074.

Harigaya, Y., and Parker, R. (2014). Fragile X Mental Retardation Protein and the Ribosome. Mol. Cell *54*, 330–332.

He, Q., and Ge, W. (2017). The tandem Agenet domain of fragile X mental retardation protein interacts with FUS. Sci. Rep. *7*, 962.

Hir, H.L., Saulière, J., and Wang, Z. (2016). The exon junction complex as a node of post-transcriptional networks. Nat. Rev. Mol. Cell Biol. *17*, 41–54.

Hosoda, N., Lejeune, F., and Maquat, L.E. (2006). Evidence that Poly(A) Binding Protein C1 Binds Nuclear Pre-mRNA Poly(A) Tails. Mol. Cell. Biol. *26*, 3085–3097.

Iossifov, I., Ronemus, M., Levy, D., Wang, Z., Hakker, I., Rosenbaum, J., Yamrom, B., Lee, Y., Narzisi, G., Leotta, A., et al. (2012). De Novo Gene Disruptions in Children on the Autistic Spectrum. Neuron *74*, 285–299.

Ishizuka, A., Siomi, M.C., and Siomi, H. (2002). A Drosophila fragile X protein interacts with components of RNAi and ribosomal proteins. Genes Dev. *16*, 2497–2508.

Izaurralde, E., Lewis, J., McGuigan, C., Jankowska, M., Darzynkiewicz, E., and Mattaj, I.W. (1994). A nuclear cap binding protein complex involved in pre-mRNA splicing. Cell *78*, 657–668.

Jolly, L.A., Homan, C.C., Jacob, R., Barry, S., and Gecz, J. (2013). The UPF3B gene, implicated in intellectual disability, autism, ADHD and childhood onset schizophrenia regulates neural progenitor cell behaviour and neuronal outgrowth. Hum. Mol. Genet. *22*, 4673–4687.

Kashima, I., Jonas, S., Jayachandran, U., Buchwald, G., Conti, E., Lupas, A.N., and Izaurralde, E. (2010). SMG6 interacts with the exon junction complex via two conserved EJC-binding motifs (EBMs) required for nonsense-mediated mRNA decay. Genes Dev. *24*, 2440–2450.

Katahira, J. (2012). mRNA export and the TREX complex. Biochim. Biophys. Acta BBA - Gene Regul. Mech. *1819*, 507–513.

Khandjian, E.W., Corbin, F., Woerly, S., and Rousseau, F. (1996). The fragile X mental retardation protein is associated with ribosomes. Nat. Genet. *12*, 91–93.

Kühn, U., and Wahle, E. (2004). Structure and function of poly(A) binding proteins. Biochim. Biophys. Acta BBA - Gene Struct. Expr. *1678*, 67–84.

Küspert, M. (2014). Untersuchung zur Rolle des La-verwandten Proteins LARP4B im mRNA-Metabolismus.

Laggerbauer, B., Ostareck, D., Keidel, E.-M., Ostareck-Lederer, A., and Fischer, U. (2001). Evidence that fragile X mental retardation protein is a negative regulator of translation. Hum. Mol. Genet. *10*, 329–338.

Laumonnier, F., Shoubridge, C., Antar, C., Nguyen, L.S., Van Esch, H., Kleefstra, T., Briault, S., Fryns, J.P., Hamel, B., Chelly, J., et al. (2010). Mutations of the UPF3B gene, which encodes a protein widely expressed in neurons, are associated with nonspecific mental retardation with or without autism. Mol. Psychiatry *15*, 767–776.

Le Hir, H., Izaurralde, E., Maquat, L.E., and Moore, M.J. (2000). The spliceosome deposits multiple proteins 20-24 nucleotides upstream of mRNA exon-exon junctions. EMBO J. *19*, 6860–6869.

Lee, K.-M., and Tarn, W.-Y. (2013). Coupling pre-mRNA processing to transcription on the RNA factory assembly line. RNA Biol. *10*, 380–390.

Lejeune, F., Ranganathan, A.C., and Maquat, L.E. (2004). eIF4G is required for the pioneer round of translation in mammalian cells. Nat. Struct. Mol. Biol. *11*, nsmb824.

Li, Z., Zhang, Y., Ku, L., Wilkinson, K.D., Warren, S.T., and Feng, Y. (2001). The fragile X mental retardation protein inhibits translation via interacting with mRNA. Nucleic Acids Res. *29*, 2276–2283.

Linder, B., Plöttner, O., Kroiss, M., Hartmann, E., Laggerbauer, B., Meister, G., Keidel, E., and Fischer, U. (2008). Tdrd3 is a novel stress granule-associated protein interacting with the Fragile-X syndrome protein FMRP. Hum. Mol. Genet. *17*, 3236–3246.

Linder, B., Fischer, U., and Gehring, N.H. (2015). mRNA metabolism and neuronal disease. FEBS Lett. *589*, 1598–1606.

Ling, S.-C., Fahrner, P.S., Greenough, W.T., and Gelfand, V.I. (2004). Transport of Drosophila fragile X mental retardation protein-containing ribonucleoprotein granules by kinesin-1 and cytoplasmic dynein. Proc. Natl. Acad. Sci. U. S. A. *101*, 17428–17433.

Liu, K., Guo, Y., Liu, H., Bian, C., Lam, R., Liu, Y., Mackenzie, F., Rojas, L.A., Reinberg, D., Bedford, M.T., et al. (2012). Crystal Structure of TDRD3 and Methyl-Arginine Binding Characterization of TDRD3, SMN and SPF30. PLOS ONE *7*, e30375.

Loreni, F., Thomas, G., and Amaldi, F. (2000). Transcription inhibitors stimulate translation of 5′ TOP mRNAs through activation of S6 kinase and the mTOR/FRAP signalling pathway. Eur. J. Biochem. *267*, 6594–6601.

Lorson, C.L., Strasswimmer, J., Yao, J.-M., Baleja, J.D., Hahnen, E., Wirth, B., Le, T., Burghes, A.H.M., and Androphy, E.J. (1998). SMN oligomerization defect correlates with spinal muscular atrophy severity. Nat. Genet. *19*, 63–66.

Lorson, C.L., Hahnen, E., Androphy, E.J., and Wirth, B. (1999). A single nucleotide in the SMN gene regulates splicing and is responsible for spinal muscular atrophy. Proc. Natl. Acad. Sci. *96*, 6307–6311.

Lunde, B.M., Moore, C., and Varani, G. (2007). RNA-binding proteins: modular design for efficient function. Nat. Rev. Mol. Cell Biol. *8*, 479–490.

Maity, A., and Das, B. (2016). N6-methyladenosine modification in mRNA: machinery, function and implications for health and diseases. FEBS J. *283*, 1607–1630.

Maquat, L.E., Tarn, W.-Y., and Isken, O. (2010). The Pioneer Round of Translation: Features and Functions. Cell *142*, 368–374.

Mazroui, R., Huot, M.-E., Tremblay, S., Filion, C., Labelle, Y., and Khandjian, E.W. (2002). Trapping of messenger RNA by Fragile X Mental Retardation protein into cytoplasmic granules induces translation repression. Hum. Mol. Genet. *11*, 3007–3017.

McKendrick, L., Thompson, E., Ferreira, J., Morley, S.J., and Lewis, J.D. (2001). Interaction of Eukaryotic Translation Initiation Factor 4G with the Nuclear Cap-Binding Complex Provides a Link between Nuclear and Cytoplasmic Functions of the m7 Guanosine Cap. Mol. Cell. Biol. *21*, 3632–3641.

Meister, G., Bühler, D., Pillai, R., Lottspeich, F., and Fischer, U. (2001). A multiprotein complex mediates the ATP-dependent assembly of spliceosomal U snRNPs. Nat. Cell Biol. *3*, 945–949.

Monani, U.R., Lorson, C.L., Parsons, D.W., Prior, T.W., Androphy, E.J., Burghes, A.H., and McPherson, J.D. (1999). A single nucleotide difference that alters splicing patterns distinguishes the SMA gene SMN1 from the copy gene SMN2. Hum. Mol. Genet. *8*, 1177–1183.

Morettin, A., Paris, G., Bouzid, Y., Baldwin, R.M., Falls, T.J., Bell, J.C., and Côté, J. (2017). Tudor Domain Containing Protein 3 Promotes Tumorigenesis and Invasive Capacity of Breast Cancer Cells. Sci. Rep. *7*, 5153.

Myrick, L.K., Nakamoto-Kinoshita, M., Lindor, N.M., Kirmani, S., Cheng, X., and Warren, S.T. (2014). Fragile X syndrome due to a missense mutation. Eur. J. Hum. Genet. *22*, 1185–1189.

Myrick, L.K., Hashimoto, H., Cheng, X., and Warren, S.T. (2015a). Human FMRP contains an integral tandem Agenet (Tudor) and KH motif in the amino terminal domain. Hum. Mol. Genet. *24*, 1733–1740.

Myrick, L.K., Deng, P.-Y., Hashimoto, H., Oh, Y.M., Cho, Y., Poidevin, M.J., Suhl, J.A., Visootsak, J., Cavalli, V., Jin, P., et al. (2015b). Independent role for presynaptic FMRP revealed by an FMR1 missense mutation associated with intellectual disability and seizures. Proc. Natl. Acad. Sci. *112*, 949–956.

Napoli, I., Mercaldo, V., Boyl, P.P., Eleuteri, B., Zalfa, F., Rubeis, S.D., Marino, D.D., Mohr, E., Massimi, M., Falconi, M., et al. (2008). The Fragile X Syndrome Protein Represses Activity-Dependent Translation through CYFIP1, a New 4E-BP. Cell *134*, 1042–1054.

Narayanan, U., Nalavadi, V., Nakamoto, M., Pallas, D.C., Ceman, S., Bassell, G.J., and Warren, S.T. (2007). FMRP Phosphorylation Reveals an Immediate-Early Signaling Pathway Triggered by Group I mGluR and Mediated by PP2A. J. Neurosci. *27*, 14349–14357.

Nicholson, P., Yepiskoposyan, H., Metze, S., Orozco, R.Z., Kleinschmidt, N., and Mühlemann, O. (2010). Nonsense-mediated mRNA decay in human cells: mechanistic insights, functions beyond quality control and the double-life of NMD factors. Cell. Mol. Life Sci. *67*, 677–700.

Niere, F., Wilkerson, J.R., and Huber, K.M. (2012). Evidence for a Fragile X Mental Retardation Protein-Mediated Translational Switch in Metabotropic Glutamate Receptor-Triggered Arc Translation and Long-Term Depression. J. Neurosci. *32*, 5924–5936.

Nimchinsky, E.A., Oberlander, A.M., and Svoboda, K. (2001). Abnormal Development of Dendritic Spines in*FMR1* Knock-Out Mice. J. Neurosci. *21*, 5139–5146.

Novoa, I., and Carrasco, L. (1999). Cleavage of Eukaryotic Translation Initiation Factor 4G by Exogenously Added Hybrid Proteins Containing Poliovirus 2Apro in HeLa Cells: Effects on Gene Expression. Mol. Cell. Biol. *19*, 2445–2454.

Oberle, I., Rousseau, F., Heitz, D., Kretz, C., Devys, D., Hanauer, A., Boue, J., Bertheas, M.F., and Mandel, J.L. (1991). Instability of a 550-base pair DNA segment and abnormal methylation in fragile X syndrome. Science *252*, 1097–1102.

Phatnani, H.P., and Greenleaf, A.L. (2006). Phosphorylation and functions of the RNA polymerase II CTD. Genes Dev. *20*, 2922–2936.

Ponting, C.P. (1997). Tudor domains in proteins that interact with RNA. Trends Biochem. Sci. *22*, 51–52.

Protter, D.S.W., and Parker, R. (2016). Principles and Properties of Stress Granules. Trends Cell Biol. *26*, 668–679.

Proudfoot, N.J. (2011). Ending the message: poly(A) signals then and now. Genes Dev. *25*, 1770–1782.

Proudfoot, N.J., Furger, A., and Dye, M.J. (2002). Integrating mRNA Processing with Transcription. Cell *108*, 501–512.

Pullmann, R., Kim, H.H., Abdelmohsen, K., Lal, A., Martindale, J.L., Yang, X., and Gorospe, M. (2007). Analysis of Turnover and Translation Regulatory RNA-Binding Protein Expression through Binding to Cognate mRNAs. Mol. Cell. Biol. *27*, 6265–6278.

Raynard, S., Bussen, W., and Sung, P. (2006). A Double Holliday Junction Dissolvasome Comprising BLM, Topoisomerase IIIα, and BLAP75. J. Biol. Chem. *281*, 13861–13864.

Rodor, J., Pan, Q., Blencowe, B.J., Eyras, E., and Cáceres, J.F. (2016). The RNA-binding profile of Acinus, a peripheral component of the exon junction complex, reveals its role in splicing regulation. RNA *22*, 1411–1426.

Sato, H., and Maquat, L.E. (2009). Remodeling of the pioneer translation initiation complex involves translation and the karyopherin importin β. Genes Dev. *23*, 2537–2550.

Schwanhäusser, B., Gossen, M., Dittmar, G., and Selbach, M. (2009). Global analysis of cellular protein translation by pulsed SILAC. PROTEOMICS *9*, 205–209.

Seki, T., Seki, M., Onodera, R., Katada, T., and Enomoto, T. (1998). Cloning of cDNA Encoding a Novel Mouse DNA Topoisomerase III (Topo IIIβ) Possessing Negatively Supercoiled DNA Relaxing Activity, Whose Message Is Highly Expressed in the Testis. J. Biol. Chem. *273*, 28553–28556.

Shatkin, A.J. (1976). Capping of eucaryotic mRNAs. Cell *9*, 645–653.

Siaw, G.E.-L., Liu, I.-F., Lin, P.-Y., Been, M.D., and Hsieh, T. (2016). DNA and RNA topoisomerase activities of Top3β are promoted by mediator protein Tudor domain-containing protein 3. Proc. Natl. Acad. Sci. *113*, E5544–E5551.

Sikorsky, T., Hobor, F., Krizanova, E., Pasulka, J., Kubicek, K., and Stefl, R. (2012). Recognition of asymmetrically dimethylated arginine by TDRD3. Nucleic Acids Res. *40*, 11748–11755.

Sims, R.J., Rojas, L.A., Beck, D., Bonasio, R., Schüller, R., Drury, W.J., Eick, D., and Reinberg, D. (2011). The C-Terminal Domain of RNA Polymerase II Is Modified by Site-Specific Methylation. Science *332*, 99–103.

Singh, G., Kucukural, A., Cenik, C., Leszyk, J.D., Shaffer, S.A., Weng, Z., and Moore, M.J. (2012). The Cellular EJC Interactome Reveals Higher-Order mRNP Structure and an EJC-SR Protein Nexus. Cell *151*, 750–764.

Singh, K.K., Wachsmuth, L., Kulozik, A.E., and Gehring, N.H. (2013). Two mammalian MAGOH genes contribute to exon junction complex composition and nonsense-mediated decay. RNA Biol. *10*, 1291–1298.

Siomi, H., Siomi, M.C., Nussbaum, R.L., and Dreyfuss, G. (1993). The protein product of the fragile X gene, FMR1, has characteristics of an RNA-binding protein. Cell *74*, 291–298.

Siomi, M. c., Siomi, H., Sauer, W. h., Srinivasan, S., Nussbaum, R. l., and Dreyfuss, G. (1995). FXR1, an autosomal homolog of the fragile X mental retardation gene. EMBO J. *14*, 2401–2408.

Siomi, M.C., Zhang, Y., Siomi, H., and Dreyfuss, G. (1996). Specific sequences in the fragile X syndrome protein FMR1 and the FXR proteins mediate their binding to 60S ribosomal subunits and the interactions among them. Mol. Cell. Biol. *16*, 3825–3832.

van Spronsen, M., and Hoogenraad, C.C. (2010). Synapse pathology in psychiatric and neurologic disease. Curr. Neurol. Neurosci. Rep. *10*, 207–214.

Stefani, G., Fraser, C.E., Darnell, J.C., and Darnell, R.B. (2004). Fragile X Mental Retardation Protein Is Associated with Translating Polyribosomes in Neuronal Cells. J. Neurosci. *24*, 7272–7276.

Stoll, G. (2015). Identification of the mRNA-associated TOP3β-TDRD3-FMRP (TTF)-complex and its implication for neurological disorders.

Stoll, G., Pietiläinen, O.P.H., Linder, B., Suvisaari, J., Brosi, C., Hennah, W., Leppä, V., Torniainen, M., Ripatti, S., Ala-Mello, S., et al. (2013). Deletion of TOP3β, a component of FMRP-containing mRNPs, contributes to neurodevelopmental disorders. Nat. Neurosci. *16*, 1228–1237.

Tamanini, F., Meijer, N., Verheij, C., Willems, P.J., Galjaard, H., Oostra, B.A., and Hoogeveen, A.T. (1996). FMRP is Associated to the Ribosomes Via RNA. Hum. Mol. Genet. *5*, 809–813.

Tarpey, P.S., Lucy Raymond, F., Nguyen, L.S., Rodriguez, J., Hackett, A., Vandeleur, L., Smith, R., Shoubridge, C., Edkins, S., Stevens, C., et al. (2007). Mutations in UPF3B, a member of the nonsense-mediated mRNA decay complex, cause syndromic and nonsyndromic mental retardation. Nat. Genet. *39*, 1127–1133.

Tarun, S.Z., and Sachs, A.B. (1996). Association of the yeast poly(A) tail binding protein with translation initiation factor eIF-4G. EMBO J. *15*, 7168–7177.

Tarun, S.Z., Wells, S.E., Deardorff, J.A., and Sachs, A.B. (1997). Translation initiation factor eIF4G mediates in vitro poly(A) tail-dependent translation. Proc. Natl. Acad. Sci. *94*, 9046–9051.

Thandapani, P., O'Connor, T.R., Bailey, T.L., and Richard, S. (2013). Defining the RGG/RG Motif. Mol. Cell *50*, 613–623.

Tripsianes, K., Madl, T., Machyna, M., Fessas, D., Englbrecht, C., Fischer, U., Neugebauer, K.M., and Sattler, M. (2011). Structural basis for dimethylarginine recognition by the Tudor domains of human SMN and SPF30 proteins. Nat. Struct. Mol. Biol. *18*, 1414–1420.

Viard, T., and de la Tour, C.B. (2007). Type IA topoisomerases: A simple puzzle? Biochimie *89*, 456–467.

Wahl, M.C., Will, C.L., and Lührmann, R. (2009). The spliceosome: design principles of a dynamic RNP machine. Cell *136*, 701–718.

Wang, J.C. (1996). DNA Topoisomerases. Annu. Rev. Biochem. *65*, 635–692.

Wang, J.C. (2002). Cellular roles of DNA topoisomerases: a molecular perspective. Nat. Rev. Mol. Cell Biol. *3*, 430–440.

Wang, H., Gate, R.J.D., and Seeman, N.C. (1996). An RNA topoisomerase. Proc. Natl. Acad. Sci. *93*, 9477–9482.

Wang, P., Lou, P.-J., Leu, S., and Ouyang, P. (2002). Modulation of alternative pre-mRNA splicing in vivo by pinin. Biochem. Biophys. Res. Commun. *294*, 448–455.

Wells, S.E., Hillner, P.E., Vale, R.D., and Sachs, A.B. (1998). Circularization of mRNA by Eukaryotic Translation Initiation Factors. Mol. Cell *2*, 135–140.

Wilson, T.M., Chen, A.D., and Hsieh, T. (2000). Cloning and Characterization of DrosophilaTopoisomerase IIIβ RELAXATION OF HYPERNEGATIVELY SUPERCOILED DNA. J. Biol. Chem. *275*, 1533–1540.

Wilson-Sali, T., and Hsieh, T.-S. (2002). Preferential cleavage of plasmid-based R-loops and D-loops by Drosophila topoisomerase IIIbeta. Proc. Natl. Acad. Sci. U. S. A. *99*, 7974–7979.

Wu, L., Bachrati, C.Z., Ou, J., Xu, C., Yin, J., Chang, M., Wang, W., Li, L., Brown, G.W., and Hickson, I.D. (2006). BLAP75/RMI1 promotes the BLM-dependent dissolution of homologous recombination intermediates. Proc. Natl. Acad. Sci. U. S. A. *103*, 4068–4073.

Xu, B., Ionita-Laza, I., Roos, J.L., Boone, B., Woodrick, S., Sun, Y., Levy, S., Gogos, J.A., and Karayiorgou, M. (2012). De novo gene mutations highlight patterns of genetic and neural complexity in schizophrenia. Nat. Genet. *44*, 1365–1369.

Xu, D., Shen, W., Guo, R., Xue, Y., Peng, W., Sima, J., Yang, J., Sharov, A., Srikantan, S., Yang, J., et al. (2013). Top3β is an RNA topoisomerase that works with fragile X syndrome protein to promote synapse formation. Nat. Neurosci. *16*, 1238–1247.

Yang, Y., Lu, Y., Espejo, A., Wu, J., Xu, W., Liang, S., and Bedford, M.T. (2010). TDRD3 is an Effector Molecule for Arginine Methylated Histone Marks. Mol. Cell *40*, 1016–1023.

Yang, Y., McBride, K.M., Hensley, S., Lu, Y., Chedin, F., and Bedford, M.T. (2014). Arginine Methylation Facilitates the Recruitment of TOP3B to Chromatin to Prevent R Loop Accumulation. Mol. Cell *53*, 484–497.

Yin, J., Sobeck, A., Xu, C., Meetei, A.R., Hoatlin, M., Li, L., and Wang, W. (2005). BLAP75, an essential component of Bloom's syndrome protein complexes that maintain genome integrity. EMBO J. *24*, 1465–1476.

Zalfa, F., Giorgi, M., Primerano, B., Moro, A., Di Penta, A., Reis, S., Oostra, B., and Bagni, C. (2003). The Fragile X Syndrome Protein FMRP Associates with BC1 RNA and Regulates the Translation of Specific mRNAs at Synapses. Cell *112*, 317–327.

Zalfa, F., Eleuteri, B., Dickson, K.S., Mercaldo, V., De Rubeis, S., di Penta, A., Tabolacci, E., Chiurazzi, P., Neri, G., Grant, S.G.N., et al. (2007). A new function for the fragile X mental retardation protein in regulation of PSD-95 mRNA stability. Nat. Neurosci. *10*, 578–587.

Zhang, Y., O'Connor, J.P., Siomi, M.C., Srinivasan, S., Dutra, A., Nussbaum, R.L., and Dreyfuss, G. (1995). The fragile X mental retardation syndrome protein interacts with novel homologs FXR1 and FXR2. EMBO J. *14*, 5358–5366.

Zhou, Z., and Fu, X.-D. (2013). Regulation of Splicing by SR proteins and SR Protein-Specific Kinases. Chromosoma *122*, 191–207.

Zhou, H., Mangelsdorf, M., Liu, J., Zhu, L., and Wu, J.Y. (2014). RNA-binding proteins in neurological diseases. Sci. China Life Sci. *57*, 432–444.

Zylka, M.J., Simon, J.M., and Philpot, B.D. (2015). Gene Length Matters in Neurons. Neuron *86*, 353–355.

9. Table of figures

10. Publications

Parts of this work have been published in the following article:

Stoll, G., Pietiläinen, O.P.H., Linder, B., Suvisaari, J., Brosi, C., Hennah, W., Leppä, V., Torniainen, M., Ripatti, S., Ala-Mello, S., et al. (2013). Deletion of TOP3β, a component of FMRP-containing mRNPs, contributes to neurodevelopmental disorders. Nat. Neurosci. *16*, 1228–1237.

11. Acknowledgements

I would like to express my thanks to all the people who helped and supported me and thus contributed to this thesis.

I especially thank Prof. Dr. Utz Fisher for the supervision, support and funding throughout this work.

I want to thank Prof. Dr. Alexander Buchberger for helpful suggestions and discussions and for examination of this dissertation as second evaluator.

I thank PD Dr. Sibylle Jablonka for being the third examiner in the oral defence.

Also, I want to thank Dr. Jens Vanselow and Prof. Dr. Andreas Schlosser for the mass spectrometry measurements and the extensive bioinformatical analysis of the data. Thanks to Jens for immense patience and the interest in this projekt. Moreover, I want to thank Dr. Elmar Wolf and Apoorva, for their support and help with ChIP experiments.

I thank all members of the department of biochemistry for collaboration, discussion and help.

Special thanks to Basti, Schorsch and Hirmchen for supervision, discussion, support (technically and mentally) and teamwork and for being great Lab members.

Many, many, many thanks to Lissy who had always helped and supported me, and always took care “that I can work” and took the load off me.

I thank Thomey and Jürgen a lot for their help with some experiments and their collaboration, but also for the discussions and understanding. Special thanks again to Jürgen for his relentless company to the chocolate machine and for always having the key.

Many thanks to Michael for helpful discussions and suggestions and his friendly ear throughout this time.

Thanks to Frau Hohmann and Andrea for their constant help in the background.

I want to thank the “lunch group” for their nice company, the conversations and discussions.

Thanks also to the running group for motivation, conversations and company.

And finally, many thanks to my family, friends and Wilhelm for their support, their empathy and immense understanding for all these years.

12. Declaration

I hereby affirm, in lieu of an oath, that I composed this doctoral dissertation (thesis) titled *"Functional characterization of the TTF complex and its role in neurodevelopmental disorders"* independently and no source materials or aids other than those mentioned have been used.

Furthermore, I confirm that this thesis has never been submitted as part of another examination process, either in an identical or in a different form I never previously acquired or tried any further academic degrees than those provided with and documented in the application form.

Würzburg, December 21, 2017 Signature